MICROFLUIDIC DEVICE FOR MICROINJECTION OF CAENORHABDITIS ELEGANS

MICROFLUIDIC DEVICE FOR MICROINJECTION OF CAENORHABDITIS ELEGANS

By

REZA GHAEMI.
B.Sc. (Sharif University of Technology, Tehran, Iran)

A Thesis
Submitted to the School of Graduate Studies
In Partial Fulfillment of the Requirements
For the Degree

Master of Applied Science
McMaster University
© Copyright by Reza Ghaemi, February

MASTER OF APPLIED SCIENCE (2014) McMaster University

(Mechanical Engineering) Hamilton, Ontario, Canada

TITLE MICROFLUIDIC DEVICE FOR MICROINJECTION OF CAENORHABDITIS ELEGANS

AUTHOR REZA GHAEMI, B.Sc.

SUPERVISOR Professor P. R. Selvaganapathy

Department of Mechanical Engineering

NUMBER OF PAGES XII, 185

ABSTRACT

Microinjection is an established and reliable method to deliver transgenic constructs and other reagents to specific locations in the animal. Specifically, microinjection of a desired DNA construct into the distal gonad is the most widely used method to generate germ-line transformation of *C. elegans*. Although, current *C. elegans* microinjection method is an effective manner for creating transgenic worms, it requirements such as expensive multi DOF micromanipulator, detailed injection alignment procedure and skilled operator which makes the microinjection process slow and not suitable for scale to high throughput. Although many microfabricated microinjectors exist, none of them are capable of immobilizing a freely mobile animal such as *C.elegans* worm. In this research, a microfluidic microinjector was developed to simultaneously immobilize a freely mobile animal such as *C.elegans* and perform microinjection by using a simple and fast mechanism for needle actuation. The entire process of the microinjection takes ~30 seconds which includes 10s for worm loading and aligning, 5s needle penetration, 5s reagent injection and 5s worm unloading. The capability of the microinjector chip for creating transgenic *C. elegans* was illustrated (with success rate between 4% to 20%)

ACKNOWLEDGEMENT

First, I am very grateful to my advisor, Professor Ponnambalam Ravi Selvaganapathy, for supervising this research and his unconditional support during the past two years. His vast knowledge and extensive level of expertise in mechanical, electrical and even biological field was indeed one of the main forces allowing this research to go forward.

Second, I am very thankful to Professor Bhagwati P Gupta for allowing me to access his laboratory's facilities and the expertise of his students. He was always there for me and truly supported the biological aspects of the research. Being a scientist, he always fascinated me with his engineering insights and skills. I am also grateful to Professors Chan Ching who always challenged me positively and made me more and more enthusiastic in advancing my research.

I thank my fellow labmates in Center for Advanced Micro-Electro-Fluidics laboratory: Wen-I Wu, Dr. Pouya Rezai, Leo Hsu and Bo Dang, Shehad Islam, Ali Shahid, Peter Lee, Siawash, Chah Zhu and Kamrul Russel, Rana Attalla, Jun Yang Harpreet Matharoo Sondos Ayyash Shinwary, Pedram Madadkar for inspiring me to get new ideas of research and for their great sense of humour. All these memories have already become great fortune in my life and I will never forget my two-year colourful life in Canada.

Finally and most importantly, I would like to deeply appreciate the everlasting love and support received from my wife, Shirin Rafeie Nejad; my parents, Mr. A. Ghaemi and Mrs. R. Momtazi; and my siblings, Masoud, Behrouz, Abolfazl, Faribal and Hamid Ghaemi. I would like to thank my second family in Canada for the kind help from Mr. B. Rafiei Nejad, Mis. M. Sefedi Esfehani and lovely sister M. Rafeie Nejad. Shirin's enduring love, encouragement, support, patience and gifted sense of humor made this journey so much easier for me. Her sacrifices, which were realized by our loss of precious time together, were for me the most painful and humbling of all. But, all these encouraged me to pursue this dream more seriously. This thesis is after all dedicated to her.

TABLE OF CONTENTS

LIST OF FIGURES

LIST OF TABLES

Chapter 1: INTRODUCTION

1.1. Motivation

Transfection is the deliberate introduction of biological material such as plasmid DNA, siRNA, proteins, dyes or antibodies into cells, embryos or a specific organ in organisms. It is an essential technique in the fields of drug discovery, genetic engineering and in-vitro fertilization [1-6]. Numerous transfection methods have been developed and customized for specific cell (or model organism) types and purpose. These methods can be broadly classified into chemical (reagent-based) biological (virus-based), and physical (instrument-based) methods. A particular sub classification of transfection is the introduction of genes that are non-native (from other organisms) to an organism into it and is known as Transgenesis.

Caenorhabditis elegans worm is a well-developed model organism for neurobiological and drug discovery studies. The simplest method for generating transgenic *C. elegans*, is to inject DNA that corresponds to the gene that needs to be expressed into the distal arm of the gonad. However, current methods of microinjection into *C.elegans* which operates in free space, requires expensive multiple degree of freedom (DOF) manipulators, detailed injector alignment procedures and skilled operator, making the injection process slow and not suitable for scaling to high-throughput. These problems of throughput and

equipment costs can be addressed by the application of microfluidic technology. Although many microfabricated microinjectors exist, none of them is capable of immobilizing a freely mobile animal such as *C.elegans* and performs microinjection by using a simpler and faster mechanism for needle actuation. High-Throughput microinjection allows larger number of chemical, genetic or pharmacological components to be rapidly tested. Through this process, active compounds, antibodies or genes, which modulate a particular bio-molecular pathway, can be identified quickly. Consequently, to solve the existing problems, a microinjection device, which can simultaneously immobilize and inject reagents via a simple injection mechanism and applicable for high throughput microinjection, is required. To achieve this aim, a simple in-plane design that allows visualization of the injection process and increases the speed of the microinjection process was developed. This design was fabricated and tested. Microinjection at the rate of 120 worms /hr were possible with this device. The injection process did not affect the viability of the worms and was found to be suitable for transgenesis. By increasing the throughput and ease of generating transgenic worms this device would be useful in drug discovery and in biological studies on diseases.

1.2. Organization

The organization of the chapters in this thesis is as follows:

Chapter 2 presents an introduction to transgenesis followed by technologies that are used for the insertion of bio-molecules into cells. Then, it provides a comparison of the methods that are currently used and their applicability to creating transgenic organisms.

Chapter 3 establishes the proposed design and describes the advantages of thsi design over other devices available in the literature. It details the functionality and operation of the device, and its potential for high-throughput. It determines the critical dimensions of the design and details some of the experiments to determine certain crucial design parameters.

Chapter 4 presents the fabrication techniques and materials used in the microfabrication and assembly of the device. After describing the needle fabrication technology, it provides an overview of the device assembly process, the setup and operation of the device.

Chapter 5 describes the experimental setup and the characterization of the device and presents the results obtained from the device. It specifies the characterization of the compliant actuation mechanism as well as the drug delivery system. The chapter ends with the results, showing the microinjection of *C. elegans* with a Methylene blue buffer solution as well as DNA solution bound to the fluorescent dye. Finally, the chapter presents the capability of the microinjector for creating transgenic *C. elegans* worms.

Chapter 6 ends this thesis by highlighting the contributions of the research, namely: performing injections in a microfluidic format, the use of compliant fluidic channels and drug

delivery systems. It then provides a number of suggestions for the future development of the device.

1.3. Contributions

The main contribution for this research is listed below:

- ✓ Recently various microfluidic devices have been developed for different cell types and model organisms. However, none of them is able to immobilize a free mobile *C. elegans* worm and perform microinjection. This device developed in this thesis represents the first microinjector capable of simultaneously immobilizing a freely mobile animal such as *C.elegans* and performing microinjection by using a simple and fast mechanism for needle actuation.
- ✓ Photolithography and 3D printing are two techniques for creating micro pattern with fine (10 μm resolution) and course (100 μm resolution) features, respectively. Many microfluidic devices such as the microinjector designed in this research required to have both feature types (fine and course) on a single mold. However, neither photolithography nor 3D printing alone could be used to create these types of master mold. To fill this technology gap, a hybrid manufacturing integrating molds from photolithography and 3D printing has been developed in this thesis. The techniques allowed to create molds with fine feature (resolution of 10 μm and height to width aspect ratio of 10) produced by photolithography as

well as course feature (resolution of 100 µm and height to width aspect ratio of 10) fabricated by 3D printing.

- ✓ The current microinjection method used for *C. elegans* worm is very slow, time consuming (~ 20 injection/hr), and required skilled operator. In this thesis a microinjector for fast, High-Throughput and simple microinjection of *C. elegans* worm, has been developed. The entire process of the microinjection took ~30 seconds (120 injection/hr) which includes 10s for worm loading and aligning, 5s needle penetration, 5s reagent injection and 5s worm unloading. This is the fastest microinjection process for *C.elegans* at this moment.

The newly developed device was shown to produce transgenic *C. elegans* for the first time (with success rate between 4% to 20%) by injecting ~150 pL (corresponding to 1 pulse at pressure level of 2 bar) of myo-2::GFP DNA plasmid into distal gonad of 25 wild-type N2 *C. elegans* worm at 56 (hr).

Chapter 2: LITERATURE REVIEW

2.1. Introduction

Transfection is the deliberate introduction of biological material, including plasmid DNA, siRNA, proteins, dyes and antibodies into cells, embryos or a specific organ in model organisms. It is an essential technique in the fields of drug discovery, genetic engineering and in-vitro fertilization [1-6]. Various approaches including chemical, biological, and physical methods have been developed for transfection.

A particular sub classification of transfection is the introduction of genes that are non-native (from other organisms) to an organism into it and is known as Transgenesis. This approach has been developed in the past few decades to create transgenic organisms. Three transgenic methods namely: Microinjection, Embryonic stem cell-mediated gene transfer, and Retrovirus-mediated gene transfer, are widely used in transgenic research. However, low transgenesis efficiency and viability still pose problem in these three methods. In this chapter, an introduction to the methods that are currently used for the insertion of genetic material into cells, embryos and the organs of animals is described first. Next, a discussion of transgenesis methods is presented. Finally, the chapter provides an introduction to the methods that are currently used for the insertion of bio-molecules into cells and in particular provides an overview of methods used for *C. elegans* microinjection.

2.2. Introduction to cell transfection

The process of introduction of foreign DNA into the nucleus of bacterial and/or mammalian cells is called transfection. The bacterial and/or mammalian cells that have received the foreign DNA are called transfectants. Typically, transfection is classified into two groups known as stable transfection and transient transfection [1]. In stable transfection, the foreign DNA is integrated with the genome of the cells [2], while in transient transfection, the foreign DNA is expressed for limited time (24 – 96 hr) and is not integrated into the genome [1]. Some applications of the transfection technology are in gene therapy, generation of pluripotent stem cell (iPS cell) and generation of interference RNA (siRNA) knock-down mutants [3-6].

One of the important applications of transfection technology is to create transgenic organisms. Transgenesis emerged in the 1990s as a technology to alter the phenotype of organisms (displayed character by animal) by changing its genetic makeup (genotype) [7]. Various methods known as recombinant DNA technologies were used to introduce the foreign gene into the DNA sequence of the host organisms. One of the main applications of the transgenesis is gene therapy, which is the modification of the genetic make-up of an individual organism to cure inherited diseases [8]. Drug discovery is another area, which uses transgenesis technology widely to created transgenic animal (e.g. mice, rat and nematodes) in order to identify and conduct preliminary validation of a drug candidate or lead compound for the treatment of a specific disease. Depending on

the cells types or model organism, various transgenic methods, have been developed. These methods are presented in the following sections in more detail.

2.3. Methods for cell transfection

Numerous transfection methods have been developed and customized for specific cell types and purpose. These methods can be broadly classified into chemical (reagent-based) biological (virus-based), and physical (instrument-based) methods. The goal of an optimized technique is high transfection efficiency, low cell toxicity, minimal effects on normal physiology, and be easy to use and reproducible.

2.3.1. Chemical methods

Chemical transfection methods use various reagents to transport genetic material (nucleic acids) into cells. Chemical transfection methods are widely used in contemporary research and were the first to be used for transferring foreign genes into mammalian cells [9-11]. These methods typically use lipids, calcium phosphate or cationic polymer (e.g. poly(ethyleneimine) (PEI), poly- L -(lysine) (PLL), poly[2-(N , N -dimethylamino)ethyl methacrylate](PDMAEMA) and chitosan). The working principle behind the all chemical transfection methods is the same. The nucleic acids are hydrophilic molecules and do not easily pass through the hydrophobic cell membrane. However, by coating the nucleic acid by a polymer or a lipid it could be made more hydrophobic and thus facilitate absorption

by the cell membrane and delivery into the cells. In lipid transfection, cationic lipids form a liposome, which then combines with nucleic acids to form transfection complex. Calcium phosphate on the other hand simply condenses the DNA and then gives, it a net positive charge. Finally, cationic polymers condense the DNA in positively charged particles. The exact mechanism of how nucleic acids pass through the cell membrane is unknown [12]. However, it is known that endocytosis and phagocytosis play important role in the process. Moreover, nucleic acids must be delivered to the nucleus for gene expression. Again, the translocation mechanism to the nucleus is not known [12]. The chemical methods are capable of delivering nucleic acids into cells in culture dish with high efficiency up to 95% [13], minimum required steps and adaptable to high-throughput systems. However, a single generic protocol cannot be used for all cell types. For each method, the transfection efficiency varies with cell type dependent on factors such as nucleic acid/chemical ratio, solution pH, and cell membrane conditions [12] and, so the process results in low transfection efficiency, especially in vivo. In addition, since there is no precise control on the number of nucleic acids and they go into the cell randomly, it would be difficult to control the dosage of the delivery by using chemical methods.

2.3.2. Biological methods

Viral mediated transfection [4], is a method that uses viruses as a specialized mechanism to transport genetic material into cells they infect and is the most common method used

in clinical research. It can be categorized into two types: *in vivo* viral gene transfection and *Ex vivo* viral gene transfection. *Ex vivo* viral gene transfection is based on the exposure of cultured cells to vectors carrying the desired gene. In this method, the target cells are removed from the organism by surgery and then are cultured *in vitro* to achieve a desired number of cells. Subsequently, the cells are exposed to the viruses that are carrying the desired gene. The viruses infect the cells and insert the desired gene into the cells' DNA. The cells are grown in the laboratory and then returned to the organism. This method can be used for various cell types with high trasfection efficiency up to 92% [14]. However, sample preparation and DNA packaging are time consuming which makes the process relatively expensive compared to other transfection methods. Moreover, this method cannot be used to incorporate a gene into a developing embryo or egg .

In vivo viral gene trasfection is based on introduction of desired gene into a vector, which is then conducted into model organisms directly via blood stream for stable genomic integration. This vector will transfer the gene of interest in the target tissue to express the target protein. This method, allows infection of specific cell types for gene delivery as is needed, (e.g. gene therapy) in a simple and high-throughput manner. However, the efficiency of the method strongly depends to the cell type and condition and they usually have transfection efficiency in order of 10% [15]. This method has not been attempted to incorporate a gene into a growing embryo or a developing egg of *C.elegans*. Moreover, in both technique (*ex vivo* and *in vivo*), DNA package size limit (the maximum base sequence that can be delivered by one virus (Replication competent ALV derived retroviruses in this case) is ~9400 bases), immunogenicity, Insertional mutagenesis and

potential hazard to laboratory personnel are other drawbacks involved [12, 16]. In addition, viral gene transfection does not allow a precise control on the doge of the delivery since there is no control on the number of viruses that infect a single cell.

2.3.3. Physical methods

Physical methods, which directly insert the genetic information into the cells or target organs, are the more recently developed methods in transfection technology. Physical methods use diverse set of physical tools (e.g. nano or micro particles, electroporation, sonoporation and capillary microinjection) to create openings in the cell membrane or tissue to transfer DNA into the cytoplasm or target organs, respectively. These techniques avoid endosomal and possibly lysomal degradation [17] involved in chemical and biological methods caused by enzymes within the cells cytoplasm. The physical methods are discussed in more details in the following sections. The physical methods avoid some of the drawbacks of the chemical and biological methods such as cell type and reagent dependency. However, they cause greater membrane and tissue damage and viability.

2.3.3.1 Ballistic particle delivery

Ballistic particle delivery is a practical transfection method, which uses nano- or micro particles (e.g. microscopic gold particles) to deliver the genes into the nucleus. It uses high pressure to force a microscale “bullet” loaded with nanoparticles and genetic

material penetrate the cell membrane. In this method, Hundreds of gold particles (with size of ~100 (nm)) are conjugated with thousands of copies of the new gene (Figure 2. 1, step 1). These particles are non-toxic, inert, and much smaller than the cells to be transferred [17-19]. A part of the new gene is marker gene (e.g. GFP marker gene) to detect cells, which express the gene. The nucleic acid/particle conjugates are accelerated with air pressure (Figure 2. 1, steps 2-5) and then shot at a batch of cells on a Petri dish plate, "gene gun" (Figure 2. 1, step 6). If the gold particle penetrated into the nucleus of the cell then, the gene may get off from gold particle and integrate into the DNA of the chromosomes. The Ballistic particle delivery was invented in 1987 to insert genetic material into plant cells, and then its applications were extended to mammalian cells in the 1990s [20]. Various factors such as the particle size, the distribution and number of DNA-conjugated particles and concentration of DNA plasmids that are conjugated onto the particles, play important role to affect the efficiency of this technique [21]. This method is simple, rapid, versatile, high reproducibility, has low DNA consumption and is cell type independent. Moreover, it can deliver single and multiple genes as well as large DNA fragments with little manipulation of cell. However, it generally has lower efficiency (up to11%) [22] compared to other physical methods or lipid-mediation transfection. In addition, preparation of microparticles and device are other challenges involved in use of ballistic particle delivery. In addition, since there is no precise control on the number of particles that hit a single cell, it would be difficult to control the the dosage of the delivery.

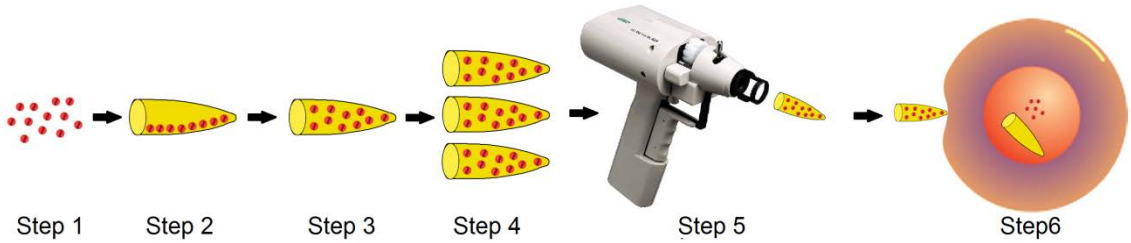

Figure 2. 1: Step 1: Precipitating DNA (black) onto gold particles (red). Step 2: loading DNA/gold into bullet (yellow). Step 3: Rotating bullet to conjugate DNA gold over inside surface. Step 4: Placing bullets into cartridges. Step 5: Loading cartridges into gun. Step 6: shooting DNA into target cell.

Adamo et al. [23] design a microfluidic-based injector to delivery macromolecules by directing a picoliter jet of a solution into the individual cells. In this design, suspended cells are introduced and lined up into a microchannel as shown in Figure 2. 2. A miniaturized nozzle is setup on the top wall of the line up microchannel and the reagent can be inserted into the cells by using a high-speed liquid jet (speed of 1–5 m/s) through the nozzle with opening diameter of ~2 μm and a length of ~10– 35 μm. A piezoelectric actuator is used to create the required pressure pulses with pressure level of ~5–40 bar for 10-30 μs to deliver ~0.1 pL of a solution of a potassium indicator (which became fluorescent upon binding with potassium inside cells) into the HeLa cells. The design is potentially a new tool for the high-throughput (they assumed the jet injector to achieve a throughput of 500–1000 injection per minute) delivery of cell impermeable compounds into living cells without compromising viability. However, efficiency and the toxicity of the method was not reported, since only a small number of cells were injected. The

device is only applicable for suspension cells and it cannot be used for mobile organisms such as worms due to the lack of the immobilization mechanism.

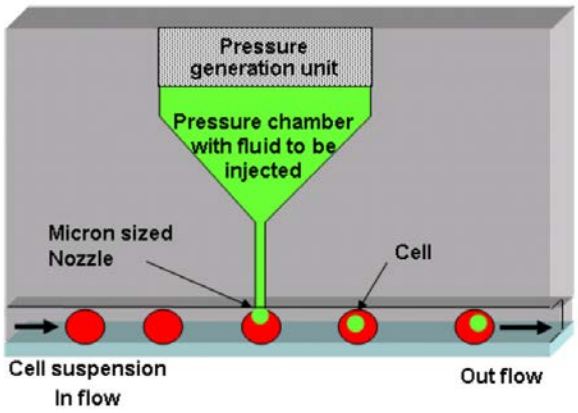

Figure 2. 2: The schematic of the jet injector. Suspended cells are lined up inside a microfluidic channel via cell suspension flow. A miniaturized jet flow (generated by pressure generator unit) through the micro size nozzle is used onto the cells to deliver the reagent (green) into the cells (red) [23].

2.3.3.2 Electroporation

Another physical method to transfer bio-molecular (e.g. DNA, proteins, etc) into the cells is electroporation (see Figure 2. 3) , which uses high-voltage electric pulses to form transient and reversible holes or pores in the cell membrane (step 2 to 3 in Figure 2. 3) [24, 25]. The pore sizes thus created are large enough to allow exogenous micro and macromolecules in the surrounding medium to enter or leave the cell (step 4 in Figure 2. 3) [26]. These pores are created because, the poor conductive cell membrane behaves similar to a capacitor and is unable to conduct DC current and an extra transmembrane potential (TMP, the difference in electrical potential (voltage) across the membrane of a

lining cell) is developed across the cellular membrane (step 2 in Figure 2. 3), which is linearly proportional to the electric field level and the cell radius. The lateral mobility of the phospholipids in the membrane causes random hydrophobic pores to develop in the membrane. At a threshold TMP of 0.5–1 V, these hydrophobic pores grow under the stress from the TMP and become hydrophilic pores. The size of the pores that are formed depends on the cell type. For example, the pores size in red blood cells was shown to be between 20-120 nm for a 0.3-ms wide, RF pulse, which oscillated at 100 kHz with an amplitude of 4-5 kV/cm [27]. This method requires fewer steps compared to other physical methods and can be applied to wide range of cell types for both stable transformation and transient gene expression with efficiency up to 96% [28]. However, viability of the cell may be affected by this technique. Although, membranes reform after brief exposures to electrical pulses, extended exposure can cause complete cellular death (due to membrane rupture) [25]. In addition, since there is no precise control on the number of nucleic acids inserted and they go into the cell randomly, it would be difficult to control the dosage of the delivery by using chemical methods.

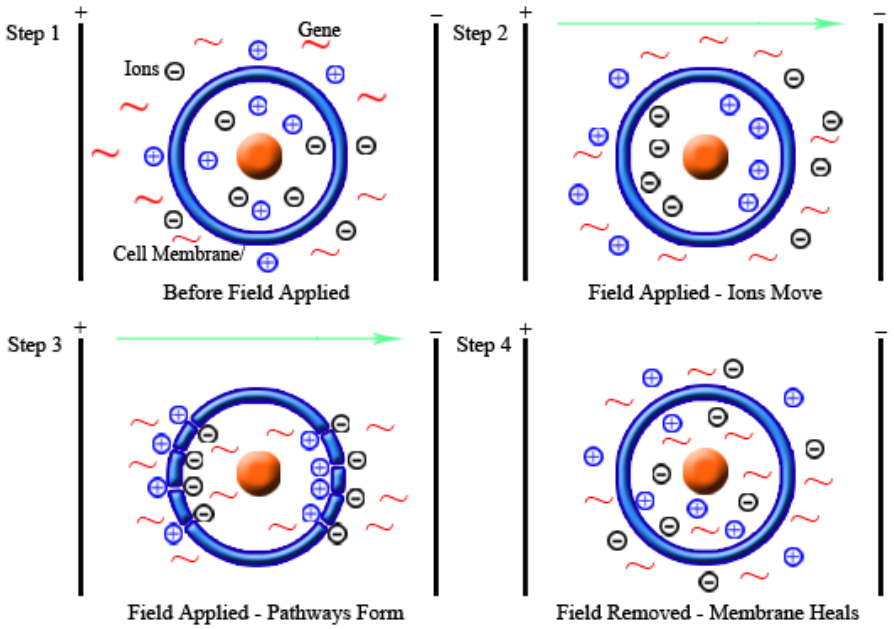

Figure 2. 3: Electroporation in a uniform electric field. Step 1: introducing the cells to the reagent (Gene, proteins, etc). Step 2: applying electrical field which polarizes the cell and the reagent. Step 3: permeabilization of the membrane creates transient holes or pores on the membrane and genes pass through the membrane. Step 4: removing electrical field (membrane heals)

Several microfluidic and miniaturized electroporation systems have been created [29-35] to transfect reagents (e.g. DNAs, proteins, etc) into endothelial cells, which can be categorized into two categories: microfluidic devices for single-cell transfection and others for multi-cell or batch transfection. One of the most important advantages of microfluidic devices over macroscale devices is that by applying microelectronic pattern techniques (e.g. photolithography process), the distance between the electrodes can be reduced which reduces the potential needed to achieve the critical electric field strengths for electroporation. In addition, the manipulation and handling of the cells are easier in microdevices since the sizes of the cells (~10 μm) are compatible with dimension of the

channel and electrodes. Moreover, other unit operations such as separation and detection could be integrated with transfection device to increase the speed and accuracy of the transgenesis process. Furthermore, the amount of the required reagent is lower than macroscale systems, and fabrication of parallel cell transfection process is simpler.

(1) Microdevices for Single cell electroporation

Lin et al. [29] designed a microfluidic electroporation system for suspended cells. In their design, the electroporation was achieved by applying 10 ms pulses of 10 V to a 0.2 mm-high, 5 mm-wide channel with integrated gold electrodes at the top and the bottom of the channel at the electroporation spot (Figure 2. 3a). This simple design was successfully applied for transfecting human hepatocellular carcinoma cells (Huh-7) with β-galactosidase and green fluorescent protein genes.

Khine et al. [30, 31] developed a microdevice which used a constriction between the two electrodes to focus the electric field (Figure 2. 4b). Moreover, the size of the constriction was well designed to enhance this effect. A gentle suction cannot pass the cells through constriction (the HeLa cell diameter (12–17 μm) was approximately four times larger than the constriction (3.1 μm)) blocking it, which increased the effect of the constriction in focusing the electric field. Upon electroporation with less that 1V using Ag/AgCl electrode, calcein release from HELA cells and trypan blue uptake was observed. However, DNA transfection has not been reported in this device.

Huang and Rubinsky [32] designed a flow-through channel electroporation microdevice with a microhole in a silicon nitride membrane applicable to cell transfection. In this design, first a flow-through containing the cells was passed on top of a silicon nitride membrane inside a channel, which was ~1.5 times the size of a cell (Figure 2. 4c). Next, the cell was captured in the microhole created in the middle of the channel by a backside pressure. Then, an electrical pulse was applied via two electrodes placed on the top and bottom of the microhole to transfer the desired foreign molecules into the cell via electroporation mechanism. The microhole in the silicon nitride membrane had a significant role to focus the electric field for the electroporation since it completely blocked the microhole. The design allowed for the transfer fluorescent YOYO-1 using 100 ms, 10 V pulses into the human prostate cells and verified the transfection by visualizing the GFP gene.

(2) Microdevices for batch cell electroporation

All the transfection devices above were based on flow-through concept. Lin et al. [29] designed a microfluidic design applicable for batch cell transfection. This device consisted of a glass substrate with interdigitated gold electrodes that was capped with a PDMS chamber (Figure 2. 4d). The device allowed for the electroporation of the surfacebound cells (Huh-7 cells, human embryonic kidney cells and HUVEC primary cells with GFP gene) by applying DC electrical field (voltage 10-100 V, pulse duration 0.1-100 ms) to the interdigitated electrode structure. In this design, the transfection

efficiency was improved by adding an extra anode above the interdigitated structure which was used to increase the local concentration of DNA plasmids near the cells at the cathodes before electroporation (the negative DNA plasmids were attracted to the cathodes by an electrophoretic potential). The transfection efficiency was enhanced as compared to experiments where no electrophoretic forces were used.

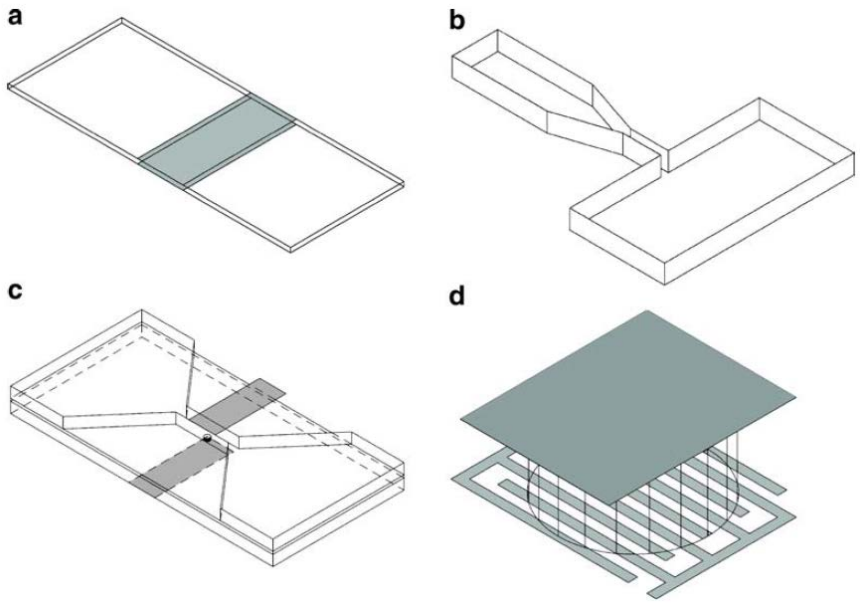

Figure 2. 4: Schematic representation of various different transfection microfluidic electroporation devices. Not to scale. a) the electroporation was achieved by applying DC pulses with integrated gold electrodes at the top and the bottom of the channel at the electroporation spot. b) HELA cells can block the constriction, which increased the effect of the constriction in focusing the electric field. c) A flow-through channel electroporation microdevice with a microhole in a silicon nitride membrane applicable to cell transfection. d) A microfluidic design applicable for batch cell transfection. consisted of a glass substrate with interdigitated gold electrodes that was capped with a PDMS chamber (adapted from Fox 2006 [33]).

2.3.3.3 Sonoporation

Sonoporation (cellular sonication) is another physical transfection method, which allows large molecules such as DNA to pass into the cells [36, 37] by applying sound (typically ultrasonic frequencies). The applied ultrasound pulse modifies the permeability of the cell plasma membrane and creates transient holes on it due to the effects of heating and cavitation. The cavitation due to ultrasound causes formation of bubbles that upon collapse produces mechanical perturbations of the cell membrane [36]. As a result of these pertubations, the transient holes form on the membrane of the cell and enhance the transport of the large molecules into the cytoplasm [37]. Ultrasound exposure is an efficient method for the transfection of bio-molecules into mammalian cells and tissues in vitro (with efficiency up to 50% for 0.4 MPa and 20 s exposures). Stable transfection rates averaged 0.34% of surviving cells [37]) and in vivo (with transfection efficiency up to 2.5% of viable cell counts in B16 mouse melanoma tumors for 400 shock wave treatments [38]). Furthermore, it is simpler as compared to other direct delivery methods such as particle bombardment and electroporation [36]. However, overexposure is a critical problem involved in this method. Extended exposure to low frequency (<MHz) ultrasound causes cellular disintegration. . In addition, since the there is no precise control on the number of nucleic acids and they go into the cell randomly, it would be difficult to control the dosage of the delivery by using chemical methods. One of the main applications of the sonoporation technology is targeted gene therapy in vivo. In a medical treatment scenario, a patient is given modified DNA, and an ultrasonic

transducer might be used to deliver this modified DNA into specific regions of the patient's body [37].

Many microdevices have been developed to use sonoporation to transfect DNA into -cells. [39, 40]. Le Gac et al [40] employed laser induced bubble cavitation in HL60 (human promyelocytic leukemia) cell suspension to enable trans-membrane transfer in a microfluidic format (Figure 2. 5). In their design, a single laser (Nd : YAG laser at 532 nm, 6 ns pulse duration) was exposed to the microchamber (see Figure 2. 5) to generates cavitation bubble with lifetimes of 10-30 μs. The cavitation bubbles can induce membrane poration of cells located in their close vicinity. Membrane integrity of suspension cells was probed by either the calcein release out of calcein-loaded cells or the uptake of trypan blue. They found 0.75 R_{max} (maximum bubble radius) as a critical interaction distance of the cavitation bubble with HL60 suspension cells.. Cells closer than 0.75 R_{max} from the cavitation bubble center became porated with a probability of 0.75%. While, other cells, which were placed farther away than four times of R_{max} were not affected. This design is very attractive as an alternative to electroporation and it has a simple fabrication process, since it can be easily applied in a microfluidic format and the material used in the device only need to be transparent to the laser pulse. However, the device is only applicable for one-layer cell structures and in several layer tissue, only the first layer can be infected. For the reason that the first layer of cells is exposed to the sound and it would absorb the DNA. Therefore, for *in vivo* experiments, the internal organs (e.g. the gonad in *C. elegans* worm) could not be infected by this technique.

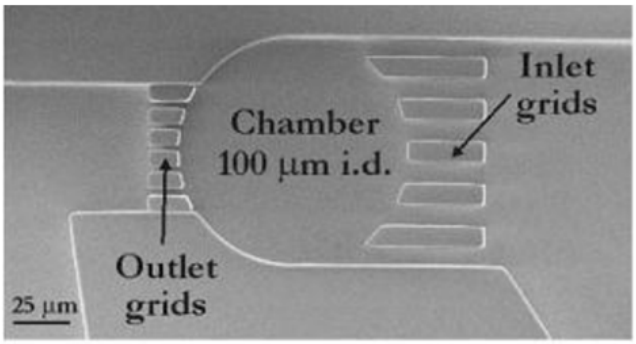

Figure 2. 5: SEM photograph of a microchamber where cells are collected, scale bar denotes 25 µm. Human leukemia HL60 cells (suspension cells) are introduced into the microsystem via inlet grids to the 100 µm diameter microchamber. Additionally, the microchamber is connected to the outlet grids to collect the cells after transfection [40].

2.3.3.4 Capillary microinjection

Capillary microinjection is a well-established technique for introducing genetic material into cells or specific organs by creating a passage through the cell membrane (*in vitro*) or tissue (*in vivo*) via a microneedle [41, 42]. Any cellular (*in vitro*) microinjection system is typically composed of three basic functions: the immobilization of the target cell or organism, the positioning and inserting of the microneedle, and delivery of the reagent in the needle into the cell or organism by control of the pressure inside. In contrast to suspension cells, the adherent cells do not require the immobilization function for the needle insertion as shown in Figure 2. 6.

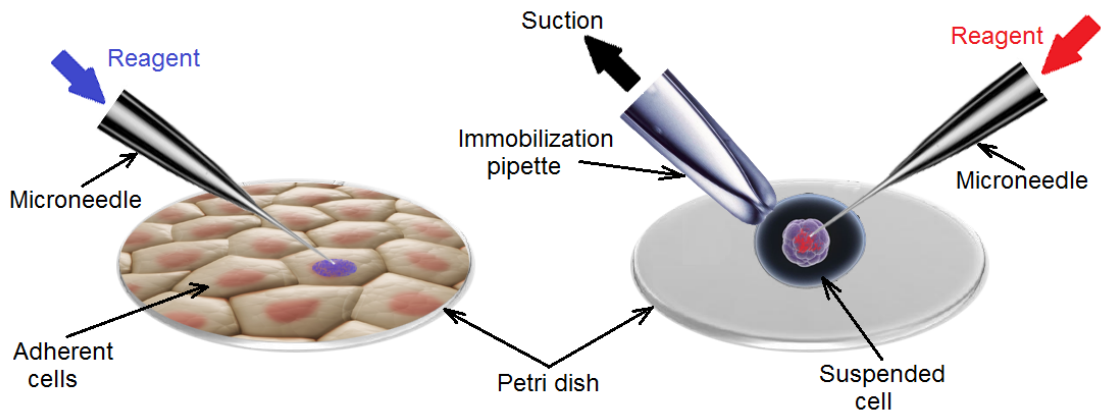

Figure 2. 6: Capillary microinjection into suspended cell (right) a nd adherent cell (left)

Using microinjection is it possible to control and meter the volume of reagents, DNA and other biomolecules that are delivered into cells, embryos and microorganisms. Typical volumes delivered are in the range of 1 nL to 1 pL [43-48] although it is possible with current technology to deliver as small as 100 fL [45] . Furthermore, there is no limitation on the materials that can be injected. These typically include DNA, mRNA, proteins and antibodies. The injection process is also independent of cell and several reagents and mixtures can be injected at the same time. Finally, microinjection allows the operator to control the location of the delivery inside a cell, embryo or a microorganism very precisely. This allows for tissue or organ specific delivery in microorganisms that is not possible by any other method.

However, manual microinjection is slow process (~15 injection/hr and depends on the operator skill and training) and requires skilled operators [49, 50]. The transfection efficiency is typically less than ~10% for in vivo model organisms [51] and ~70% for in

vitro cells and embryo microinjection [52], again strongly depending on operator's skills (in some conditions, transfection efficiency of 96% have been reported [53]). Automated microinjection [54] is relatively fast (up to 1500 injection per hour) but requires expensive equipment. One of the main applications of the capillary microinjection is in generation of transgenic organisms. In addition, embryonic stem cell-mediated gene transfer is another application for capillary microinjection method [55].

A number of Lab-on-a-chip microinjector have been engineered for microinjection of suspended cells, Drosophila embryo, Zebra fish embryo as well as adherent cells. Lab-on-a-chip microinjection reduces cell damage, reagent dead volume and is amenable for high-throughput. Generally, they can be classified into two groups based on the mechanism of the needle insertion: active needle actuation and passive needle actuation.

(1) Microinjector with active needle actuation

This group of devices use mechanical systems such as a micropositioner to move the microneedle into a cell, embryo or organism that has been held stationary. Chun et al. [43] designed a MEMS device for suspended cell injection consisting of one microarray injection capillary and a complementary array of microchambers for immobilizing the cells as shown in Figure 2. 7. The device consists of an array of hollow chambers with small microholes (5 μm diameter and 100 μm depth) at its bottom (see Figure 2. 7). The cell suspension is spread on the microchamber array and is trapped in these microchambers though suction. Next, an array of microneedles (1 μm in thickness, 30 μm

in length and 5 μm in diameter) made of SiO_2, corresponding to the pattern of the microchambers. Then, the microneedle array is aligned and inserted into the cells. Pneumatic pressure was used to deliver reagents into the cells. Although the design is suitable for high throughput microinjection, its fabrication process is complex and expensive as it involves multiple steps of bonding and reactive ion etching (RIE). Moreover, the cell trapping mechanism is not suitable to immobilize live model organisms such as *C. elegans* and drosophila larva that cannot be pinned through suction at one location.

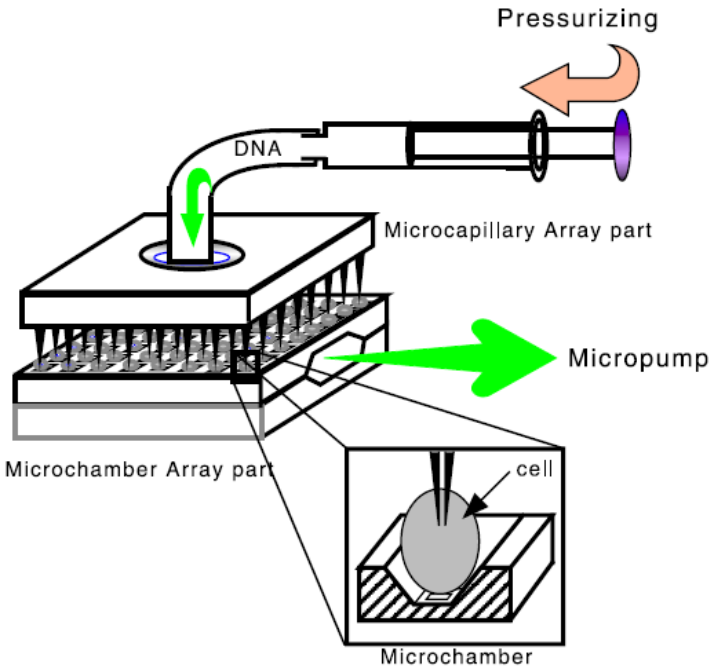

Figure 2. 7: Microarray injection device [43]

Lee et al. [44] presented a hybrid system consisting of a glass microneedle, integrated with a PDMS microvalve for controlled fluid delivery (Figure 2. 8). The device consists

of a glass microneedle (fabricated via traditional micropipette pulling) inserted into the PDMS based microchannel (80x80 mm) and bonded. Two kinds of cored glass needles (ID/OD = 7/10 µm and 17/22 µm) with length of 7-10 mm was used for injection. A microfluidic valve integrated with the microchannel close to the microneedle serves as a flow control device to meter and control fluid delivery. The design allowed for controlled delivery of volumes less than 1 (nL) of water. Although this device integrates flow control and reduces dead volume at the tip of the microneedle it still requires a micropositioner and skilled operator to align and position the needle for insertion.

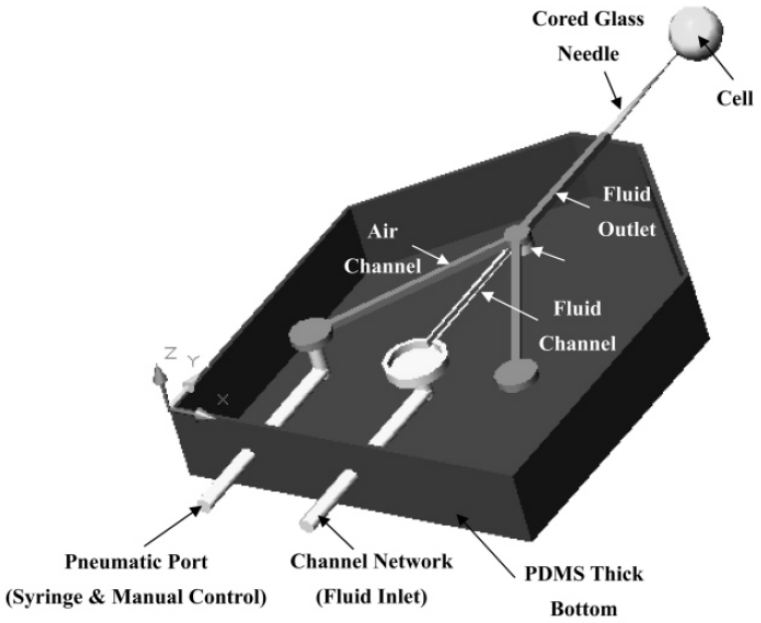

Figure 2. 8: Micro-valve mediated microinjection control. The reagent is transferred through the fluid channel connected to fluid inlet toward the core glass needle. The air channel connected to the pneumatic port is used to close/open the pneumatic valve on the fluid channel [44].

Gentil et al. [45] modified the atomic force microscope (AFM) tool to perform precise cellular injections. They redesigned the AFM probe tip to consist of a sharp tip that has an internal hollow core to allow fluid flow through it (see Figure 2. 9a). Figure 2. 9b shows the scanning electron micrographs of the microfluidic probe tip with the small orifice (~200 nm) above the sharp tip that is used to flow reagents into the cells. In operation, the precise positioning and force feedback control of the AFM was used to insert the tip of the probe to any location inside the cell while observing it with an inverted microscope.

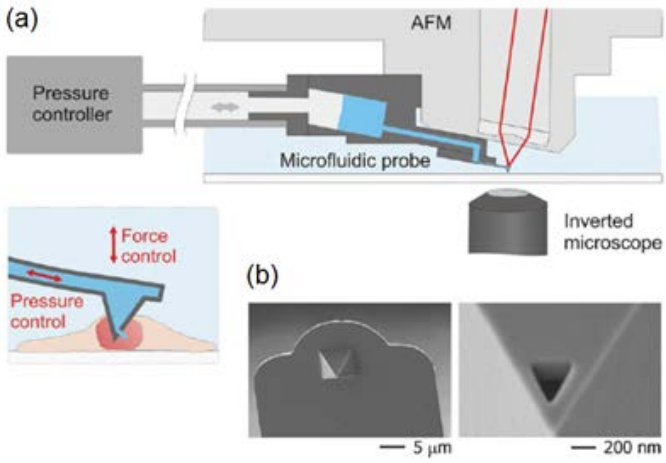

Figure 2. 9: a) Schematic representation of the intranuclear injection using fluidic force microscopy. The setup features an inverted microscope, an AFM, and a microfluidic probe connected to a pressure controller. Optical-, force- and pressure-monitoring are performed simultaneously along the entire intranuclear injection process. b) Scanning electron micrographs of a FluidFM injection probe; a triangular aperture was milled by focused ion beam at the front facet of the pyramidal tip [45].

The intranuclear injection of 300-1000 (fL) Lucifer yellow CH (LY) into Hela cells was performed with a success rate of 100% with no adverse effect on the cells. The device

enabled quantitative and functional injections into single cell nuclei and showed optimal injection efficiency and cell viability. The deflection of the needle can be controlled via adjusting the pressure inside the needle. A force sensor was placed on the tip to measure the injection force (Figure 2. 9a). Moreover, the pressure control through the microchanneled probes allowed the precise, tunable delivery of femto- to picoliter volumes. However, the use of AFM to provide actuation and control of the injection makes it expensive compared to other microfluidic methods. Moreover, AFM tips may not be suitable for injection into internal organs of organisms such as *C. elegans* and drosophila larva that are placed far deeper into the body that the size of the tip. In addition, precise positioning requires significant time that may be determinetal to high-throughput operation.

(2) Microinjector with passive needle actuation

In contrast to microinjector that require active needle actuation, other designs fix the position of the needle in the device and push the target (cells, embryo, etc) to the needle for insertion . Adamo et al. [46] designed a microfluidic format single cell microinjection system. In their design, the needle is fixed at the corner of a bend in the microchannel through which the cells flow as shown in Figure 2. 10. In order to perform the injection valve 1 (V1) is opened and valve 2 (V2) is closed which pushes the cell flowing in the microchannel and impinges it on the needle. (Figure 2. 10a). Next, the reagent is delivered through the microneedle while the pressure on the cell due to the fluid flow in

the microchannel is minimized (Figure 2. 10b). Finally, the cell is released from the needle by opening the valve 2 (V2) and closing the valve 1 (V1) which pushes the cell into channel B and out of the device (see Figure 2. 10c). Hela cells were used to test the effect of cell transit (without injection) inside the device on the cell viability. Their results showed no differences in cell viability between the two conditions with 98% cell viability one hour after passage through the chip. They also injected ~2.5 (pL) of a fluorescent marker (dextran, tetramethylrhodamineMW10 000) within 0.5 (s) into Hela cells to visualized injection process.

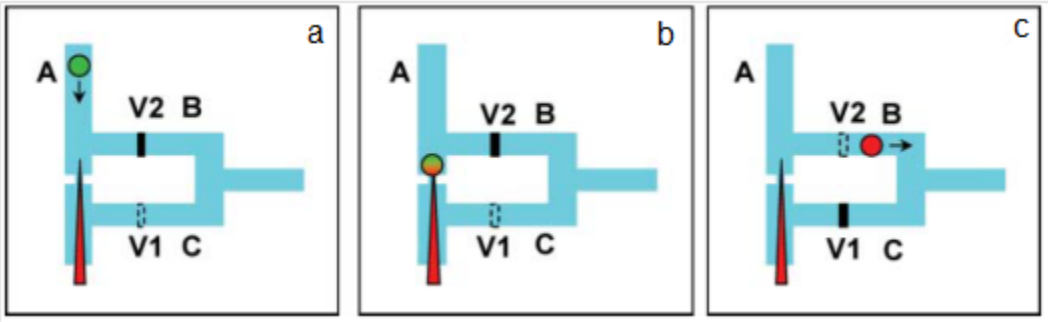

Figure 2. 10: Microfluidic cell injection method. a) Cell is moved by the fluid stream towards the microneedle, valve 1 (V1) is opened and valve 2 (V2) is closed. b) The cell is pierced by the injection needle and injected. c) V2 is opened and V1 is closed which causes a reversal of flow to lift the cell off the needle and transport it along channel B and out of the device [46] .

The advantage of this design is that it is simple and suitable for high-throughput cell microinjection. However, control of insertion depth is not possible as its position is not controlled actively. The dynamics of the flow and the position of the cell in the flow determine the location of the insertion and the position of delivery of the material into the cell. The other drawback is that the size of the cell is a critical factor for injection. If they

are too large then, they might clog the channel, and if they are too small then the injection needle might lyse the cell. Furthermore, the needle assembly is complex and requires precision to ensure that the tip extends into the channel a given length. Finally, the design cannot be used for live organisms such as *C. elegans* and drosophila larva where the insertion has to be deep into the tissue.

A similar microfluidic device was designed by Delubac et al. [47] by using a Pyrex-silicon-Pyrex sandwich structure for Drosophila embryo injection as shown in Figure 2. 11. A surface micromachined silicon nitride microneedle suspended inside a microchannel was used for injection. Embryos are sequentially inserted into the channel and oriented for insertion using a sheath flow such that the posterior end of it faces the microneedle. Once oriented, they are pushed towards the needle which insert into them in a similar fashion as the previous device. Then the reagent is delivered into the embryo using a pressure pulse to the microchannel attached to the microneedle. The total time from loading and injection was 2s.

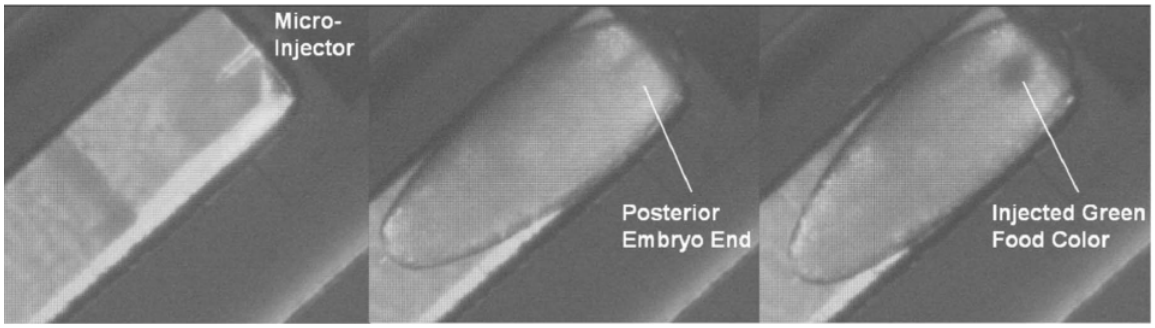

Figure 2. 11: Images of an embryo arriving at the injector and being injected with green food color[47].

To examine the effect of mechanical stress on embryo viability, they cycled the embryos inside the channels and subsequently stored under a 1 mm thick Klearol oil film in a humid environment (surrounded by water in a closed container). The results showed a survival of 93% of embryos. They used suppression of eGFP (Enhanced Green Fluorescent Protein) expression by a siRNA (Small Interfering RNA) that blocks it as a way of demonstrating injection efficiency. The embryos were monitored for about 4 (hr) post fertilization and they showed an injection efficiency of 25%. The device was suited for performing automated screens based on drosophila embryos as well as generation of transgenic drosophila lines. However, similar to the work done by Adamo et al [46], the length of the needle, which penetrates into the embryo, is constant. Therefore, the device is unable to inject the reagent into more than one location inside the embryo (selectively being able to inject into the different area of the embryo). Moreover, the design cannot be used for live organisms such as *C. elegans* and drosophila larva due to lack of the immobilization system.

Noori et al. [48] developed a simplified capillary microinjection system for zebra fish embryo by confining the injection needle to a single degree of freedom. Figure 2. 12a, shows the working principle of the design. A pulled microinjection needle (15 mm OD, 7.5 mm ID tip) is embedded into a channel collinear to the suction capillary. The device was fabricated by soft photolithography process and the reagent was accurately delivered with electroosmotic dosage control by using DC voltage in the range of 5-25 (V) corresponding to the flow rate of 3-14 (pL/s). The suspended embryo is immobilized by applying suction in a hollow glass capillary (1 mm OD, 0.5 mm ID), which is embedded

into a channel (1 mm wide, 1.5 mm deep) perpendicular to the target. The insertion of the microneedle is controlled via a compliant deformation of the PDMS substrate on two separated glass substrates – one fixed and the other moving in the range of 0-800 (µm). They injected Methylene blue solution by applying a 25 V potential for 10 s to the embedded electrodes to demonstrate the functioning of the device in four steps as shown in Figure 2. 12b.

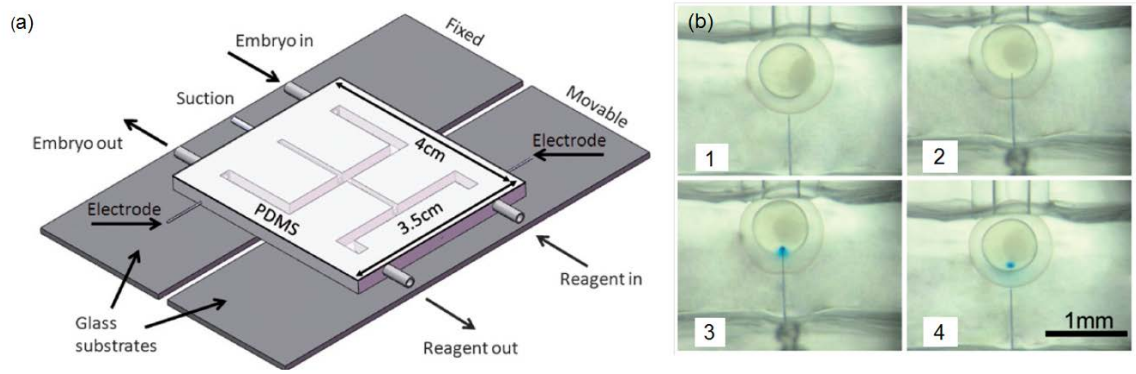

Figure 2. 12: Microinjection with electroosmotic flow control. a) the embryos are introduced through the "Embryo in" and then the suction channel is used to capture the embryo. Next, the needle was inserted into the embryo by moving the movable substrate. Subsequently, DC voltage applied to transfer the reagent into the embryo. b) Four steps of injection process 1) embryo capturing, 2) needle insertion, 3) reagent delivery and 4) needle removing [48]

The design is suitable for high-throughput microinjections with integrated pre- and post-processing operations. The injection mechanism is significantly simpler than current methods due to using a single degree of freedom for injections. However, similar to the works done by Adamo et al. [46] and Delubac et al. [47], the needle assembly requires

precise mechanism for manipulating the needle position to ensure that the tip extends into the channel at a given length. The design is suitable for injection into spherical shape target, but its immobilization system cannot be used for injection into live organisms such as *C. elegans* and drosophila larva.

2.3.4. Summary of the transfection methods

A summary of the advantages and disadvantages of transfection methods discussed in section 2.3.1 to 2.3.3, including chemical, biological and physical has been listed in Table.

Table 2. 1: Summary of the advantages and disadvantages of transfection methods

Class	Methods	Advantages	Disadvantages
Chemical	- Cationic polymer - Calcium phosphate - Cationic lipid - Cationic amino acid	- No viral vector - High efficiency - Easy to use - No package size limit - Lots of commercial - product are available	- Not always applicable for - *in vivo* transfection - chemical toxicity to some - cell types - Not possible to target - specific cell - Single method cannot be - applied for all cell types - For each method, the - efficiency varies with cell - type and conditions - No control on the dosage of delivery

Biological	Virus-mediated	- Easy to use - Applicable for in vivo - transfection	- DNA package size limit - Immunogenicity - Low efficiency - Insertional mutagenesis - No control on the dosage of delivery
Physical	- Ballistic particle delivery	- Simple, rapid and high - reproducibility - Low DNA consumption - Cell type independent - Can deliver single and - multiple genes as well as - large DNA fragments - without little - manipulation of cell	- Low efficiency - Expensive equipments - Cannot be used for internal - organs at *in vivo* transfection - No control on the dosage of delivery
	- Electroporation - Sonoporation	- Simple, rapid and high - reproducibility - High efficiency - Cell type independent - Fewer steps compared to - other physical method	- Hard to use for *in vivo* - transfection - Hard to target specific cell - Demands experimenter skill, - laborious procedure - No control on the dosage of delivery

- Microinjection	- Well-established - technique for in vivo - transfection - Simple principle and - independent of cell type and - reagent - Several types of reagents - can be injected in the - same time or in defined - sequences - The only method for - injection of specific - organs in *in vivo* - transfection with precise control on the dosage	- Expensive equipments - Slow process - Required skilled operators

From this survey, it can be found that capillary microinjection has a number of advantages over other methods, which make it an ideal method to deliver various reagents into a specific organ inside the model organisms such as *C. elegans.* However, the problems that need to be addressed to make it viable for clinical applications are low throughput, dedicated and complex procedure with expensive equipments.

2.4. Transgenic *C. elegans*

C. elegans worm is a model organism that is widely used in the study of disease processes and in drug discovery. It has a number of favourable attributes such as small size, rapid life cycle, fully mapped neuronal circuits and developmental process that make it suitable for these studies. Furthermore, is transparent body allows visualization of internal body structures, organs and cells that facilitate biological understanding of disease processes. These are studied typically using *in vivo* genetic regulation assays and high throughput molecular screens (HTS) or through behavioural studies such as chemotaxis, thermotaxis, mechanotransdutivity as well as electrotaxis where an external stimuli induces a behavioural response [56, 57]. A crucial part of these assays and studies is generation of transgenic worms that have particular genes up or down regulated so that they can be contrasted with the wild type in their functioning. Transgenesis is a relatively new technology that introduces control sequences such as RNAi that could potentially up or down regulated a gene present in the organism or genes external to the organism, artificially to create mutant species [1-6]. These methods are very precise and mutants with various genes knocked down have been developed to systematically study the influence of these genes in functioning of the animal. Transgenic species are typically generated by capillary microinjection of the worms and delivery of the RNAi or DNA into the gonad.

2.5. *C. elegans* microinjector

A typical microinjection setup currently used for generating transgenic C.elegans is shown in Figure 2. 13. It consists of 6 parts: (1) 40x optical lens, (2) three degree of freedom stage, (3) needle holder, (4) three degree of freedom needle actuator, (5) pressure driver and (6) needle actuator driver.

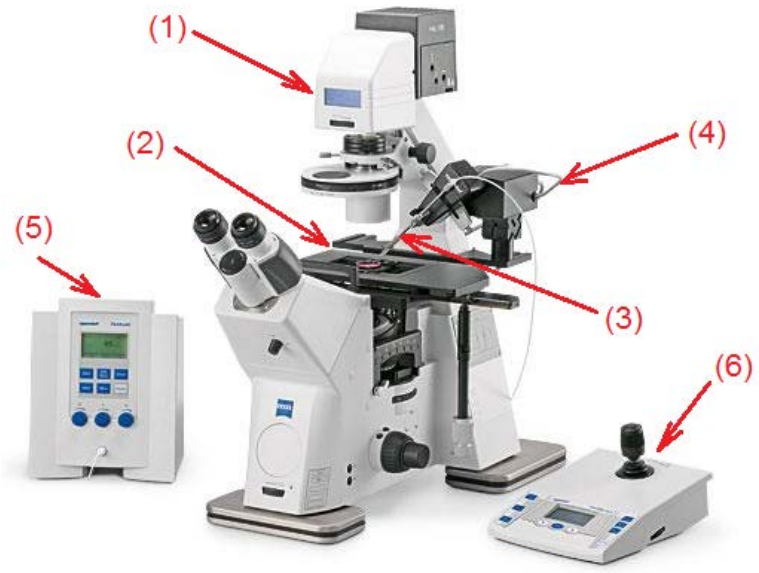

Figure 2. 13: (1) Inverted Microscope for Injections with 40x optical lens (2) three degree of freedom stage (3) needle holder (4) three degree of freedom needle actuator (5) pressure driver (6) needle actuator driver (Adapted from *eppendorfna.com*).

The simplest method for generating transgenic *C. elegans*, is to inject DNA that corresponds to the gene that needs to be expressed into the distal arm of the gonad (shown schematically in Figure 2. 14). The wild type adult worm have two gonads, each bent into a U-shape. As schematically shown in Figure 2. 14b, the adult ovary is

composed of a common compartment of cytoplasm containing multiple nuclei (syncytium). Oocytes are formed when plasma membranes enclose individual germ-line nuclei in close proximity to the bend in the gonad (Figure 2. 14). Therefore, in order to maximize the number of oocytes containing the genetic material of interest, injections are performed into the cytoplasm of the syncytium (Figure 2. 14c) [58]. The conventional microinjection method for creating transgenic worms has been described below.

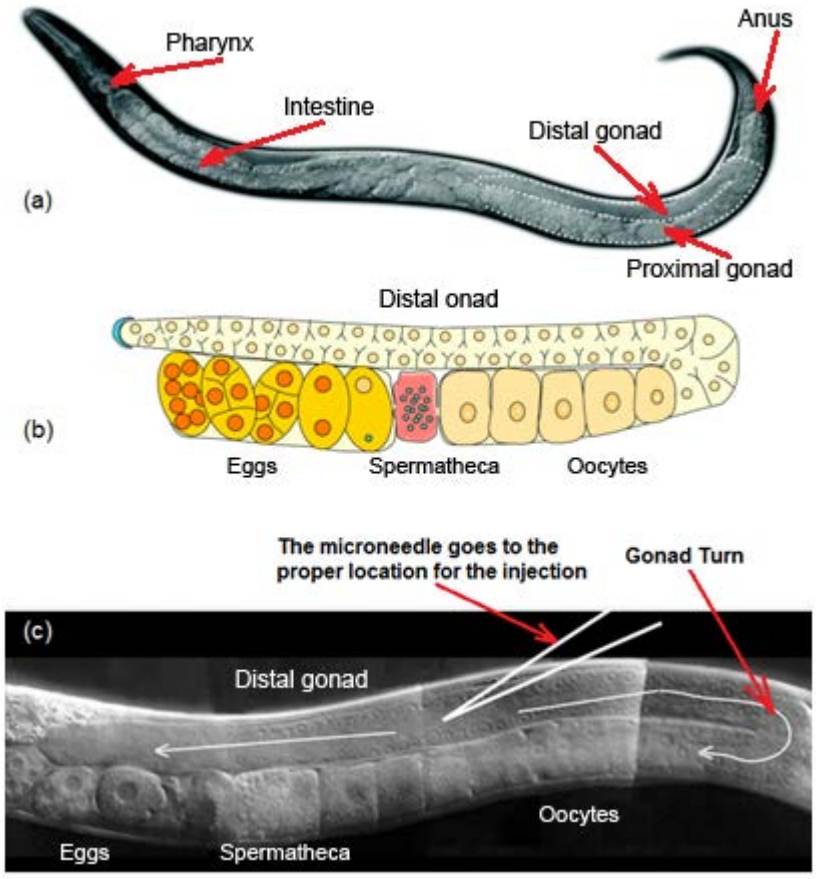

Figure 2. 14: The *C. elegans* reproductive system. a) The location of the U-shape gonad inside the worm. b) schematic of the gonad and its reproductive system ((a) and (b) from: *celldiv.com*). c) The proper location of the microinjection shown on the gonad (from: *wormbook.org*)

First, a drop of oil is spread on an injection pad and place under a dissecting microscope on top of a small Petri plate cover (Figure 2. 15a). Next, a healthy worm from a bacteria-free region of an NGM plate is picked with a naked pick and transfer to the oil drop (Figure 2. 15b). The function of the oil (Halocarbon Oil Series HC-700, CAS#9002-83-9, from Halocarbon Products Corporation) is to minimize the worm motion for needle insertion. Then, the microneedle (OD = 5 µm, ID = 3µm and taper angle of 88^{o}) is aligned and inserted into the target gonad (Figure 2. 15c). Afterward, the DNA is transferred into the gonad (Figure 2. 15d). The primary goal is to put as much of plasmid DNA in the gonad as possible so that the injected reagent reaches the gonad turn (shown in Figure 2. 14c). However, it is important to note that the optimal amount of injection is 200 pL. If a sub optimal amount is injected then the plasmid may not be integrated into the genome of the developing oocytes and the offspring worm will not express the gene. If a larger amount is injected then the internal pressure of the worm increases which could potentially be catastrophic to the worm causing death. Finally, the needle is removed from the gonad and the worm is plated on an NGM plate for recovery. In case of a successful microinjection, the next generation of the worms (progeny) will express the new gene as an extra chromosome in the worm genome, which usually is verified by GFP marker.

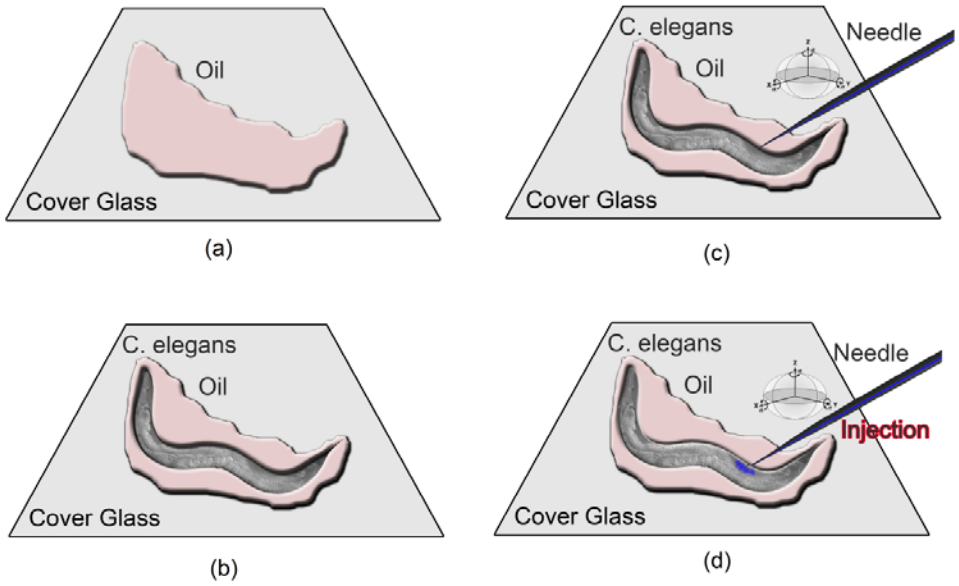

Figure 2. 15: Steps of *C. elegans* capillary microinjection

Microinjection is a well-establish technique for creating trasnsgenic *C. elegans* and its transfection efficiency is higher than two other transgenic methods (i.e. embryonic stem cell-mediated gene transfer and retrovirus-mediated gene transfer). However, the expensive equipment (e.g. high degree of freedom manipulator) and complex procedures (e.g. needle aligning) make the process time-consuming, slow and consequently inefficient and relatively difficult for high-throughput *in vivo* genetic/drug screen studies.

Recently, Zhao et al. [59] designed a microfluidic chip-based *C. elegans* microinjection system for investigating cell–cell communication *in vivo* (Figure 2. 16). The device consists of one inlet channel, twelve suction channels, one outlet channel and one open chamber as shown in fix-a. A buffer channel, S1 (contains suction channel with 20 µm width and 40 µ height) connected to the inlet channel (50 µm height and 80 µm width)

was designed to slow down the flow velocity of the worm at the exit of the inlet channel before immobilization process as shown in Figure 2. 16a. In addition, it prevents the worm from being loaded into main suction microchannels from head or tail. The main suction channel are used to immobilize the worm, while the channel S2 is designed to avoid the head (or tail) of the worm being inserted into immobilization channel. The open chamber, shown in Figure 2. 16a, allowed the microneedle to have access to the worm for injection.

The injection process consists of six steps. First, an adult worm was manually introduced into the inlet channel by using positive pressure (Figure 2. 16b). Next, channel S1 (see Figure 2. 16c) was used to capture one end of the loaded worm by suction, as it entered into the open chamber from the inlet channel. Then, the worm was completely immobilized against the sidewall by main suction channels. The other end of the worm was captured by channel S2 (Figure 2. 16d). Subsequently, the microneedle was inserted into the worm using an external micro-manipulator (similar to conventional method) and the single intestinal cell was microinjected with chemical agonist for stimulation (Figure 2. 16e). Afterward, the worm was loaded into the outlet channel by suction when the negative pressure on the main suction channels and channel S1 were released (one end was still caught by channel S2) as shown in Figure 2. 16f. Finally, to unload the worm, the negative pressure on channel S2 was released (Figure 2. 16g).

Their design was used for on-chip microinjection of *C. elegans* and investigation of intercellular calcium wave (ICW) propagations *in vivo*. They were able to immobilize the

worms for long-term (200 s) on the lateral immobilization system by applying suction. Using an external micro-manipulator, similar to conventional method, chemical stimulation was delivered to single intestinal cells of the immobilized worms by microinjection. This microfluidic platform can be a useful tool for studying cell–cell communication in multicellular organisms *in vivo*. However, using an external high degree of freedom (DOF) micro-manipulator for needle aligning and insertion still makes the process slow and consequently inefficient and relatively difficult for high-throughput *in vivo* genetic/drug screen studies.

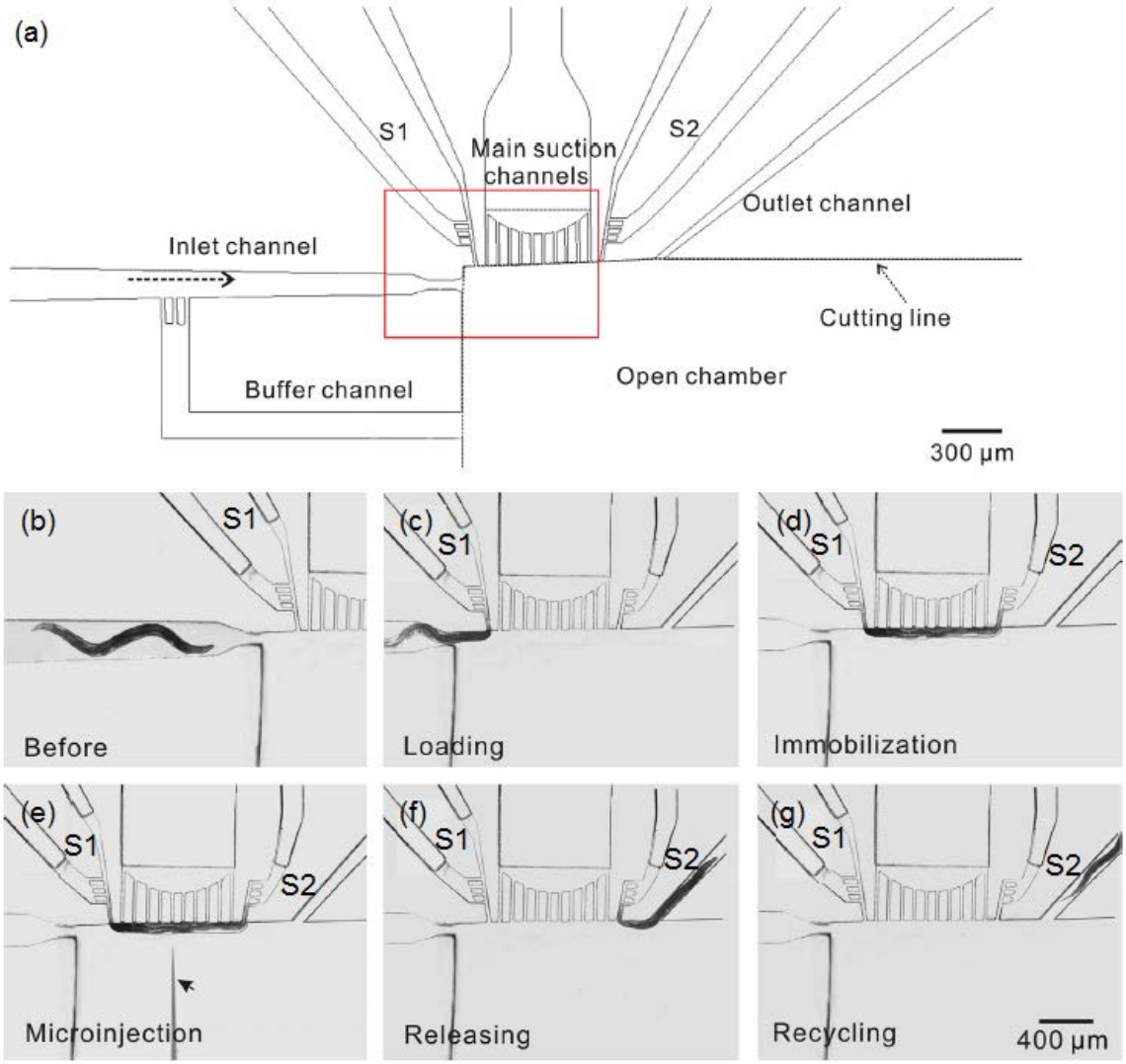

Figure 2. 16: Operation procedure for the microinjectionof *C. elegans* on the developed microfluidic chip. b) An adult worm was manually injected into the inlet channel by using positive pressure before immobilization. c) Once an end of the loaded worm was exposed into the open chamber, channel S1 caught this end of the worm by suction. d) After the rest of worm was completely pushed into the open chamber, the worm body was caught against the sidewall by main suction channels. The other end of the worm was caught by channel S2. e) The single intestinal cell was microinjected with chemical agonist for stimulation. Arrowhead indicated the glass capillary needle. f) The negative pressure on the main suction channels and channel S1 were released, the rest of the worm was loaded into the outlet channel by suction and the one end was still caught by channel S2. g) Negative pressure on channel S2 was released to evacuate the worm (adapted from Zhao et. al [59]).

2.5.1. Components of a *C. elegans* microinjection system

A typical *C. elegans* microinjection process is composed of four steps: (1) Worm immobilization, (2) worm and needle aligning, (3) needle insertion and (4) reagent transfer. The following section examines the critical factor involved in each steps. Various microfluidic systems have been developed to automate various unit operations for experimentation on *C. elegans* for behavioral studies and for neuronal imaging. However, there has been relatively little development in development of a microinjection system for *C.elegans*. In the following sections, some of the components that have been developed for worm handling in literature will be reviewed and their relevance and suitability for use in the microinjection system assessed.

2.6. Immobilization system

As described in section 2.5, high viscose oil is used in conventional *C. elegans* microinjection to immobilize the worm for needle aligning and insertion. Although, this process is simple to use and low cost, it is manual and slow; thus, it is not suitable for high-throughput microinjection. Various on-a-chip immobilization systems have been recently designed for high-throughput *C. elegans* subcellular-resolution imaging and laser microsurgery [60-67]. None of them have been used for *C. elegans* microinjection, while a few of the designs can be redesigned for this purpose. The designs can be divided in two categories; active and passive systems.

2.6.1. Active microfluidic immobilization systems

The active systems such as compressive immobilization, lateral suction and thermal immobilization, need external actively controlled actuation mechanism to keep the worm immobilized during the imaging.

2.6.1.1 Compressive immobilization

The principle behind this method is immobilization of *C. elegans* using an inflatable membrane that squeeze the worm in a cavity in order to halt undesired motion as schematically shown in Figure 2. 17a [60]. In this design, an elastic membrane is pressurized and it compresses the *C. elegans* against the walls of the channel to restrict its motion; consequently, the worm is immobilized and ready for imaging. The amount of membrane deflection is critical factor to define the dimension of the trap area which is function of the applied pressure on the membrane. The deflection of the membrane for the pressures air pressures from 0 to 35, 70, 105, 140 and 175 kPa have been shown by taking two-photon images of cross-sectional profiles of the microchannel in Figure 2. 17b. This design was used to immobilize the worm and then to perform femtosecond laser nanoaxotomy while minimally affecting the worm and can easily be automated to enable high-throughput genetic and pharmacological screenings as shown in Figure 2. 17c [60].

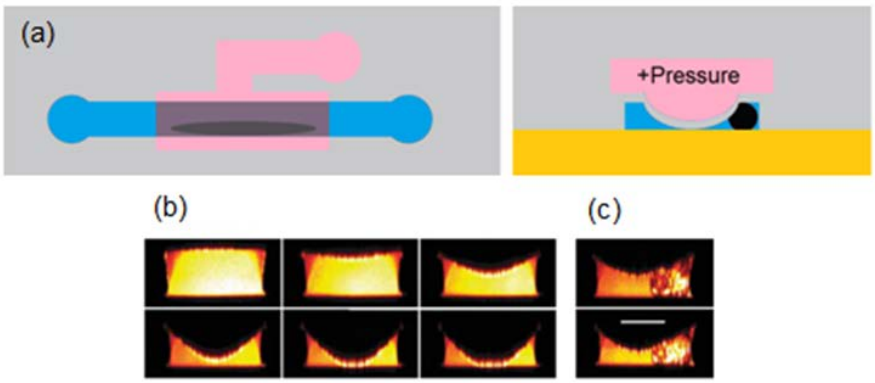

Figure 2. 17: Immobilization using a pressurized membrane. a) Schematic of the design: A thin membrane is flexed downward by the application of pressure through a microfluidic channel above the main chamber where a worm is captured. b) Two-photon images of cross-sectional profiles of the microchannel in the trap area for increasing air pressures from 0 to 35, 70, 105, 140 and 175 kPa. c) Cross-sectional two-photon images of a trapped worm at 105 and 140 kPa. Scale bars, 50 µm [60].

2.6.1.2 Lateral suction

The fundamental principle behind the method is that an array of microchannel, which are smaller than the cross sectional dimension of the worm are used to apply suction, capture and immobilize the worm body at multiple locations as schematically is shown in Figure 2. 18a. Rohde et al. [61] designed a microfluidic chip for high-throughput and rapid worm screening and imaging using lateral suction immobilization system (Figure 2. 18b). In this design, a single suction port, which enables capture and isolation of a single animal from a group and a channel array that linearly orients the captured worm by aspiration were developed [61, 52]. The author described that although, this design is capable of capturing and positioning a free worm into the microchannel, it could not fully immobilize worms for long-term studies and imaging as the suction channel dimensions

do not taper with the cross section of the worm at its different locations from head to tail. Therefore, another feature, a pressurized membrane, has been added to the design to fully immobilize the worm after capturing [61] . In Figure 2. 18c, a single worm is shown trapped by multiple suction channels with mec-4::GFP-expressing touch neurons.

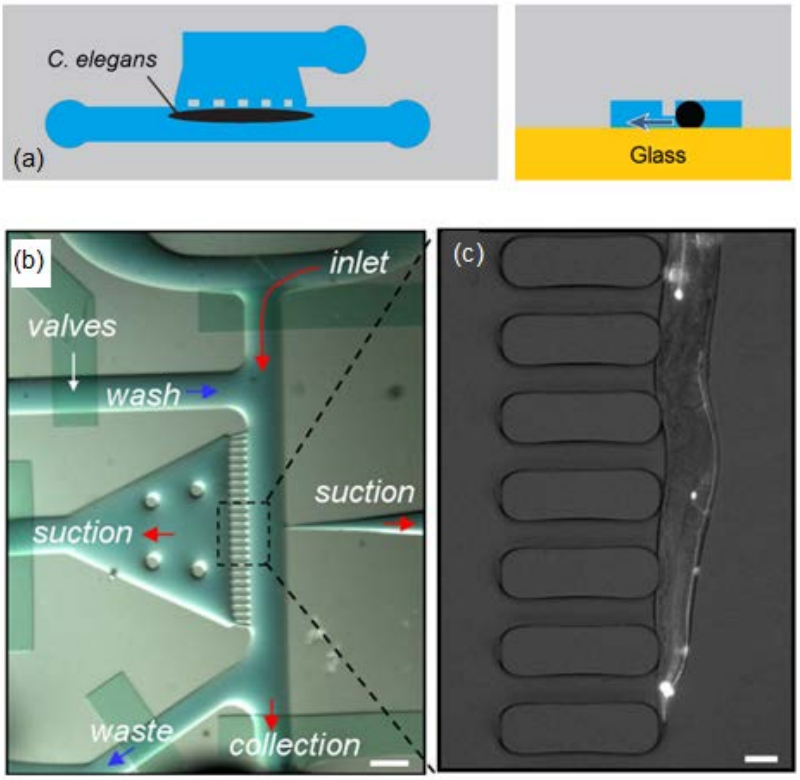

Figure 2. 18: Immobilization using a lateral suction. a) schematic of the lateral suction immobilization. A channel array is used to hold *C. elegans* linearly. b) Image of the on-chip sorter with its immobilization system (Scale bar: 500 µm). c) A single worm is shown trapped by multiple suction channels. A combined white-light and fluorescence image is taken by a cooled CCD camera with 6.5-µmpixels and a 100-ms exposure time through a *x10* magnification, 0.45 N.A. objective lens with (Nikon). mec-4::GFP-expressing touch neurons and their processes are clearly visible. (Scale bar: 10_m.) [61, 62]

2.6.1.3 Thermal immobilization

Another approach enabling immobilization of *C. elegans* in microfluidic channels uses cooling to stop animal motion. MacMillan et al. [63] found that an decrease in temperature reduces the locomotion of *C. elegans* on a Petri dish. Chung et al. [64], used this phenomena and fabricated a microfluidic device featuring a channel containing cooled liquid below a central imaging chamber as schematically shown in Figure 2. 19a. In this automated design as shown in Figure 2. 19b, the worms are loaded first into inlet channel. Next, similar to lateral suction technique, a single worm is positioned at proper location. Then, a cold fluid flow (~4°C) is used to reduce the temperature and immobilize *C. elegans* for imaging as shown by blue channel in Figure 2. 19b. Finally, the worms are sorted into two different groups based on the feedback taken from the experiment into outlet 1 or outlet 2. In Figure 2. 19b, the channels were filled with dye to show specific features: blue, temperature control channel; green, valves; and red, sample-loading channel. This allowed fast cooling of the animals for rapid analysis of gene expression patterns in freely moving animals and sorting of various phenotypes automatically. However, the worm is immobile it is not fixed in its location and can move about inside the wide channel. Therefore, this method of immobilization it will not provide enough mechanical support needed for needle penetration.

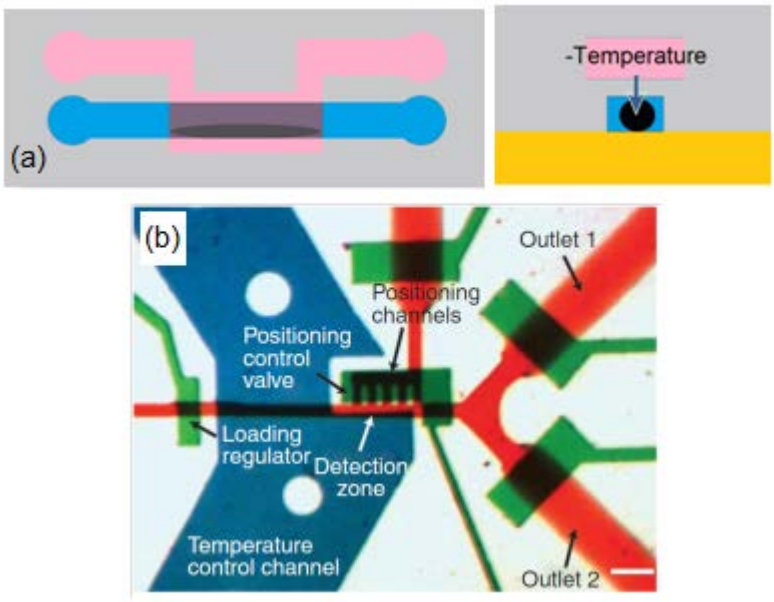

Figure 2. 19: a) Schematic of Immobilization using cooling. Cold fluid (~4°C) in the pink layer can be used to immobilize *C. elegans* in the blue layer. b) Optical micrograph of the microchip's active region (boxed region in c). The channels were filled with dye to show specific features: blue, temperature control channel; green, valves; and red, sample-loading channel. Scale bars100 µm [64].

2.6.2. Passive microfluidic immobilization systems

In contrast to active systems, the passive systems use the external sources to only trap the worm (as a trigger), while in the rest of the process, the system does not need external sources. Exposure to CO_2 and compression channel are two types of the passive microfluidic systems, which have been described in the following sections.

2.6.2.1 Exposure to CO_2

The in vitro experiment showed that the exposure to CO_2 immobilized *C. elegans* for long-term (1-2 hr) studies [65]. Chokshi et al. [66] demonstrated that the gas permeability of PDMS could be used to immobilize *C. elegans* in microfluidic format for high-throughput screening and imaging. In this method similar compressive immobilization (Figure 2. 20), CO_2 gas was diffused into the bottom chamber through the gas permeable PDMS membrane from a top channel and exposed to the chamber where the worm was placed (from the pink layer into the blue layer as shown in Figure 2. 20). One minute exposure to CO_2 immobilized the animals as it has been shown previously in non-microfluidic environments [65]. The CO_2 method offers the additional advantages of long-term immobilization (1–2 hours) and reduced photobleaching, if fluorescent imaging during immobilization is required. Moreover, post-immobilization worm locomotion speed analysis on a food-free agar showed that 1 (hr) immobilization by CO_2 could reduce the worm speed from 95 µm/s (the speed of the control sample) to 67 µm/s. Although, worm is immobilized robustly in this design and the lateral access to the gonad is feasible, the size of the worm is smaller than the size of the microchannels, and the immobilized worm is not held stationary into microchannel. Furthermore it will not have enough mechanical support for needle penetration.

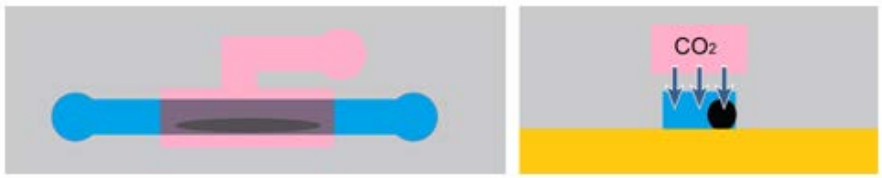

Figure 2. 20: Schematic of the immobilization system by CO_2. The gas permeability of poly(dimethylsiloxane) (PDMS) allows diffusion of CO_2 from the pink layer into the blue layer containing the animals, immobilizing them [66].

2.6.2.2 Tapered microchannel

All of the microfluidic devices for immobilization presented previously used microfluidic valves to control fluidic flow. Even though these valves offer fast and accurate control of flow within microfluidic channels, they imposed an extra complexity in device fabrication and operation that may be undesirable for certain experiments. Hulme et al. [67] introduced an a tapering microfluidic channel that used to compress the worms into narrowed channel and immobilize then, as schematically shown in Figure 2. 21a. The size of the narrowed channel is well-designed to passively halt the locomotion of the *C. elegans* and prepare it for imaging (see Figure 2. 21b). Moreover, a branched channel structure has been used to distribute animals among a 128 array of trap channels for high-throughput immobilization. This design allowed for passive loading and immobilization of multiple animals (Figure 2. 21). It is important to note that the lack of active control in this design prevents straightforward recovery of a specific animal within the array. Moreover, the recognition of the worm anatomy was difficult since the worm was squeezed in the narrowed channel and it distorted the anatomy of the worm.

In short, many on-chip immobilization systems have been recently designed for *C. elegans* subcellular-resolution imaging and laser microsurgery [62-65] which can be divided in two categories; active and passive systems. Tapered microfluidic channels (Figure 2. 21) are suitable for rapid and high throughput immobilization for the reason that they operates passively (does not need external source to keep the worm immobilized during the injection) in simpler manner and have simpler fabrication process . However, there are some issues with current passive immobilization methods. The primary of which is that the internal structures such as gonad are not clearly visible due to compression of the body in the lateral dimension. Therefore, using this design for an application that requires the visual observation of the internal organs (e.g. microinjection) might require modification of the channel design.

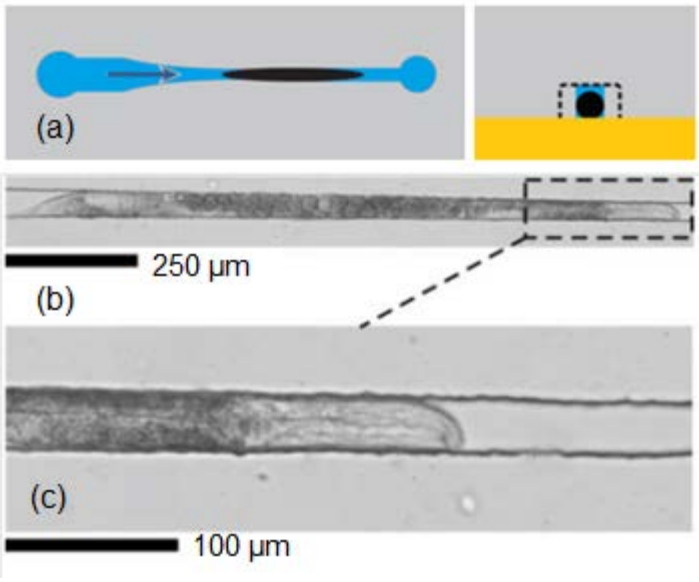

Figure 2. 21: a) Schematic of Immobilization via tapered channels. b) A tapered channel can passively immobilize *C. elegans* by flowing the animals toward a channel that gradually narrows in width [66].

2.7. Needle actuation

An actuator is required to accurately align and insert the needle into the gonad. Generally, three approaches have been applied to achieve this goal. In the first approach, the needle is directly connected to a micropositioner and actuated. For example, in conventional *C. elegans* microinjector, high precision hydraulic micromanipulators are specifically designed to perform this function (see Figure 2. 22). The micromanipulator is capable to provide high precision, low drift, smooth responsive motion, and long and reliable product life. However, this technique requires expensive multiple degree of freedom (DOF) manipulators, detailed injector alignment procedures and skilled operator which makes the injection process slow and not suitable for scaling to high-throughput.

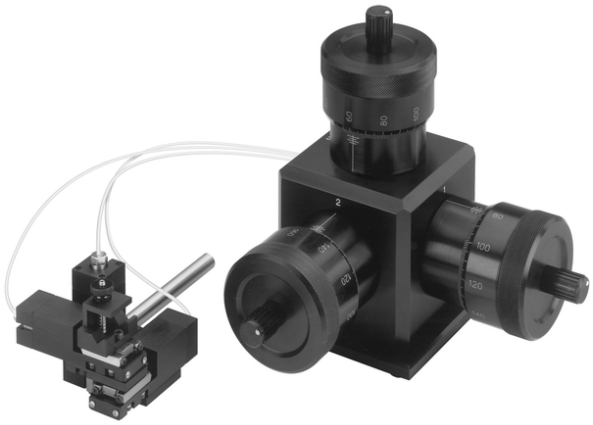

Figure 2. 22: Three degree of freedom micromanipulator used for c. elegans microinjection (updated from: *somascientific.com*)

In the second approach, the needle is fixed at a certain distance and the target cell or organism is pushed toward the needle by using fluid flow. Adamo et al. [46] and Delubac

et al. [47] used fluid flow to insert the fixed needle into cell and Drosophila embryo, respectively (Figure 2. 10 and Figure 2. 11). Consequently, the needle assembly requires precise mechanism for manipulating the needle position to ensure that the tip extends into the channel at a given length. The passive immobilized needle prevents active manipulation and position of the needle tip inside the cell or organism either pre or post injection and therefore may not allow operations that require delivery to specific cells or body locations as in transfection.

The third approach is needle actuation by using a compliant mechanism. Compliant mechanisms are well-established designs for microfluidic format microinjections. Noori et al. [48] actuated the needle insertion via a compliant deformation of the PDMS substrate on two separated glass substrates – one fixed and the other moving. They are single-piece structures and self-integrated with microchannels. However, micromanipulator is still required to actuate the mechanism. Many mechanisms have been designed in order to reduce the input to a single degree of freedom motion as described in the next chapter.

2.8. Needle-Tissue interaction

Needles are commonly used to cut the barrier tissues and connect the desired organ to the reagent chamber. As noted previously, tissue damage is one of the critical problems involved in capillary microinjection. In order to minimize damage a careful study of the

interaction of the needle with the membrane/tissue is needed. A number of variables e.g. insertion method, needle characteristics, and tissue characteristics, influence the mechanical interaction between needle and biological tissue and consequently the amount of tissue damage that arises as a result [68]. Theoretical models that describe the interaction between needle and tissue, in terms of loads and displacements, has developed in recent years [69-71]. However, experimental data from needle insertions into living biological tissue are rather difficult to come by due to both practical and ethical reasons.

2.8.1. Influence of insertion method

Generally, the needle insertion is composed of three phases, which can be distinguished by the position of a needle relative to a tissue boundary as shown in Figure 2. 23 [68].

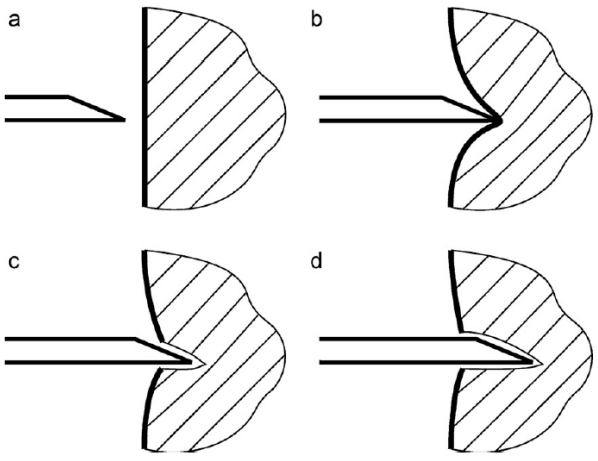

Figure 2. 23: Basic phases in needle insertion: a) no interaction; b) boundary displacement; c) tip insertion; d) tip and shaft insertion [68].

Initially in the insertion process, the tissue boundary deflects due to the load applied by the needle tip, but the needle tip does not penetrate the tissue, which is called “tenting” and is shown Figure 2. 23b, f [68]. When the stress caused by the tip of the needle is increased above a certain critical value, the relative velocity between needle and tissue boundary starts to increase (indicating that puncture has occurred) and a crack will be initiated in the tissue and the needle will begin to penetrate into the tissue [72]. Subsequently, in the second phase (tip insertion), the tip of the needle penetrates into the tissue and the cross-sectional area of the tip is increased Figure 2. 23c. Consequently, the cut made by the sharp edges of the tip is wedged open and the crack in the tissue-boundary is enlarged [73], which can cause two types of the crack growth process known as cutting (gradual, stable crack growth) and rupture (sudden, unstable crack growth). Once the crack is initiated, in the third phase (tip and shaft insertion), the contact area between tip and tissue and the size of the hole at the boundary almost remains constant. Only the contact area between shaft and tissue increases as the needle penetrates more into tissue. Cutting (or rupture) and friction forces, are two forces which act on the needle during this phase. During this phase, the force on the needle originates from two sources: the needle is subject to cutting (or rupture) forces at the tip, and to a varying friction force that is due to the increasing contact area between shaft and tissue [74].

2.8.1.1 Insertion velocity

Insertion speed affects the puncture force (i.e. force required to initiate cutting) and frictional force during needle penetration in biological tissue [75, 76] . It was observed

that the puncture force decreases and friction force increases with increasing insertion velocity, however, the strength of these effects depends on the type of tissue. Heverly and Dupont [75] found that the puncture force decreased with increase in velocity up to 75 mm/s when a 19 G (ID/OD = 0.69/1.07 mm) diamond tip needle was inserted into porcine heart (epicardium and myocardium), ex vivo. The puncture force was velocity independent at higher speeds (75-250 mm/s). They concluded that the cutting force and tissue displacement could be minimized by maximizing velocity. Another investigation performed by Mahvash and Dupont [76] found that the beveled needles also show similar behavior. In the case of microneedles, Rousche and et al. [77] found that the skin deformation, which has direct correlation with puncture force, could be reduced by increasing insertion velocity. In the experiment, a 10x10 array of needle-shaped electrodes (1.5 mm length, diameter of 80 µm at its base and tapers to a fine point at the tip) was inserted into feline cortex by using a pneumatically actuated impact insertion system at speeds from about 1 to 11 m/s. The minimum array insertion speed of 8.3 m/s was necessary for a complete insertion of all 100 electrodes in the array to a depth of l.5mm into the tissue. However, the dimension of the tip has not been reported in the study. Consequently, despite the size of the needle, the amount of force needed to cut a path and consequently the amount of tissue damage can be reduced by increasing the insertion velocity. However, by increasing the insertion velocity, it will be difficult to control the depth of the insertion and there would be optimize condition between maximum velocity and the capability of the insertion control system (either manual or automatic).

2.8.1.2 Axial rotation

The axial rotation of the needle during insertion can affect both tissue displacements prior to puncture as well as the frictional force generated during puncture [78-80]. Abolhassani et al. [78] found that axial rotation typically reduces the friction force in chicken breast by up to 10%, which leads to less tissue damage. The method was based on insertion of 18 G beveled needles at a constant translational velocity of 10 mm/s with rotational frequencies ranging from 0.02 Hz–0.42 Hz (1 rpm to 25 rpm) for both continuous rotation and rotational oscillation with amplitudes of 10^{o}, 30^{o}, and 90^{o} for each frequency. Meltsner et al. [79] found that the total axial force in porcine gel and in beef has been decreased by up to 50% by inserting 17 G beveled needles and 17 G conical needles into porcine gel and into beef phantoms. Langevin et al. [80] found that rotation of acupuncture needles before pull-out (needle grasp) increased pull-out force up to 150% in live human skin. Consequently, needle axial rotation is reduced the friction force as well as cutting force, which corresponds to less tissue damage. However, needle rotation might be difficult to imply in microscale device because of complexities involved in fabrication process.

2.8.1.3 Insertion location and direction

The location at which the needle is inserted and the direction of needle insertion with respect to the tissue are critical factor for a thorough understanding of needle–tissue interaction mechanics since biological tissue is typically inhomogeneous and anisotropic.

Both experimental and numerical data related to effects of insertion location or direction on mechanical response of the tissue (axial, frictional force, pull-out forces and etc) are limited. Only, Suzuki et al. [81] explored the effects of insertion angle (30^o and 45^o) on axial force and hole shape during penetration of a polyethylene membrane by two catheter tips with different multifaceted bevels ("Lancet" and "Backcut") at 3.3 mm/s (20 insertions per condition). The result shows that axial force at 30^o was significantly lower (approx. 40%) than for 45 only for the "Backcut" type. Consequently, the insertion angle is a critical factor for tissue-damage mechanism and at certain angle (for specific tissue) it may cause minimum tissue damage.

2.8.2. Influence of needle characteristics

2.8.2.1 Diameter

The outer diameter of the needle can affect the puncture force. Podder et al. [82] showed that puncture force increased with corresponding increase in diameter of diamond tip needles from 17G to 18 G (ID/OD = 1.27/0.84) in both human tissue (clinical procedures on 20 patients -10 patients per needle size, with a total of 52 insertions) and in silicone rubber. Okuno et al. [83] obtained the same conclusion for the slope of the force-position curve (which represents the frictional force) in silicone. In addition, Okamura et al. [84] and O'Leary et al. [85] observed that increased diameter is aggravated the effect of tip type in silicone rubber. In the microscale, Davis et al. [86], used individual hollow metal microneedles (tip radii of 30 –80 µm, wall thicknesses between 5 µm to 58 µm (solid

tips) and length of 500 µm) were inserted into the skin of human to examine the effects of the area of needle tip (effect of the outer diameter) on the insertion force. The results showed that despite the thickness of the wall, the insertion forces varied from 0.1 to 3.0 N and have an approximately linear coloration with the area of the needle tip, which can be defined as sharpness. Consequently, to minimize the tissue damage, the needle diameter should be as small as possible. However, decrease of needle diameter will increase the required pressure to drive flow through the needle.

2.8.2.2 Tip type

The tip of the needle is used to create a passage through tissue. As described in section 2.8.1, the insertion is typically a combination of cutting and wedging phenomena. The amount of force needed to cut a path and consequently the amount of tissue damage, depend on the shape of the needle tip. The most common needle tip shapes are depicted in Figure 2. 25 [68].

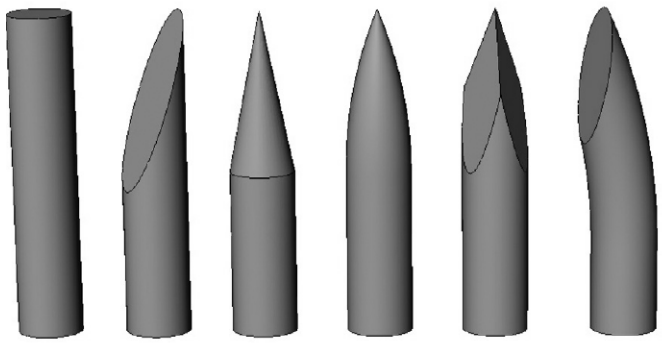

Figure 2. 24: Basic needle tip shapes (left-to-right): blunt, beveled, conical, Sprotte, diamond (Franseen), Tuohy [68].

It has been observed that conical needles diamond tip trocar needles generate higher peak axial force compared to beveled needles during insertion into biological tissue.

Westbrook et al. [87] showed that conical needles created higher peak axial force than multifaceted bevel needles by manually inserting into excised bovine dura. (For various needle sizes and with bevel parallel to the fiber direction). Mahvash and Dupont [76] compared the peak axial force between diamond tip needle and beveled needle by inserting 19 G (ID/OD = 0.69/1.07 mm) diamond tip trocar needles and 18 G (ID/OD = 1.27/0.84) beveled needles into porcine heart ex vivo at a wide range of velocities. They observed that the diamond tip needle generated a peak axial force roughly twice as high as for the beveled needle, regardless of its smaller diameter compared to bevel needle.

Okamura et al. [84] examine the effects of the number of the cutting edges on slope of the force-position curve (which defines the friction force during insertion). They showed that friction force during insertion (represented by the slope of the force-position curve) decreases with increasing number of cutting edges (conical beveled diamond) in silicone rubber and was increased by increase in needle diameter.

In the microscale, Davis et al. [86], used individual hollow metal microneedles (tip radii of 30 –80 μm, wall thicknesses between 5 μm to 58 μm (solid tips) and length of 500 μm) were inserted into the skin of human to examine the effects of tip on the insertion force. The results also indicated that irrespective of the outer diameter, thin-walled hollow needles (5μm thickness) and solid needles (58 μm thickness) with the same outer diameter at the tip required the same insertion force. Therefore, for hard tissue, which

cannot dimple into the needle bore during the insertion, the wall thickness does not play significant role in tissue damage mechanism.

Therefore, bevel needles generate less peak axial force, less tissue damage as a result compared to other needle types. However, their fabrication in microscale devices would be more complex rather than conical needles, which can be easily produced by various techniques such as pulling and wet etching.

2.8.2.3 Lubrication

The effect of the lubrication on peak axial force is significant on artificial material regardless of the type of the needle [68]. Lubrication decreases the peak axial force and tissue damage as a result. Systematic studies on the effect of lubricants in insertion into biological tissues have not been performed. However, it has been hypothesized that the moisture released due to cutting of biological tissue may serve as lubricant [68].

2.9. Reagent delivery

Two different methods have been used for reagent transport in microinjection devices. These are capillary pressure microinjection (CPM), which uses pressure driven flow (PDF), and electroosmotic flow (EOF), which is caused by the movement of charge within the fluid, for reagent transport. CPM is a well established and the simplest technique to inject a wide range of substances, including naked DNA, RNA, antibodies

and nanoparticles into cells with high transfection efficiency (up to 100%) and low cytotoxicity [88, 89]. The delivered volume is determined by the magnitude and duration of the applied pressure pulse. However, precise volume control remains a problem and the reagent delivered into cells may vary by a factor of 5 or more, resulting in significant variability and low reproducibility [89]. The use of pressure for injections imposes limitations on CPM. When the diameter of the needle is decreased (to avoid tissue damage and increase the cell viability [90]), the required pressure to push reagent through is increased non linearly. Notably, current CPM tools are at their limit (diameter > 0.2-0.5 μm) due to the high pressures needed to dose using nanoneedles which is beyond the ~500-600 kPa range of commercial systems.

Using electroosmotic flow (EOF) technique for reagent transport, solves some of the problems related to pressure driven flow. In this method, one of the electrodes is the injection needle and the other electrode is the medium in which the cells are growing. Application of an electric field leads to transport of the charged molecules in the fluid filling the needle, such as the DNA and proteins, through the needle and into the cell. The technique allows the use of smaller injection needles since it does not use pressure for reagent transport. The flow velocity for electroosmotic flow (EOF) injection at steady state can be determined by [91] :

$$v_x = -\frac{\varepsilon_\omega \varepsilon_0 \zeta}{\eta} E_x \qquad (2\text{-}1)$$

Where, $\varepsilon_0, \varepsilon_\omega, \zeta, \eta$ and E_x are the dielectric permittivity of a vacuum (ε_0 = 8.854 × 10^{-12} C/Vm), the local relative dielectric permittivity (or dielectric constant) of the liquid, zeta potential, viscosity and applied electric field strength across the channel, respectively. According to the equation, electroosmotic flow (EOF) depends only on applied electric field and the properties of the fluid. While, the flow rate in the pressure injection depends on applied pressure, tip diameter and taper angle, consequently, variations between pipettes can result in significant variations in output. It is, however, independent of the chemical properties of the reagents to be delivered. One of the disadvantages of electroosmotic flow (EOF) is that the rate of delivery of reagent is slow as compared to the pressure injection. Furthermore, it is difficult to quantify the actual flow delivered to the cells due to diffusion and efflux from the pipette tip, which needs to be balanced by the application of a retaining current [92].

2.10. Summary

This chapter provided an overview of existing cell transfection methods, introduced microfluidics and microfluidics based injection systems. It was concluded that capillary microinjection has a number of advantages over other methods for creating transgenic *C. elegans*. However, the problems that need to be addressed to make it viable for low cost

and high-throughput applications are expensive multiple degree of freedom (DOF) manipulators, detailed injector alignment procedures and slow immobilization mechanism.

Chapter 3: Conceptual Design

3.1. Introduction

As described in previous chapter, *Caenorhabditis elegans* worm is a well-developed model organism for neurobiological and drug discovery studies. Microinjection is an established and reliable method to deliver transgenic constructs and other reagents to specific location inside the worm [58]. However, current methods of microinjection into *C.elegans* which operates in free space, requires expensive multiple degree of freedom (DOF) manipulators, detailed injector alignment procedures and skilled operator, making the injection process slow and not suitable for scaling to high-throughput. These problems of throughput and equipment costs can be addressed by the application of microfabrication and microfluidic technology. Although many microfabricated microinjectors exist [43-48, 59], none of them is capable of immobilizing a freely mobile animal such as *C.elegans* and perform microinjection by using a simple and fast mechanism for needle actuation. Such an automated design, will allow high-throughput microinjection that could be used for drug discovery assays. Through this process, active molecules, antibodies or genes, which modulate a particular biomolecular pathway, can be identified quickly. This chapter describes the design criteria, conceptual design and design layout of a microinjection device, which can simultaneously immobilize worms

and inject reagents via a simple injection mechanism and is amenable for high throughput microinjection .

3.2. Design Criteria

Capillary microinjection adapted to a microfluidic format was determined to be appropriate for this application based on the survey of literature presented in the previous chapter. An automated microinjection device will require (i) a loading and immobilization system to position the worm at the appropriate location, (ii) an actuation mechanism to move the injection needle into the worm and (iii) a reagent delivery system to deliver precise amounts of reagents into the injected location.

3.2.1. Loading and immobilization system

Loading channel is required to transfer the *C. elegans* worms from their culture plate on which they are grown to the injection zone. The primary design criteria for the loading channel is that its dimensions should facilitate the transport of worms while not damaging them in this process. In addition, it should be able to sequence the worms such that only one worm can reach the immobilization region at one time. The length and diameter of the young adult *C. elegans* is 45 µm and 1000 µm, respectively and it has in-plane sinusoidal swimming pattern with the amplitude of 100 µm. Therefore, loading channel dimensions in the range of 200 µm to 400 µm in width and 50 µm to 100 µm in depth

would be suitable and would facilitate easy and damage free transport of worms while also sequencing them into a file for immobilization.

A young adult *C. elegans* worm is a live and mobile animal. The primary design criteria for immobilization are that it should be simple and fast to operate and fixes the position of the body and various internal organs of the worm for injection. Additional criteria include that the immobilization system does not damage the worm and allows visualization of the internal organs of subsequent injection. The immobilization process should happen as quickly as possible and a typical time of ~1-2 min is acceptable. In order to avoid dehydration of the *C. elegans* worm during microinjection, the humidity and temperature should be approximately in the range of $20^o\ C < T < 25^o\ C$ and $90\% < \Phi < 100\%$, respectively.

3.2.2. Needle Actuation Mechanism

3.2.2.1 Needle Tip Size

The function of needle tip is to create a passage through the tissue in which it is inserted. The shape of the tip and its size (inner and outer diameter at the tip) play significant roles in tissue-needle interaction and tissue damage. The primary design criterion is that the size of the needle tip should be a small fraction of the worm size to minimize tissue damage while being large enough to allow easy delivery of reagents. Since, the diameter of a young adult *C. elegans* worm is ~45 μm, a needle tip that is $1/10^{th}$ its size would be a suitable compromise. Indeed, the typical needles used in conventional microinjection are

approximately 3 µm. Therefore, needles with tip sizes in the range of 3 µm to 6 µm can be considered suitable.

3.2.2.2 Capillary size

Conventional capillaries used in microinjection have OD of 1000 µm and ID of 500 µm. However, these capillaries are too large for integration with microfluidic devices where the channel dimensions are 50-100 µm. Therefore, fused silica microcapillaries that are used in high performance liquid chromatography are investigated here for use as microneedles. These microcapillaries are available in a variety of sizes from 90-600 µm. In order to match with the device dimension and for successful integration, microcapillaries with OD of 90 um were chosen.

3.2.3. Needle Actuation

The goal of the microinjection is to inject biomolecules into the gonad of the worm, when it is immobilized. The gonad of *C. elegans*, is cylindrical in shape with the diameter and length of 20 µm and 200 µm, respectively as shown previously in Figure 2. 14. Therefore, the actuation mechanism employed for the needle movement should have the resolution of at least 5 µm ($1/4^{th}$ of the size of the gonad) for successful insertion. Moreover, the range of the needle motion should be at least as large as 400 µm along the

gonad (2 times of the gonad length) and 100 µm across the gonad (2 times of the gonad diameter) to fully span the gonad during the injection.

3.2.4. Reagent delivery

A typical worm at its prime reproductive stage has a volume of ~ 1.4 nL. In conventional microinjection, injected volumes are ~ 15% (200 ± 20 pL) or more of the worm's body volume. Since close to 100 worms are injected in each batch, this amounts to a total reagent volume of ~20 nL is needed. Therefore a storage capacity of ~ 1-1.5 µL would be sufficient given a reasonable dead volume of the system.

3.3. Device Layout and Working Principle

The microfluidic microinjection device, designed here is composed of five parts: Loading, immobilization, needle actuation mechanism, reagent delivery and unloading system as shown in Figure 3. 1. First, the young adult *C. elegans* worms are transferred from the agar plate to the device via the loading system (Figure 3. 1, step 1). A passive immobilization mechanism (narrowed channel) is used to trap and immobilize the mobile worm for needle insertion (Figure 3. 1, step 2). Once the worm is immobilized, the injection needle is precisely moved into the worm for delivery of the reagents by using a single degree of freedom (DOF) compliant mechanism coupled to a micropositioner (Figure 3. 1, step 3). Then, the reagent is delivered into the gonad of the worm via a

capillary pressure microinjection (CPM) technique, which uses pressure driven flow (PDF) (Figure 3. 1, step 4). Finally, the worms were transported to the outlet chamber via a M9 buffer from washing channel to outlet chamber, and then worms were plated on agar plate using a micropipette (Figure 3. 1, step 5). This section explains the working principle and design parameters for these five steps.

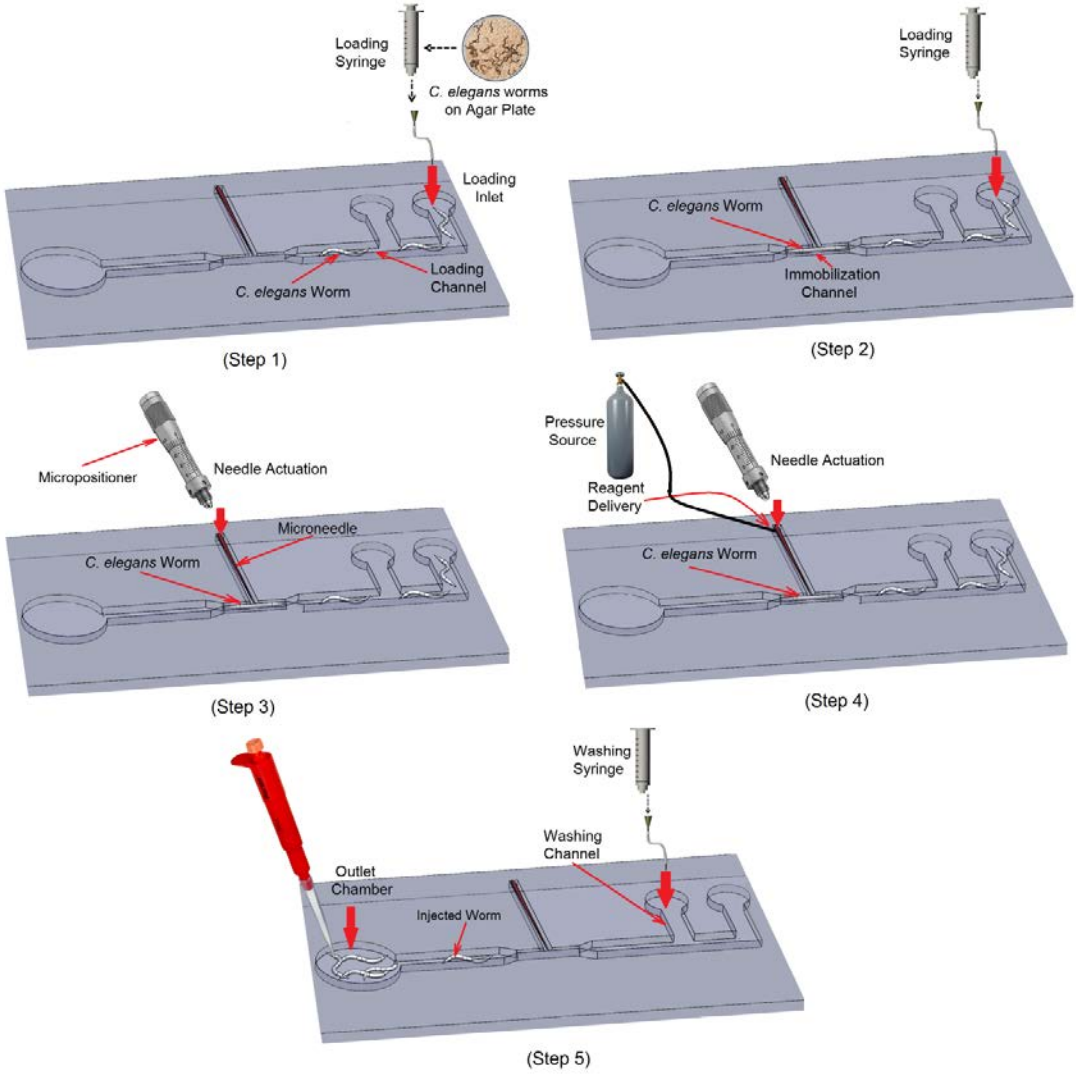

Figure 3. 1: Schematic sequences of the conceptual design. Step 1: Loading, Step 2: Immobilization, Step 3: Needle actuation, Step 4: Reagent delivery and step 5: unloading

3.3.1. Worm Loading System

The young adult *C. elegans* worm is mostly cultured on agar plate. Thus, a method was required to transport the worms from the agar plate into microchannels. To do this, a loading system consisting of two syringes, flexible plastic tubes and the microchannels on the microfluidic chip was designed (Figure 3. 2).

Initially the worms are washed and transferred from the agar plate into a syringe, which is attached to the inlet of the device. Next, the worms are introduced into the device by pressurizing the syringe by using a pressure source as illustrated in Figure 3. 2.

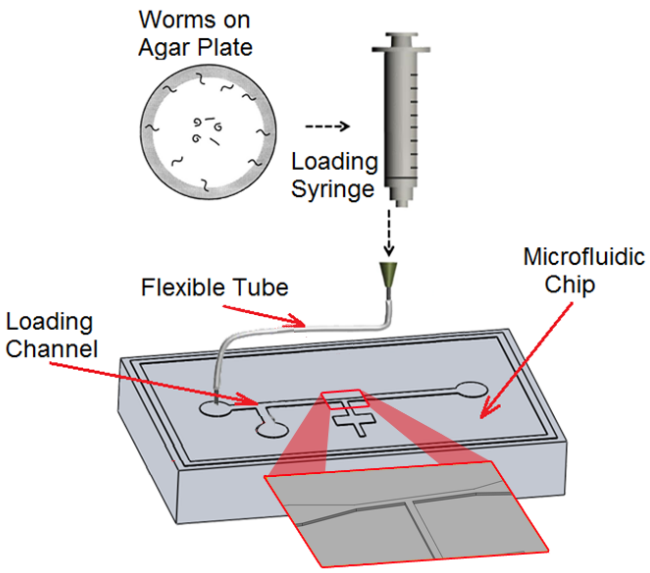

Figure 3. 2: Schematic of loading system. Worms were washed from agar plate and transferred into syringe. Then loading syringe and washing syringe were connected into loading channel via the plastic tubes.

According to design criteria described in section 3.1, the width and depth of loading channel was defined to be 300 µm and 65 µm, respectively. The reservoir diameter was

set as 3 mm and the inner and outer diameter of the flexible tube (ID of 1/32” and OD of 3/32”) was chosen. To transfer the worms to the tube, a 3 mL syringe was selected which is controlled by a constant pressure source.

3.3.2. Worm Immobilization

An immobilization mechanism was required to trap and immobilize the mobile young adult *C. elegans* worm for needle insertion, after loading the worm into the device. As described in previous chapter (section 2.6), many on-chip immobilization systems have been recently designed for *C. elegans* subcellular-resolution imaging and laser microsurgery [1-3] which can be divided in two categories; active and passive systems. In this design, tapering microfluidic channels (the schematic of the shown in Figure 3. 3a), a passive system, suitable for rapid and high throughput immobilization was selected as it is simple to operate and easy to fabricate. Furthermore, the process does not need an external source to keep the worm immobilized during the injection. However, there are some issues with current passive immobilization methods. The primary of which is that the internal structures such as gonad are not clearly visible due to compression of the body in the lateral dimension. A visual comparison between a free mobile *C. elegans* worm and immobilized worm is shown in Figure 3. 4. It can be clearly seen that the internal structures such as gonad are not distinguishable in the passive immobilized worm due to compression of the body in the lateral dimension. Therefore, a number of

redesigns for passive immobilization were developed that will simultaneously allow visualization of internal structures of the *C.elegans*.

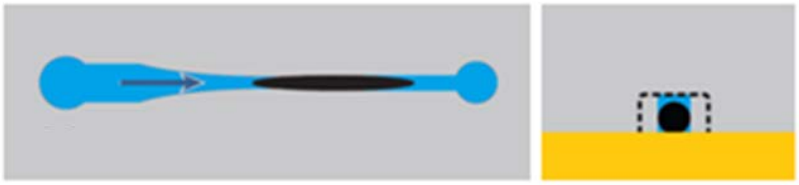

Figure 3. 3: (a) Schematic of imobilization via tapered channels. A tapered channel can passively immobilize *C. elegans* by flowing the animals toward a channel that gradually narrows in width

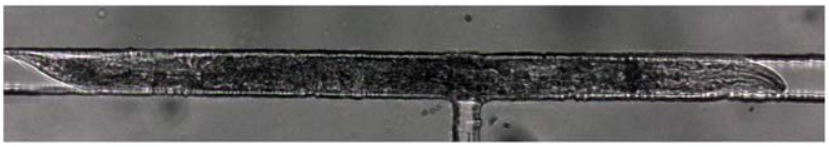

(a) *C. elegans* in narrowed Channel

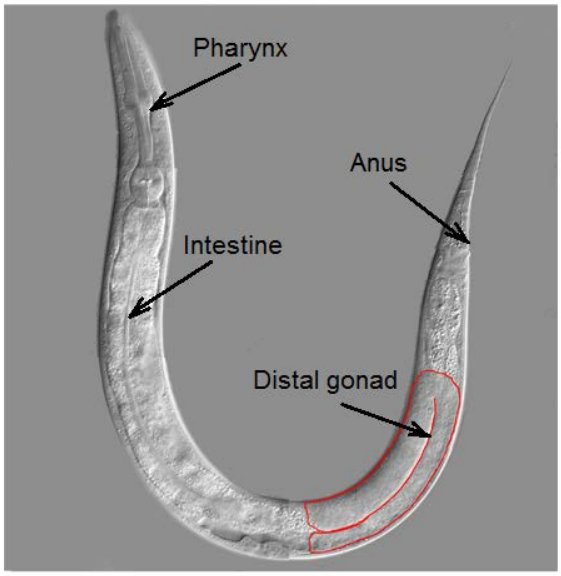

(b) Free mobile C. elegans

Figure 3. 4: a) *C. elegans* worm inside the immobilization channel. The internal organs such as gonad is not clear in this design in compared to b) a free mobile *C. elegans* (up dated from: *www.elvesys.com*)

3.3.2.1 Single Layer vertical compression Immobilization

Vertical compression of the worm using a narrow channel (25 µm width and 70 µm depth) as it is conventionally done for passive immobilization, packs all the anatomical features of the worm into a small area and make visual recognition of the gonad very difficult (Figure 3. 3b). Initially, designs with larger widths (30, 35, 40 and 45 µm) which produce lesser compression were designed to improve visualization of the gonad and yet achieve immobilization. Although this design improved visualization of the gonad, it was not able to capture the worm consistently due to the increased width.

3.3.2.2 Single Layer Horizontal Immobilization

Unlike in the previous design, where the worm was compressed from the sides (right and left), in the new design, it was compressed from top and bottom via a narrowed channel with 25 depth and 55 µm width as shown in Figure 3. 5. This design was successful in fully immobilizing the worm for large durations of time (more than 10 minutes) as well as in enabling clear visualization of the gonad for microinjection. However, this new geometry misaligned the compressed section of the worm from the needle tips. The depth of the narrowed channel was uniformly 25 µm from the top; while, based on design criteria, the depth of the needle channel was more than 55 µm in order to accommodate a 90 um capillary. Consequently, the central axis of the immobilization channel and needle channel was not in the same plane, which might create condition where the needle could

be inserted into PDMS layer (the PDMS layer under immobilization channel) instead of worm.

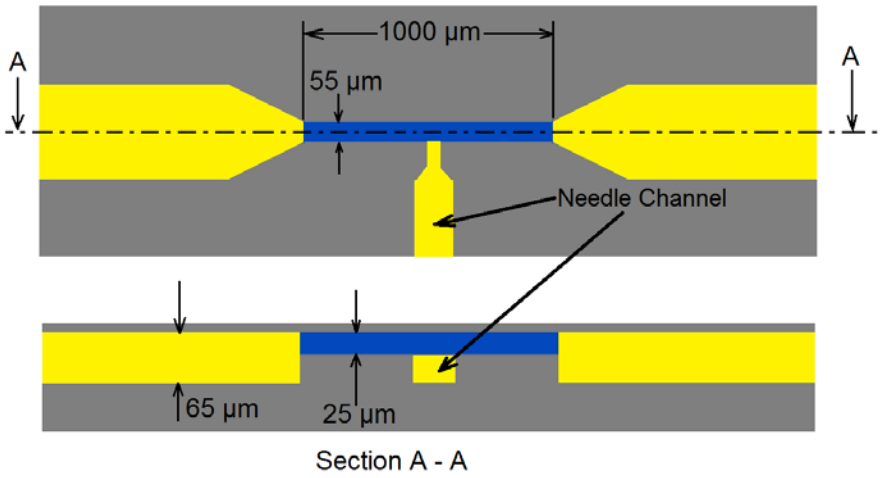

Figure 3. 5: Modified trapped channel for *C. elegans* immobilization. In contrast to previous design [5], C. elegans was squeezed from top and bottom via a narrowed channel with 25 depth and 55 µm width.

3.3.2.3 Two Layer Horizontal Immobilization

In order to retain the advantage of passive immobilization by compression from top and bottom via a narrowed channel as well as to allow centering of the worm for microneedle insertion, a new hybrid design was developed. In this design, the narrowed channel had 25 µm depth with 55 µm width. However, the depth in the middle section of the immobilization channel, called as “injection area”, had a length of 100 µm and a depth of 65 µm (Figure 3. 6). The narrowed portions of the immobilization channel would allow easy visualization of the internal organs as well as allow consistent immobilization as shown in Figure 3. 8. While the enlarged region at the center, will allow centered injection as shown in Figure 3. 7.

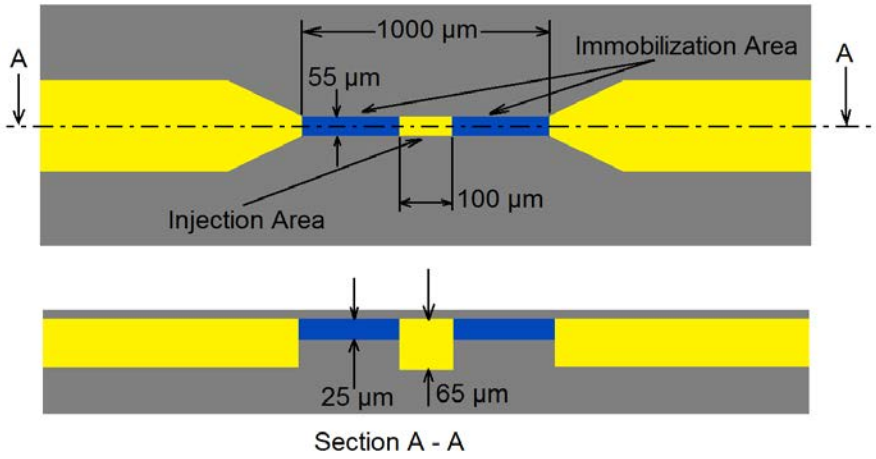

Figure 3. 6: The final design of the immobilization system. the narrowed channel had 25 µm depth with 55 µm width. The depth in the middle of the narrowed channel with length of 100 µm was increased to 65 µm where called as “injection area”.

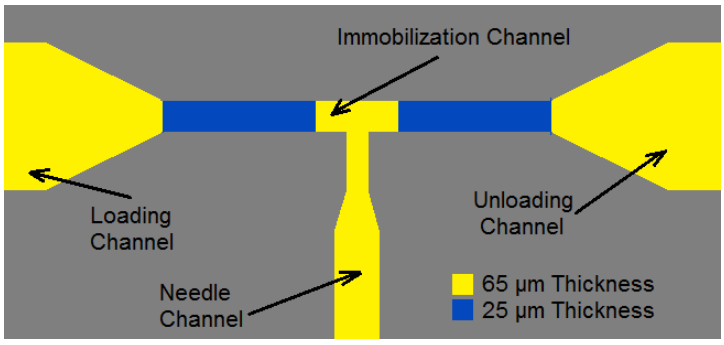

Figure 3. 7: Schematic of the microinjector channels composed of four channels: Loading channel, needle channel, immobilization channel and unloading channel

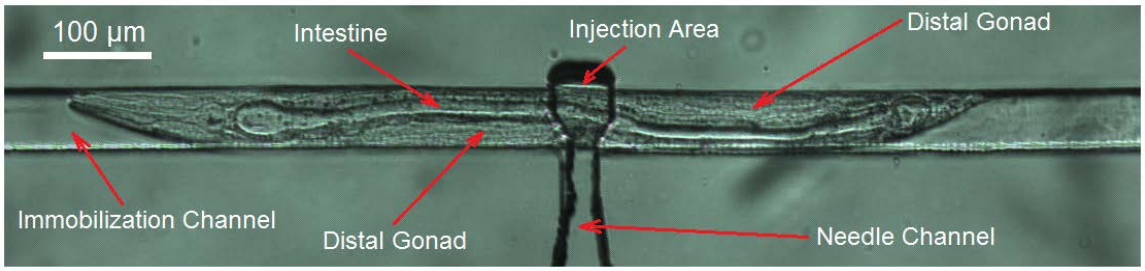

Figure 3. 8: An immobilized *C. elegans* worm inside the final design. The picture shows that the narrowed portions of the immobilization channel would allow easy visualization of the internal organs as well as allow consistent immobilization

3.3.3. Needle Actuation

Once the worm is immobilized, the injection needle should be precisely moved into the worm for delivery of the reagents. In conventional *C. elegans* microinjection, the microneedle is connected to expensive multiple degree of freedom (DOF) micropositioner to align and actuate the microneedle for insertion. This is because the worm is not immobilized in a fixed location with respect to the needle; instead it is in free space necessitating multiple DOF micropositioners. This technique requires detailed injector alignment procedures and skilled operator, which makes the injection process slow and not suitable for scaling to high-throughput. A device that fixes the relative position of the worm and the injection needle will allow a simpler mechanism for needle actuation to be used. The design of such an actuation mechanism should be compatible with immobilization system and applicable for high-throughput manner.

As described in the previous chapter (section 2.7), compliant mechanisms have been used for microinjection in a microfluidic format. Although, many types of compliant systems

have been recently used in microfluidic platforms [10-12], none of them has been used for microinjection of *C.elegans*. By immobilizing the worm at a fixed location in the device and integrating the microinjection needle within the device, a simple single DOF complaint mechanism (as shown in Figure 3. 9) can be used in the place of conventional multi DOF micromanipulator to inject into the distal arm of the gonad. The mechanism described here provides a simple in-plane injection scheme that was low-cost, fast and does not require a skilled operator.

The system composed of three parts: a movable block, a fixed block and a thin flexible membrane that connects the two blocks (see Figure 3. 9a). The microneedle was attached to the movable block and it could move relative to the fixed block inside the needle channel similar to prismatic joints. The location of the needle channel inside the movable and fixed block was indicated in Figure 3. 9a and the bottom view of the compliant mechanism was shown in Figure 3. 10. When the movable block was pushed by a micrometer or microactuator (the displacement “D” in Figure 3. 9b), it deflects the flexible membrane and subsequently, moves the microneedle inside the needle channel (the displacement “d” in Figure 3. 9b). The configuration of the compliant mechanism after actuation is shown in Figure 3. 9b. After unloading the movable block, the stored potential energy in membrane (PDMS membrane was used as a spring) drives back the movable block to the stationary point (similar to the condition in Figure 3. 9a). Since the outer diameter of the shank of the needle was 90 µm, it gently tapers down to the needle tip of 3 to 6 µm, the dimension of the needle channel on the fixed and the movable block was designed as shown in Figure 3. 10b (The depth of the channels was 70 µm). This

ensured that the microneedle could smoothly move in fixed block at the tip while being tightly attached to the movable block.

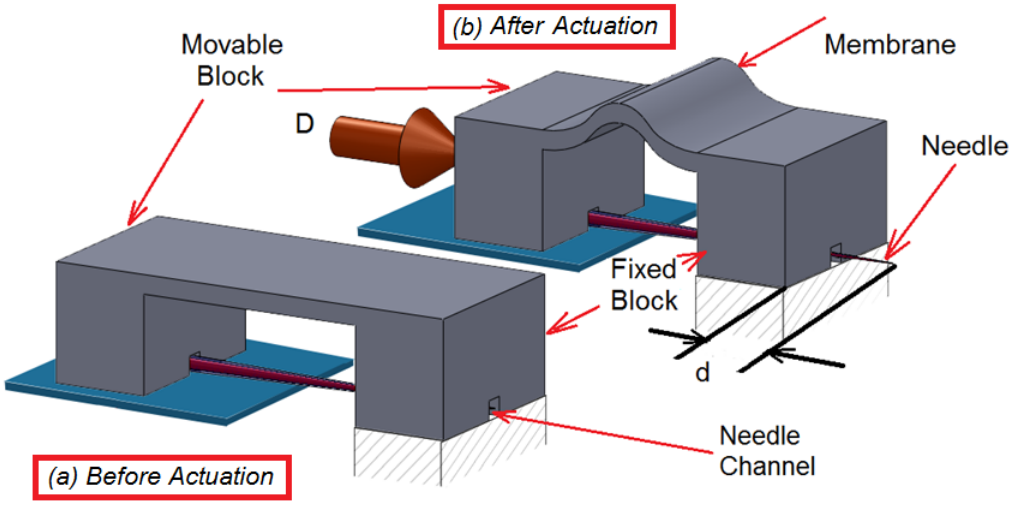

Figure 3. 9: The conceptual design of the compliant mechanism. a) Before actuation. b) After actuation. The motion of the micromanipulator "D" deflected the PDMS membrane subsequently moved "d" the needle inside the needle channel in fixed block. The bottom view of the complaint mechanism is shown in Figure 3. 10.

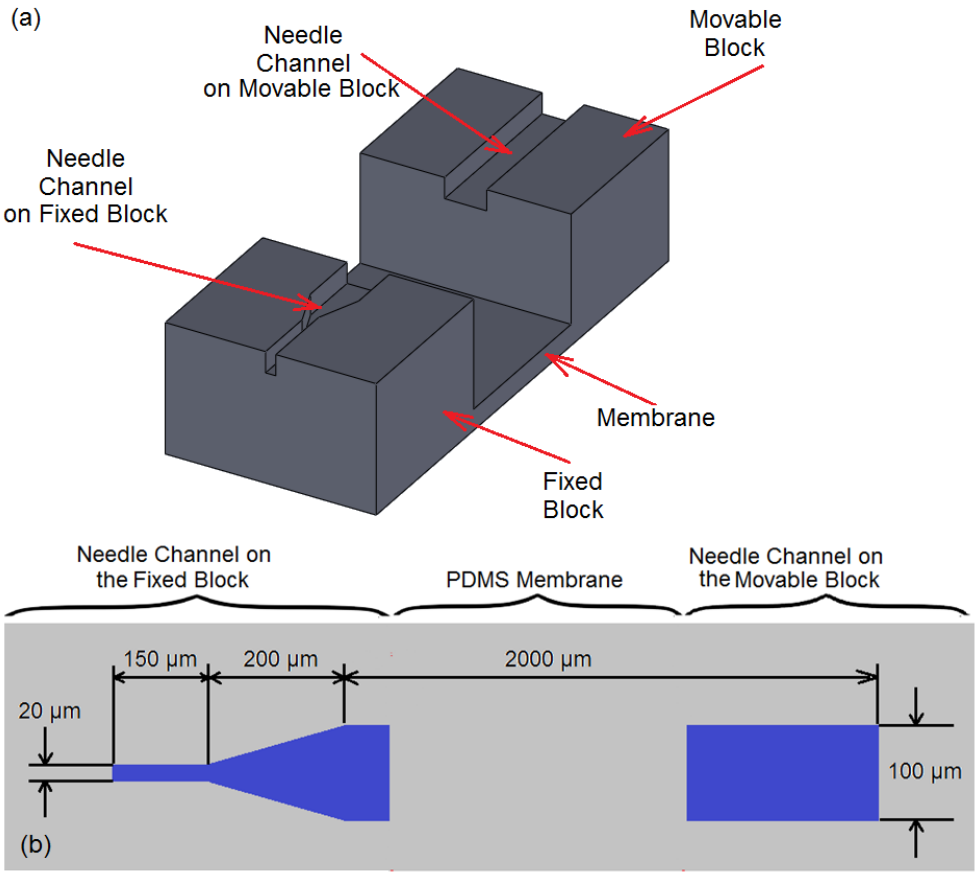

Figure 3. 10: a) Bottom view of the complaint mechanism. b) the geometry of the needle channel. The thickness of the channel was uniformly 70 µm

In order to integrate the complaint mechanism with loading and immobilization system, The fixed block (see Figure 3. 10a) was extended and the loading and immobilization channel were integrated on it as shown in Figure 3. 11. This design allowed the needle to be smoothly was inserted into immobilization channel while its tip was centered with immobilization channel.

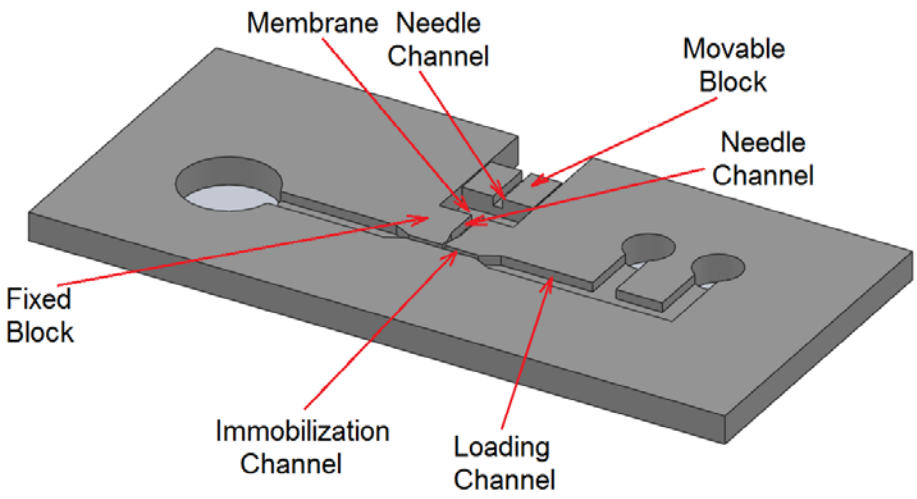

Figure 3. 11: This schematic shows how compliant mechanism was integrated to loading and immobilization mechanism. The fixed block was extended and loading and immobilization channel were created on it.

The stiffness of the mechanism relates the applied displacement (input "D" Figure 3. 9b) with the needle motion (output "d") for semi-static actuation (the frequency of actuation < 0.1 Hz). Therefore, the design parameters of the compliant system were described in terms of the stiffness of the mechanism. Since the thickness of the movable and fixed blocks was significantly higher (20 times) than PDMS membrane and micropositioner, they can be considered much stiffer and as rigid bodies. Figure 3. 12 shows schematic of compliant mechanism modeled using 1 dimensional springs.

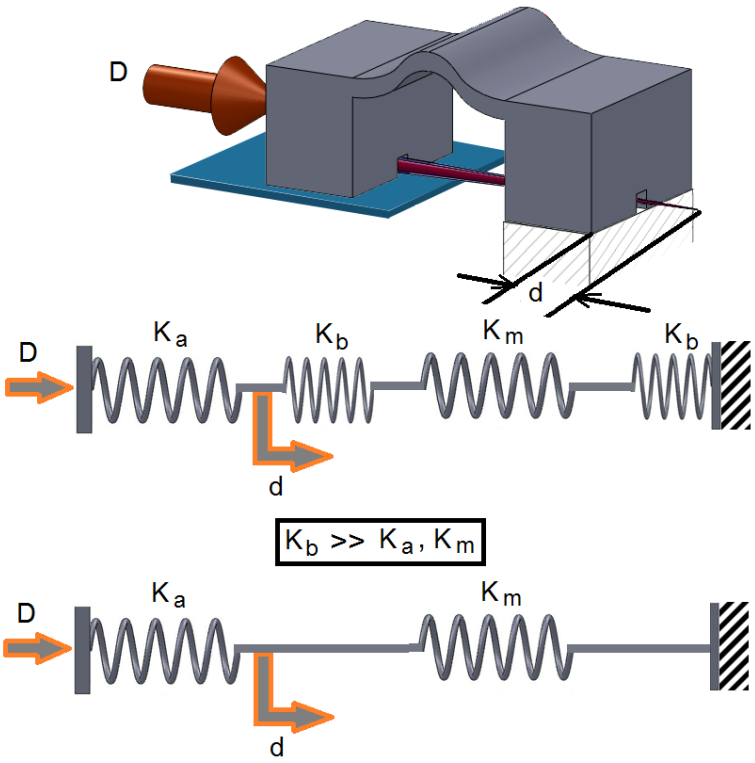

Figure 3. 12: Schematic of compliant mechanism. The mechanism was model by 2 DOF springs. The stiffness of the movable and fixed blocks was significantly higher than PDSM membrane and micropositioner. Therefore, the simpler model composed of K_a and K_m.

The correlation between the applied displacement (input) and needle motion (output) could be calculated as:

$$d = \left(\frac{K_a}{K_a + K_m}\right) D \qquad (3\text{-}1)$$

Where, K_a, K_b and K_m were the stiffness of the manipulator, movable (and fixed) block and PDMS membrane, respectively. It is important to note that the movable and fixed block have almost the same dimension; therefore they have nearly the same stiffness.

The stiffness of the micromanipulator was constant during the characterization of the device. While, the stiffness of the PDMS membrane was defined by the geometry of the membrane (width, height and thickness). Therefore, by tuning the dimension of the PDMS membrane, the desired correlation between applied displacement (input “D”) and needle motion (output “d”) was generated.

A compression test performed on movable block, determined its stiffness (n=3) to be 960 N/m. It was desired that the stiffness of the movable block should be 20 times of the stiffness of the PDMS membrane. Therefore, the design parameter of the PDMS membrane were selected (as listed in Table 3. 1), in order to achieve the stiffness of 48 N/m. Such a membrane allowed robust control (with resolution of the 5 µm as desired in design criteria) of the needle motion by using manual single axis micropositioner attached to the movable block.

Table 3. 1: Design parameters of compliant system related to the dimension of the PDMS membrane

Parameters	**width**	**height**	**Thickness**
Values	7 mm	5 mm	1 mm

3.3.4. Reagent Delivery

The final part of the device is design of the reagent delivery system. Two different methods have been used for reagent transport in microinjection devices. These are capillary pressure microinjection (CPM), which uses pressure driven flow (PDF), and electrophoresis, which utilizes electrokinetic flow (electrophoresis) for reagent transport.

CPM is most broadly used since it is the simplest, fast and most direct way to inject extracellular material into a target (cytoplasm or nucleus or specific organ) without cell or reagent restrictions. However, the volume delivered into the target is not accurate and it may diverge by a factor of 5 or more. In addition, if the size of the needle was reduced, then, the required pressure for dosing will increases rapidly which might exceed the tolerance of the connectors. Therefore, microneedles smaller than a few micrometers in inner diameter are not suitable for PDF. Moreover, the mechanical shock caused by application of a pressure pulse for reagent delivery might damage the target cell or organs. Electrophoresis overcomes this (mechanical shock) problem since the flow rate is more gentle compare to PDF. However, the process is slow which can affect the throughput of the device. In addition, the voltage required for electrophoresis flow is high which might affect the viability of the target. In this design, capillary pressure microinjection (CPM) was selected as the method of the reagent delivery since it is fast and highly suitable for high-throughput microinjection.

The design of the reagent injection system is shown in Figure 3. 13. It consists of a reagent chamber and microneedle. In conventional microinjection, the microneedle itself is used as reagent reservoir since the dead volume of the pulled microneedle (typically 50 mm in length and ID of 0.5 mm) is ~ 9 µL which is larger than the total volume of the reagent required for a set of microinjection (usually ~2 µL). However, the dead volume of the needle (with OD = 90 µm, ID = 20 µm, length of 80 mm) used in this design is extremely small (~25 nL) and could not accommodate all the reagent needed for a set of injections. Therefore, the microneedle was connected to a larger glass capillary (ID = 0.5

mm, OD = 1 mm, length = 25 mm) in order to store the reagent during microinjection as schematically shown in Figure 3. 13. The reservoir can be connected subsequently to either to a pressure source for pressure driven flow (PDF) or to conductive electrode for electrokinetic flow.

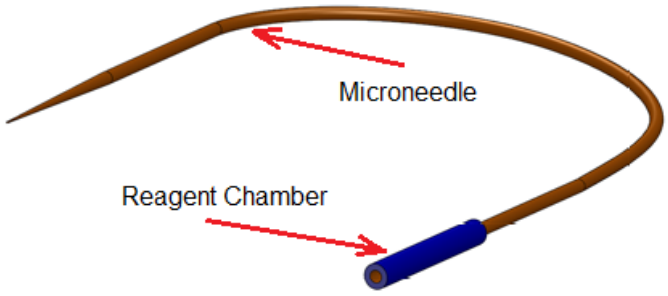

Figure 3. 13: schematic of the microneedle (OD = 90 µm, ID = 20 µm, length = 80 mm) connected to the reagent chamber (ID = 0.5 (mm), OD = 1 (mm), length = 25 (mm)).

3.3.5. Worm Unloading and Plating

Once the reagent was delivered, the worm should be unloaded from the immobilization channel and plated on standard agar plate for recovery. Towards this task, several designs were investigated. In the first design, as shown in Figure 3. 14, suction applied through a syringe at the outlet interconnect was used to remove the injected worm and transport it to the outlet. However, application of a suction pressure at the outlet also tends to transport worms from the loading reservoir that have not yet been injected into the outlet. In order to avoid this, another channel called “washing channel”, (see Figure 3. 14) was added and connected to a reservoir of DI water. In this design, the loading channel was

closed and the washing channel was open during the unloading phase removing only the injected worm into the outlet syringe. Then, the injection cycle including loading, immobilization, injection, unloading, was repeated for other worms. However, worms accumulated in the dead zones in the outlet reservoir and none of the worms that were injected could be extracted out.

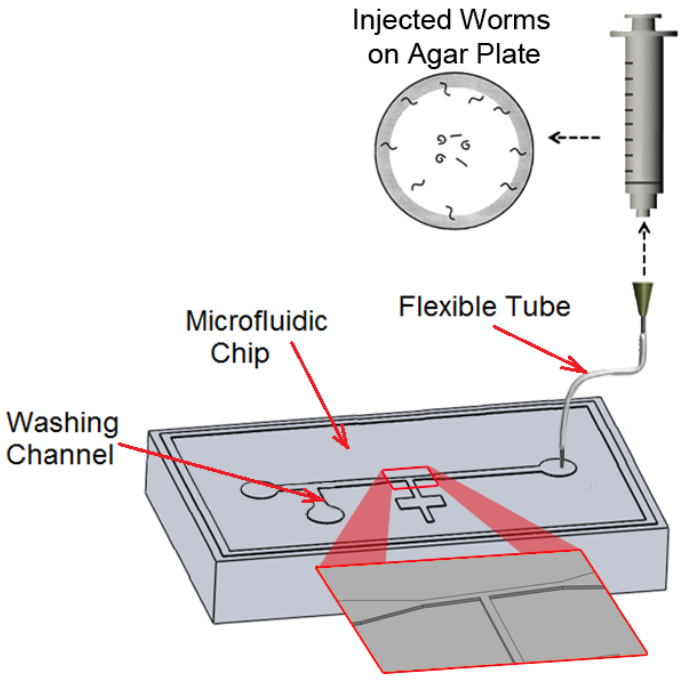

Figure 3. 14: The schematic of the first design for unloading system. A syringe was connected to the outlet interconnect and once a worm was injected, it was used to apply suction and remove the injected worm to the syringe. The flow is through washing channel to the outlet syringe.

Therefore, the injection process was modified to inject a large number of worms and extract them together. This process modification allowed extraction of a few worms (30% of the injected worms) but was deemed not efficient.

In the next design (as schematically shown in Figure 3. 15); the outlet reservoir was left open to atmosphere by punching a hole such that there are no dead zones for accumulation of the worms. When an individual worm was injected, the loading channel was closed and the worm was manually pushed out by using a syringe connected to the washing channel to the open outlet reservoir. The open reservoir also allowed easy pick up of individual worms immediately after injection by using a micropipette and then plate it on agar plate as shown in Figure 3. 15. Then, the injection cycle was repeated to another worm. The efficiency of the worm extraction of this design was 100% and the total time to perform this process was less than 2 minutes.

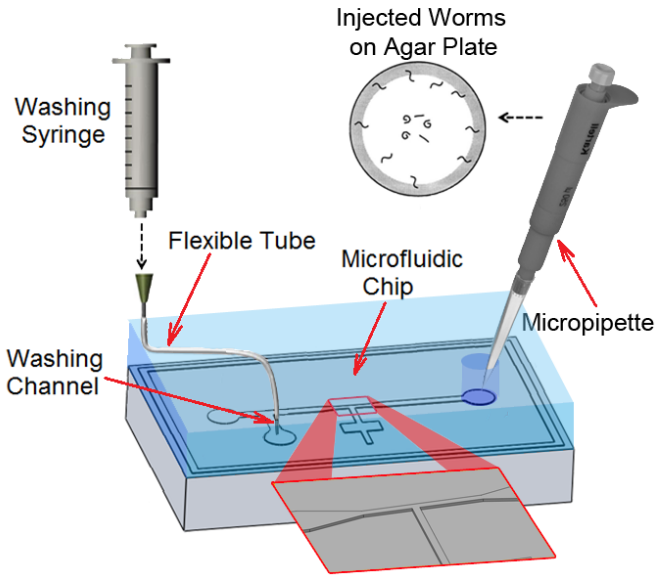

Figure 3. 15: The schematic of the final design for unloading system. The outlet reservoir was left open to atmosphere and the worm was manually pushed out by using a syringe connected to the washing channel to the open outlet reservoir and then it was picked up from the reservoir using micropipette and plated on agar plate.

3.4. Advantages over Existing Methods and Devices

In this chapter, an in-plane design to visualize the injection process better and to increase the speed and simplicity of the microinjection process was developed. The device (Figure 3. 16) consists of (i) a narrowed channel to immobilize the worm physically, (ii) a one DOF complaint mechanism to actuate the needle and (iii) a microchamber attached to a microneedle for reagent transport. Unlike conventional injection where anesthesia, cooling or injection oil is used, the *C. elegans* worm was physically and passively immobilized as it is faster and avoids dehydration which is a significant issue. Use of a single DOF complaint mechanism in the place of conventional multi DOF micromanipulator to inject the distal arm of the gonad provides a simple in-plane injection scheme that is low-cost, fast and does not require a skilled operator. Pressure pulses are used to transfer reagents from a microchamber through the microneedle into the gonad of the worm. After injection, worms are transferred to the outlet chamber.

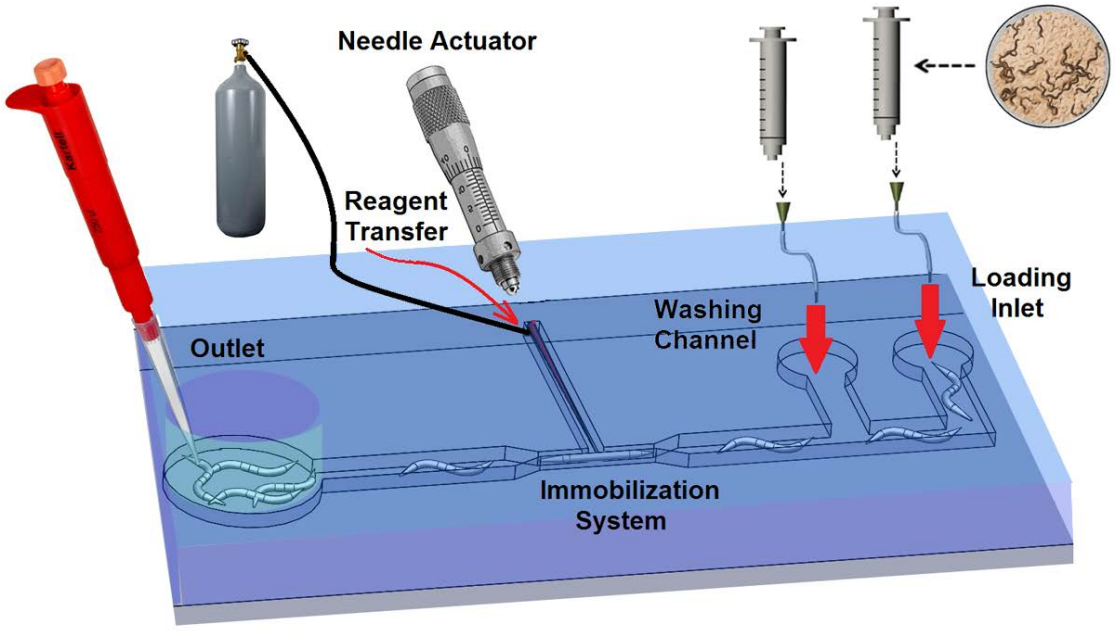

Figure 3. 16: Schematic of all components of the microinjector

3.5. Summary

This chapter introduced the proposed device, its working principles and advantages over existing devices and methods. The device overall maintains the advantages of capillary microinjection such as high transfection efficiency and low cytotoxicity, while eliminating the problems associated with low throughput and complexity in operation caused by using high degree of freedom actuators. The next chapter will focus on the fabrication of the device.

Chapter 4: Device Fabrication

4.1. Introduction

The design criteria and the conceptual design of the microinjector have been discussed in the previous chapter. This chapter introduces the fabrication techniques and materials used in the assembly of the device. First, the needle fabrication based on pulling method, is described. Next, the process flow for PDMS device fabrication using soft photolithography technique is detailed.

4.2. Device fabrication

4.2.1. Needle fabrication

The design criteria for the microinjection needle is described in Section 3.2 and has the following dimensional constraints as listed in Table 4. 1.

Table 4. 1: The design Criteria of needle fabrication

Design Criteria	**Min**	**Max**
The inner* diameter of the tip	3 µm	6 µm
The taper length	250 µm	450 µm

* the inner and outer diameter of the conical needle was assumed the same at tip

The typical method to create microneedle for *C. elegans* microinjection is based on pulling of borosilicate glass capillary (Figure 4. 1a). In this method, two sides of the glass capillary with 0.5 mm ID and 1 mm OD are clamped while a certain tension force is applied along the capillary. Then by increasing the temperature in the middle of the capillary via electro thermal filament and pulling it simultaneously, the capillary will be pulled and microneedle can be created (Figure 4. 1c and d).

The fabricated needle (3 µm tip diameter, 87^{o} taper angle) has proper dimension for *C. elegans* microinjection, but it is not compatible with microfabricated device as the outer diameter of the original glass capillary is 1 mm and it cannot be simply assembled into a typical microchannel in closed format microfluidic devices. Therefore, the microneedle should be produced from glass capillary with outer diameter of less than 100 µm.

Flexible fused silica capillaries, with a large range of standard sizes from 2 µm to 700 µm internal diameters and 90 µm to 1000 µm outer diameters, are used as chromatography columns in analytical chemistry applications such as Gas Chromatography (GC), Capillary Electrophoresis (CE) and Capillary Liquid Chromatography (CLC or LC) (see

Figure 4. 2). The smallest outer diameter of these commercially available capillaries (20 µm ID x 90 µm OD) was suitable and could be integrated with a microfluidic device. However, the softening temperature (the temperature for pulling) of fused silica capillary (1665 °C) is higher than borosilicate glass capillary tubes (820 °C). Therefore, the required thermal energy for pulling of fused silica capillary cannot be generated by standard pulling machines. Consequently, a custom-built fused silica capillary pulling machine was designed and built.

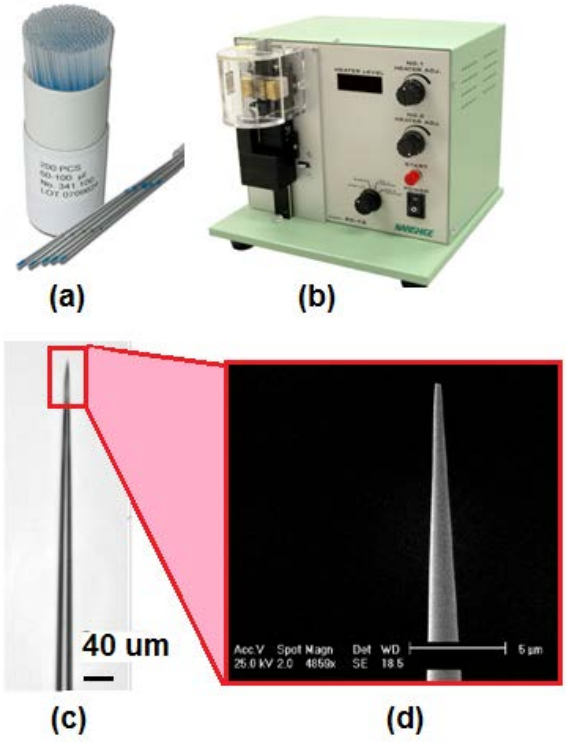

Figure 4. 1: a) A box of borosilicate glass capillary with 1mm OD and 0.5 mm ID, b) The PC-10 is designed specifically for pulling 1mm~1.5mm O.D. borosilicate glass capillaries (up dated from: *narishige-group.com*). c) Thick Walled Glass (1.0mm x 0.50mm, BF100-50-10), 0.6-0.9µm tip, 6-8mm taper (400x) and d) Scanning Electron Microscopy of a Microinjection Pipette (~5,000x mag)

(updated from: *www.sutter.com*)

Figure 4. 2: a) Flexible fused silica capillary, b) The cross section of the capillary (updated from: *www.polymicro.com*)

The custom-built puller consisted of five parts: fixed and movable blocks, spring, guide bar and a lighter (see the schematic in Figure 4. 3a). The fixed and movable blocks were used to clamp the capillary at two sides. The guide bar was designed to restrict the motion of the movable block to an axial motion (prismatic motion). The spring and lighter were used to apply required tensile force and heat, respectively.

Once the capillary (20 µm ID x 90 µm OD) with the length of 15 cm was clamped at the two ends, the spring with stiffness of 5.2 (N/m) was in a compressed state imposing a force on the movable block. A displacement gage (Δx) with resolution of the 1 mm was setup along the spring on the guide bar; therefore, the tensile force applied can be determined as $F = K.\Delta x$; where K is the stiffness of the spring and Δx is the readout displacement from the gage. As a result, applied force could be varied to create different shapes of the microneedle using the setup shown in Figure 4. 3b. A lighter (MICRO-JET TOOL, MJ-320, Canada) capable of generating a blue flame at 1300°C with the diameter of the flame (where it encounters with capillary) of 2.5 mm was positioned at the mid point between the two blocks.

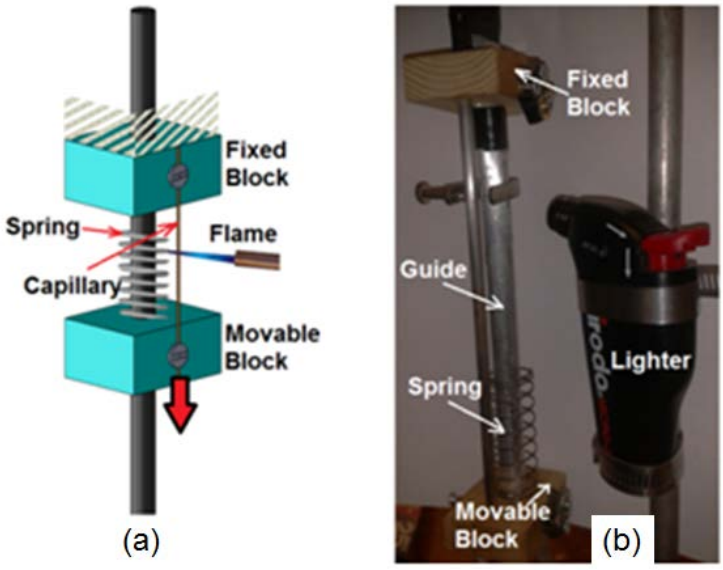

Figure 4. 3: a) Schematic of pulling system, b) The needle fabrication setup

Since the temperature of the flame is constant when it meets the capillary, tensile force applied to the capillary becomes the only parameter that determines the needle shape and the pulling time. Forces in the range of 0-60 (mN) were applied on the capillary to fabricate the desired needle shapes and dimensions. The results shown in Figure 4. 4, reveal three different types of the microneedle shapes can be obtained. When the forces were below 20 mN, the microneedle created had taper longer than 650 µm as shown in Figure 4. 4a. When the force was between 20-40 (mN), the taper length of 300 µm to 400 µm was obtained as shown in Figure 4. 4c. Finally, the forces higher that 40 mN produced microneedles with taper shorter than 150 µm Figure 4. 4b. The range of force between 20-40 mN was found to be suitable for the kind of needle that desired (Table 4. 1) in design criteria (see Figure 4. 4c). Because of surface tension between the needle, water inside the needle channel and the glass substrate, microneedle with taper length larger than 400 µm was stick to glass substrate, which did not allow the needle to be

aligned with worm during needle insertion. The needle pulling processes mostly took 120s to setup the capillary and 2s to perform the pulling).

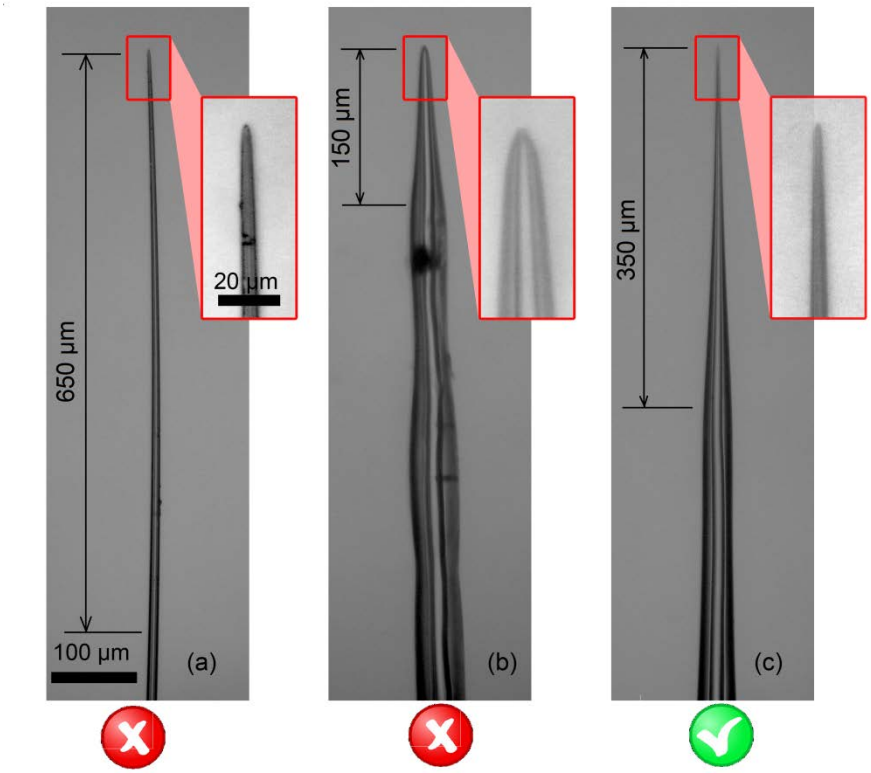

Figure 4. 4: Three different types of the microneedles fabricated by the custom-made pulling machine. a) The microneedle with the taper length (650 µm) larger than maximum allowed taper length (450 µm). b) The microneedle with the taper length (150 µm) shorter than the minimum allowed taper length (250 µm). c) The microneedle with proper taper length (250 µm) for *C. elegans* microinjection

Once the pulling process was performed, the two microneedles (the needles clamped to fixed and movable block, respectively) were removed from the blocks. The microneedle formed on the stationary block was always completed melted and deformed as it remains in the flame even after the capillary has been pulled and the tips have snapped. (Figure 4. 5a). In contrast, the micro needle clamped to the movable block was pulled away from

the high temperature zone after the tip snapped and was able to cool down quickly (Figure 4. 5b); therefore, it could be used in subsequent fabrication.

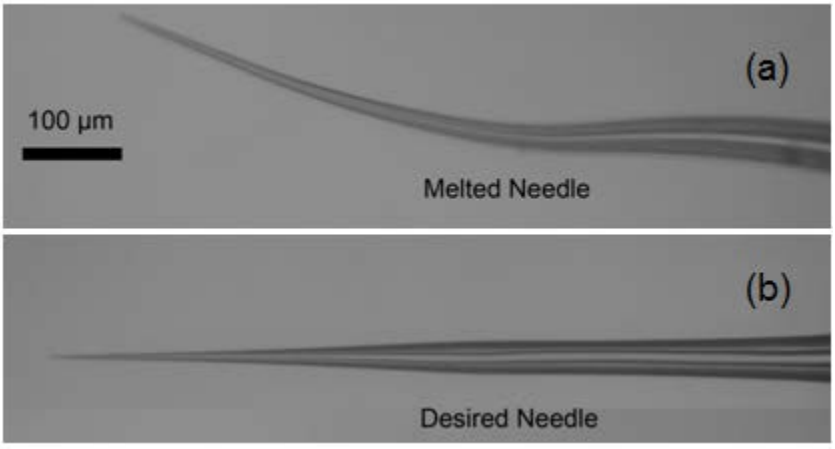

Figure 4. 5: Two fabricated microneedle after pulling of the capillary. a) The melted needle, the microneedle which received extra heat and was melted after pulling due to the lack of the timing control on lighter. b) The desired needle, the microneedle clamped to the movable block which immediately put down the high temperature zone after pulling

In most cases, the inner diameter of the pulled microneedle is blocked or has very small inner diameter. Thus, post fabrication Hydrofluoric Acid (HF) wet etch, was performed to open the tip of the microneedle, which allowed to create inner diameter of 3 µm for each microneedle. The end of the needle was connected to a larger capillary (OD = 1mm, ID = 0.5 mm, length = 15 mm) using epoxy glue as shown in Figure 4. 6. The volume of the epoxy glue for sealing should be less than ~1 µL. If more epoxy was used for the sealing, then the glue could fill the entire chamber because of capillary force. Note that the larger capillary can be cut from the standard borosilicate glass tubes (Microdispenser Capillaries, 3-000-210-G, Alpha Laboratories, Hampshire) using glass scraper.

Moreover, it should be noted that the larger capillary was used as the reagent chamber in the future experiments.

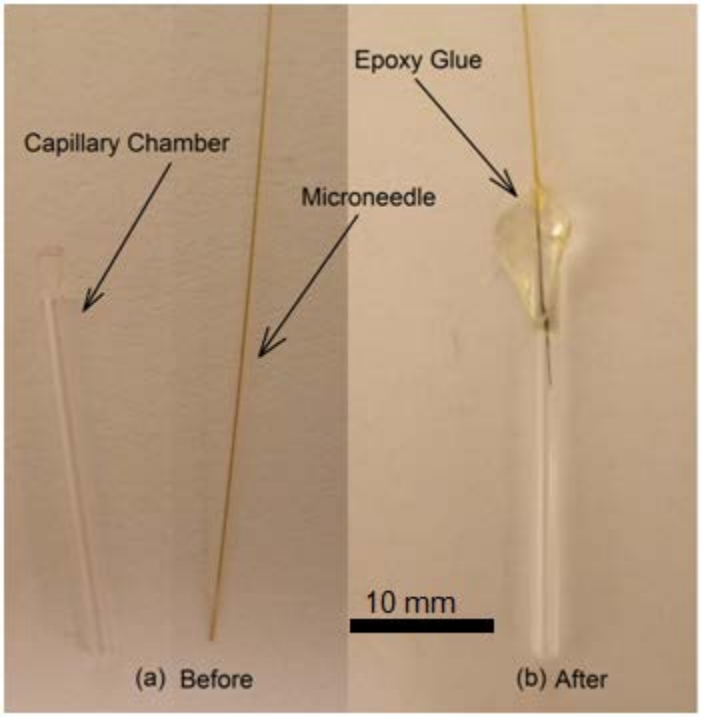

Figure 4. 6: The demonstration how the standard capillary was connected to the microneedle using Epoxy glue and it was used as the reagent chamber using. The capillary has the dimension of OD = 1mm, ID = 0.5 mm, length = 15 mm and the tail of the microneedle has OD = 90 µm and 0.5 mm of the microneedle is inserted into the capillary

The epoxy glue was cured for 20 minutes and then the chamber was filled by DI water using stainless steel needle (30 G x 1/2 in., BD PrecisionGlide™, Canada) connected to 1 mm filtered syringe (PN 4612, Acrodisc® 10 mL Syringe Filters with 0.2 µm Supor® Membrane, Pall Corporation, USA). Next, the chamber was connected to PVC tube (Thermo Scientific Nalgene 180 PVC Tubing, 1/32 x 3/32, Canada) and then to 10 mL syringe that can be used to apply manual pressure. Afterwards, the microneedle was

introduced into 49% HF for 5s and then into 10% HF for 30s while maintaining a small flow of DI water through the inner bore using the syringe. This cycle was repeated a number of times to create an open needle with outer diameter in range of 3-6 µm.

4.2.2. Device fabrication

The fabrication of microinjector device is a multi-step process consisting of PDMS chip fabrication using soft-lithography technique, fabrication of the compliant mechanism and final assembly of the microneedle with the PDMS chip. The process flow for the device fabrication is shown in Figure 4. 7. First, the master mold was fabricated using photolithography. Next, interconnects were placed on the master mold and PDMS prepolymer was cast on it. Finally, the PDMS elastomeric chip was peeled of the mold, microneedle assembled into it, and bonded to a glass slide.

4.2.2.1 Mold fabrication

There are two conventional techniques to transfer the CAD design to the master molds for PDMS casting: Photolithography and 3D printing. Although, the resolution of the photolithography process (1 µm) is finer than 3D printer technique (100 µm), its maximum achievable thickness (150 µm with aspect ratio of 10:1) is smaller than 3D printed structures (2000 µm with aspect ratio of 5:1)

In the conceptual design (described in section 3.3), the microinjector device consists of features in two different size ranges. The loading, unloading, immobilization and needle

channels are in the size range of 20 µm and require accuracy of definition of 10 µm while, the compliant system is in the size range of 1000 µm and require accuracy of definition of 100 µm. Consequently, neither photolithography nor 3D printing alone could be used to create the master mold. Instead a hybrid approach is used here. Firstly, photolithography was used to create the fine features on silicon wafer and 3D printing then produced the course features. Subsequently, both molds created separately werw assembled into one master mold.

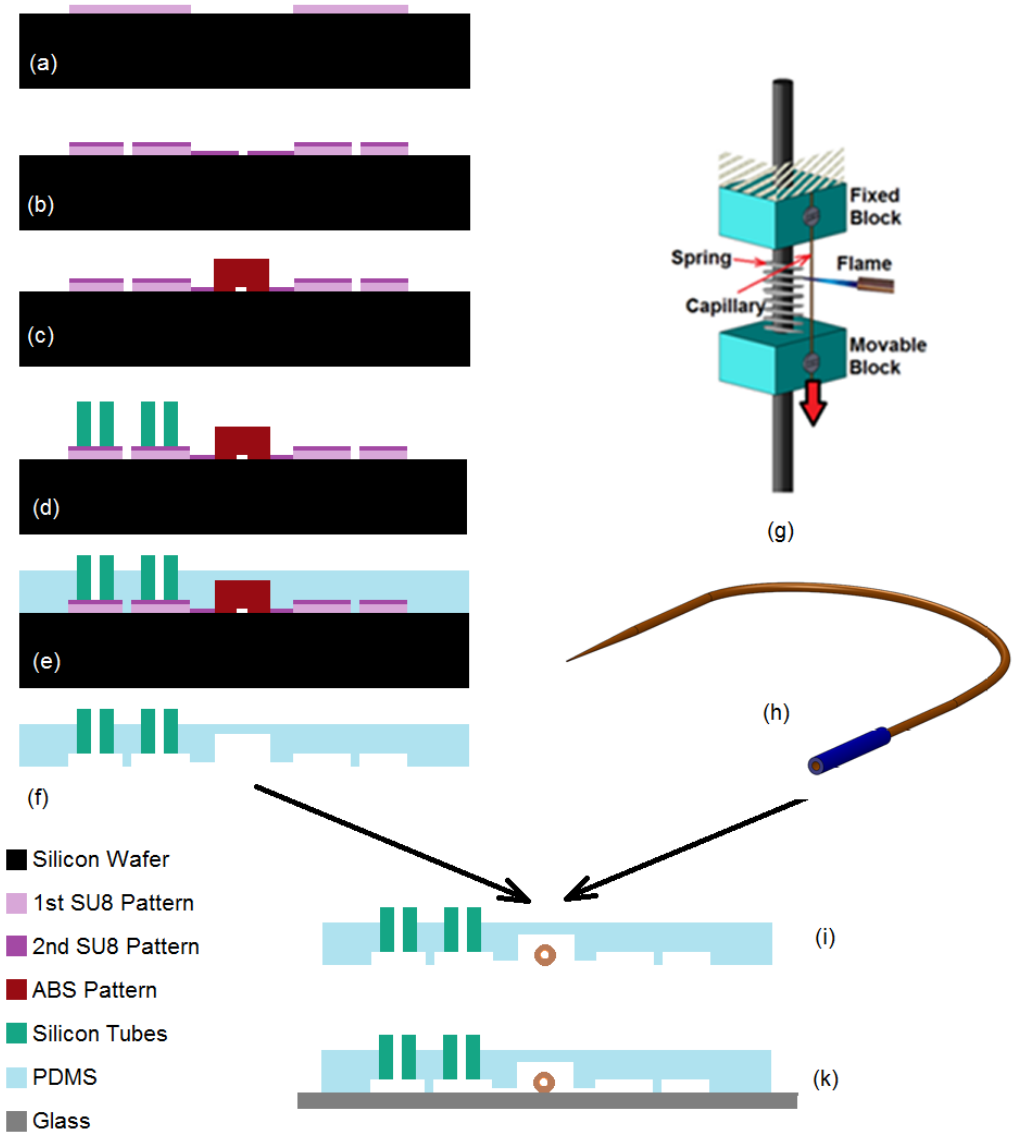

Figure 4. 7: The flow process of the device fabrication. a) pattering of the first SU8 layer with thickness of 50 µm. b) pattering of the second SU8 layer with thickness of 25 µm on the first layer. c) the ABS part created by 3D printer is attracted to fabricate a hybrid master mold. d) the interconnectors (silicone tubes) were place on SU8 pattern. e) PDMS (1:10) was casted on the mater mold to create a 3 mm device layer and 1 mm PDMS membrane for compliant mechanism. f) The PDMS substrate was peeled off from the master mold. g) the microneedle is pulled from fused silica capillary and h) connected to larger capillary for introducing the reagent. i) The microneedle and PDMS chip were assembled together k) the PDMS chip was bonded to the glass slide using dry oxygen bonding.

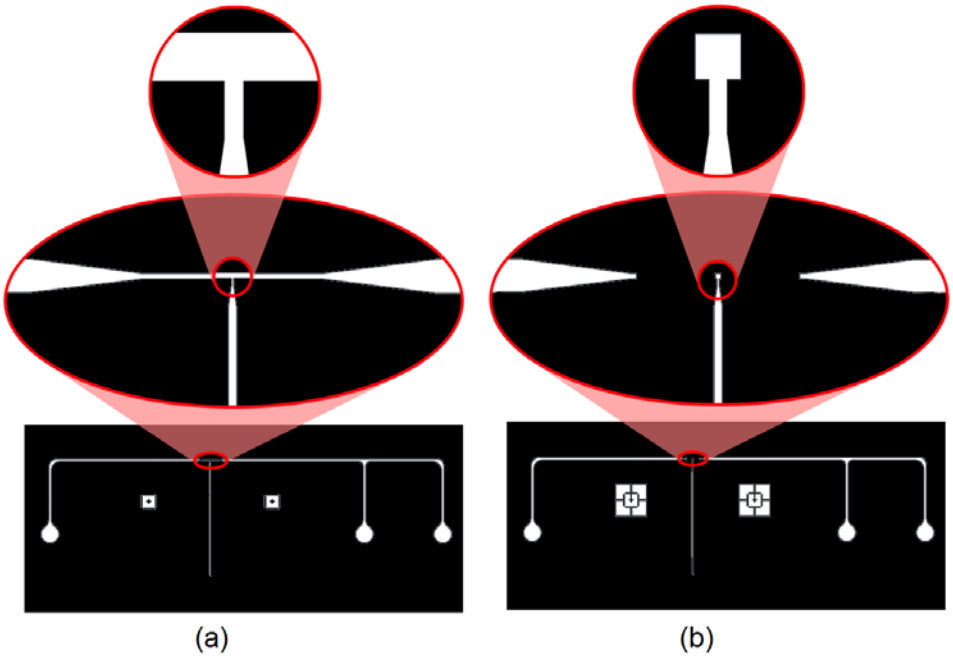

Figure 4. 8: The microchannel pattern for the first a) and second layer b) of the microchannels

The process for making the mold is as follows. First, a Silicon (Si) wafer with 76 mm diameter (University Wafer, MA. USA) was cleaned and dried. Next, the wafer was treated by oxygen plasma at 50 Watts for 1 min to remove any residue on the top surface. Then the negative photoresist (SU-8-2075, Mircochem Corp, MA, USA) was spun on the wafer at 3500 rpm which produced a SU8 layer of thickness of 50 µm. The wafer was baked to evaporate the remaining solvent. Subsequently, the photomask of the first layer (Figure 4. 8a) and the wafer were aligned in a mask aligner and exposed to UV (365 nm) with power of 4.6 mW for 40 sec. Then, after unloading the wafer from the mask aligner and post-exposure baking, the SU8 pattern was developed using the developer to remove the photoresist in the unexposed area.

Subsequently, the same process was repeated to create the second layer of the pattern (Figure 4. 8b) over the first layer with a thickness of the 25 µm. Finally, the mold was post-baked to increase the stiffness of structure.

In order to create the features related to compliant mechanism, first an ABS block with the dimension of 3.5x3 mm^2 base and 1.2 mm height was 3D printed. Next, a thin layer (~50 µm) of 1:2 (PDMS to curing agent) PDMS pre polymer was spun and microcontact printed on the bottom of the block. Then, the block was attached to the SU8 structures on silicon wafer (at a distance of 1cm from the immobilization channel) to create the final composite mold as shown in Figure 4. 9. Finally, the mold was heated (150^o C for 5 minutes) to cure the PDMS.

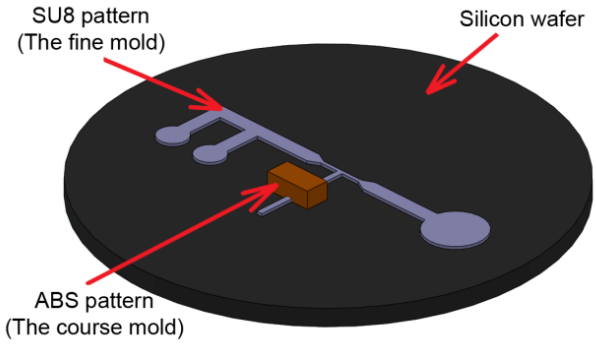

Figure 4. 9: The master mold composed of two types of molds (course and fine features). The SU8 pattern on Silicon wafer defined the fine features with resolution of 10 µm and the ABS pattern used to create the course features with minimum resolution of 100 µm.

4.2.2.2 Interconnects

In order to have access to the inlet and washing channel, silicone tubes with ID 1.5 mm and OD of 4.8 mm and 10 mm length were used. The tubes were placed on the

corresponding reservoirs on the SU8 mold (see Figure 4. 10). This method allowed complete integration of the interconnects with PDMS device with excellent sealing.

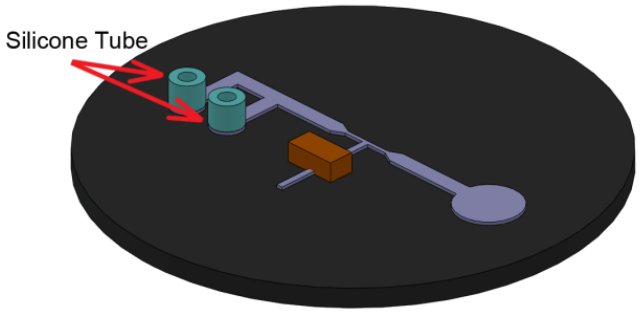

Figure 4. 10: The master mold after putting silicon tubes (ID 1.5 mm of and OD of 4.8 mm and 10 mm length) on the SU8 patterns in order to have access to the inlet and washing channel after PDMS casting.

4.2.2.3 PDMS casting

The next step after mold fabrication was PDMS casting. First, Polydimethylsiloxane (PDMS) pre-polymer mixture (Sylgard 184 kit,Dow Corning Corp., MI, USA; 10: 1 ratio of the base and crosslinker) was cast on the master mold, and cured at room temperature for 24 h. The volume of the dispended PDMS pre polymer (25 mL) into 10 cm (diameter) Petri dish corresponded to a thickness of 3 mm and 1 mm in the PDMS chip and compliant mechanism section, respectively. Next, the PDMS elastomer was peeled off from the master mold, the extra PDMS was trimmed and the outlet chambers was punched out with a biopsy tool with diameter of 8 mm. Next, the PDMS substrate was cut along the red lines as shown in Figure 4. 11a to make the compliant mechanism described in section 3.3.3 and shown in Figure 4. 11c. In this configuration, the movable block

(Figure 4. 11b) was connected to the PDMS membrane via “Line A”. In addition, the fixed block and PDMS membrane were connected together by “Line B” (Figure 4. 11b). Finally, a small amount of the PDMS prepolymer usually seeps into the silicone tube during PDMS casting process due to its low surface energy. Therefore, after curing and peeling off the PDMS, the insides of the interconnects were punched using a biopsy tool to connect open them.

4.2.2.4 Needle Integration

The next step is the integration of the microneedle into the PDMS substrate. Firstly, the PDMS substrate was inverted and placed under optical microscope (100-200x magnification) such that the microchannel features are accessible from the top for needle integration. Next, the microneedle was gently placed on the PDMS substrate, positioned and aligned so that the tip of the microneedle was at a distance of ~100 µm to 200 µm from the immobilization channel. Then, the shank of the microneedle assembly was inserted into needle channel on the movable block as schematically shown in Figure 4. 12a. Since the size of the needle channel on the movable block was a good fit with the outer diameter of the needle itself, it held the needle tightly at that location and prevented any further movement of the needle during subsequent processes. Next, a droplet (~1 uL) of the PDMS pre polymer (4: 1 ratio of the base and crosslinker) was spread on the movable block to fully attach the microneedle to the movable block. After rapid curing the PDMS glue (see the black apot on the movable block in Figure 4. 12a) using a flame,

the PDMS chip, as shown in Figure 4. 12b, was taken off from the microscope for bonding.

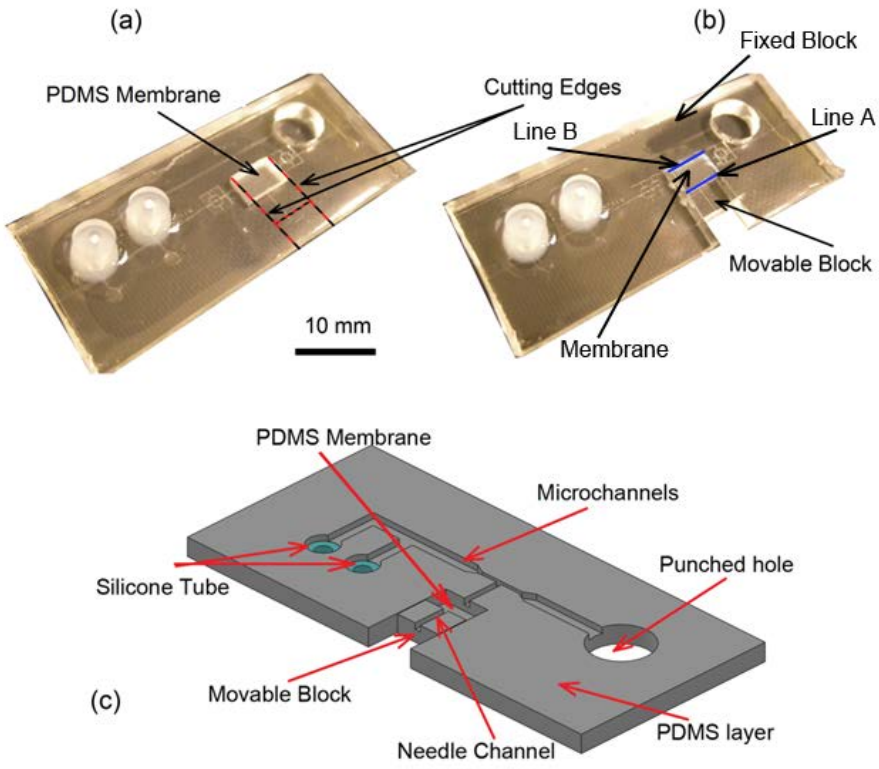

Figure 4. 11: Steps and schematic of PDMS chip cutting and pouching a) The PDMS chip after trimming and pouching. b) The PDMS chip after cutting and releasing the movable block. c) Schematic of different parts of the PDMS chip after casting

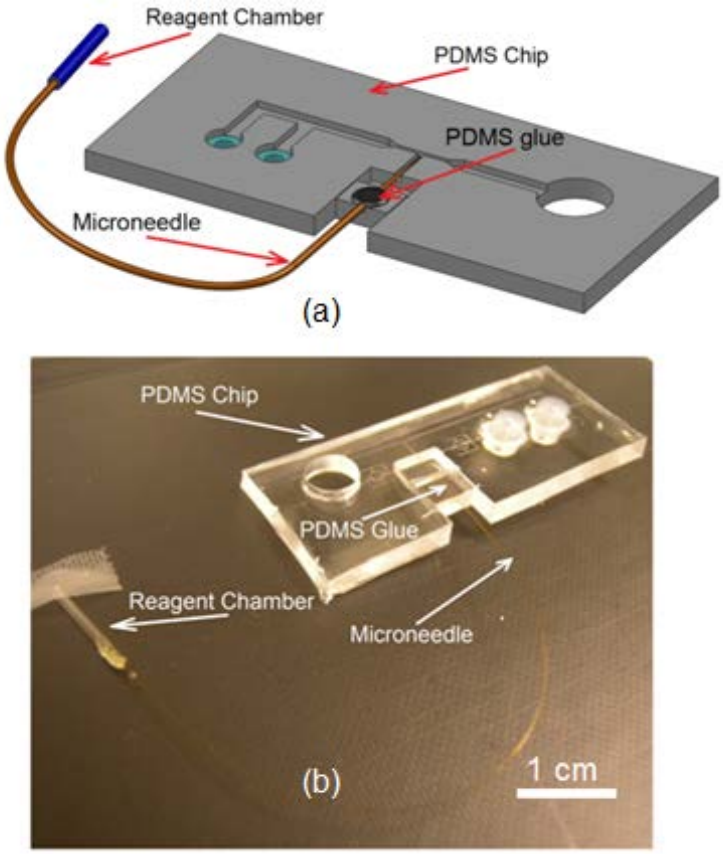

Figure 4. 12: a) A schematic of the needle assembly processes and different parts of the chip. b) The PDMS chip after needle assembly

4.2.2.5 Bonding

Bonding is the final step in the fabrication of the injection device. The PDMS substrate and a 75x25 mm^2 glass slide were exposed to 50W oxygen plasma for 70s. Since the plasma machine worked in low level of the pressure, the DI water present inside the reagent chamber when opening the tip evaporated. Therefore, after taking off the PDMS chip from the plasma machine, the reagent chamber was filled with reagent which is required for microinjection. A thin layer of grease was then spread on the movable block to reduce the friction of the motion during the needle actuation. Afterwards, the PDMS

chip was placed under microscope and a 10 mL syringe was connected to the reagent chamber. By pressurizing the reagent chamber, the needle was tested for suitable operation and clogging. If the needle was clogged, a sharp and clean scalpel was used to gentle touch the tip of the microneedle which dislodges any residue accumulated at the tip and opens the microneedle. It is important to be note that the force during the touching should not be high that breaks the needle. Finally, the glass slide was placed on the PDMS chip and the bonding process was completed. The fabricated microinjector as shown in Figure 4. 13 was ready for operation.

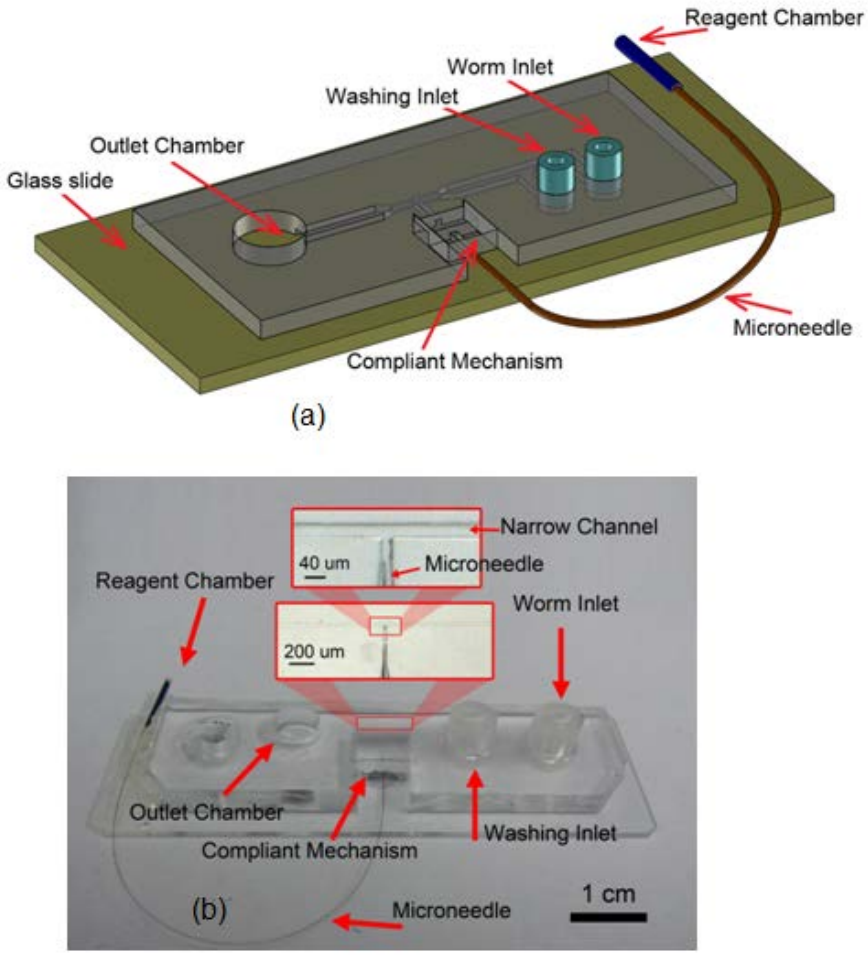

Figure 4. 13: A schematic a) and PDMS chip of final *C. elegans* microinjector

4.3. Summary

This chapter provides an overview of the materials used in the fabrication of the device, fabrication process as well as the sample preparation. The fabrication process generally followed traditional soft lithography techniques, just different slightly in the mold fabrication process. The next chapter covers the characterization and testing of the device.

Chapter 5: Device Characterization and Results

5.1. Introduction

This chapter details the characterization of the device and presents the results obtained. Various components of the device including the loading system, immobilization channel, compliant mechanism and reagent delivery system were characterized. The chapter also presents the results achieved, specifically the injection of Methylene blue, Green fluorescent Protein (GFP) dye as well as results of creating transgenic worms.

5.2. Experimental setup

The experimental setup (Figure 5. 1) consisted of three major parts: Fluidic system, optical system and the microfluidic device. The fluidic system which was used to introduce the worms into the device and deliver reagents into the worm, consisted of a pressurized air tank at 4 (bar), pressure regulator (2000 Series Regulator, ARO, Ingersoll Rand, USA) and a solenoid valve (S10MM-30-12-3, 3-Way Normally Closed, Pneumadyne, Inc., USA). The optical system that was used to observe, control and record the injection process consisted of an optical microscope (Model 500 LumaScope, Etaluma, Inc, CA), digital camera (Flea3 FLs-U3-32S2C, Point Grey Research, Inc. Canada) and software (Labview©, flyCapture2© software). The microfluidic device,

which was used to perform the injection into *C. elegans* worm, consisted of a microinjector chip (whose fabrication was described in previous chapter) and a micropositioner (Micrometer fine focus linear stage, Model A LHFF, Line Tool Co. PA).

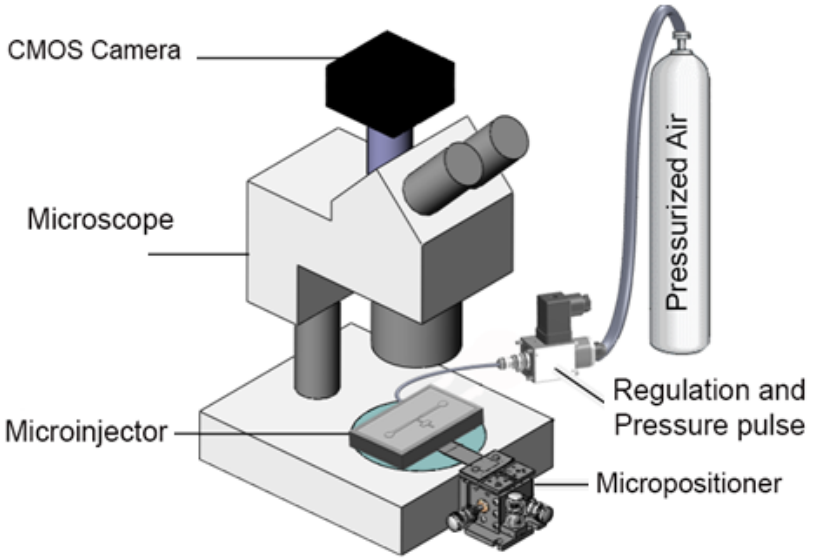

Figure 5. 1: Experimental Setup used for *C. elegans* microinjection consisted of three major parts: fluidic system, optical system and microchip

The micropositioner which was attached to the movable block on microfluidic chip was used to actuate the microneedle for injection. Although, the minimum resolution of the micropositioner was 10 µm (as defined by the marking on the shank of the screw gage), displacements of less than the maximum resolution (~2 µm) can be achieved by controllably rotating the screw partially between two markings under visual feedback. The air pressure tank was connected to the reagent chamber on microinjector chip through a pressure regulator and a solenoid valve and is capable of generating adjustable pressure pluses for reagent delivery. The solenoid valve was used to control the duration

and number of the pulses for each individual injection. The microfluidic injector was installed under optical microscope (Light Microscope, Leica, Canada) and a CMOS camera mounted on it was used to record the video of the injection processes. After injection, a 200 µL micropipette was used to transfer the injected worms into the standard nematode growth (NG) agar plates for recover after injection.

5.3. Worm culturing

For all the experiments described in this thesis, wild-type N2 Bristol *C. elegans* grown at 20°C on standard nematode growth (NG) agar plates containing OP50 Escherichia coli as a food source, were used [93] In order to obtain age-synchronous populations, bleach treatment was performed [94]. First, 2 mL of a bleach solution (800 µL of 4 N NaOH and 1200 µL of 5% NaOCl) was added to a 4 mL suspension of gravid hermaphrodites in M9 physiological buffer (3 g KH2PO4, 6 g Na2HPO4, 5 g NaCl, and 1 mL 1 M MgSO4 dissolved in 1 L distilled water). Next, this mixture was incubated at room temperature for 3 min to lyse worms and release fertilized eggs, which were subsequently washed and allowed to hatch in M9 over 24 h to produce a synchronized population of arrested L1 larvae. Finally, animals were transferred to NG agar plates containing *E. coli* bacteria and allowed to develop normally.

5.4. Results

5.4.1. Proof of concept and preliminary testing of the microinjection system

This section describes the proof of concept and preliminary testing of the microinjection system including the loading, immobilizing system and needle actuation. To transfer the wild-type N2 *C. elegans* worms from agar plate into the microfluidic device, the worms were first washed off the plate into a test tube using M9 physiological buffer. Next, 1 mL of this solution containing the worms was transferred into a 3 mL syringe connected to the inlet of the device through a 20 cm long PVC tube as shown in Figure 5. 2.

by using manual pressure on the syringe the worm was moved into the mouth of the narrowing region of the immobilization channel as shown in Figure 5. 3a. Then application of a small manual pulse pushed it into the immobilization channel as shown in Figure 5. 3b. Subsequently, the position of the worm in the channel and its alignment with the position of the injection needle was adjusted by inserting (Figure 5. 3c) or withdrawing (Figure 5. 3d) the plunger in the syringe as appropriate. The time for worm loading and aligning into the immobilization channel was around 6 s and 4 s, respectively. This experiment showed that the worm could be successfully loaded and aligned into the immobilization channel manually in 10 s. However, various factors such as the dimension of the loading channel and immobilization channel, the pressure level, duration of the pressure could affect the loading and aligning time. Therefore, the loading system and its operation was fully characterized in the next section.

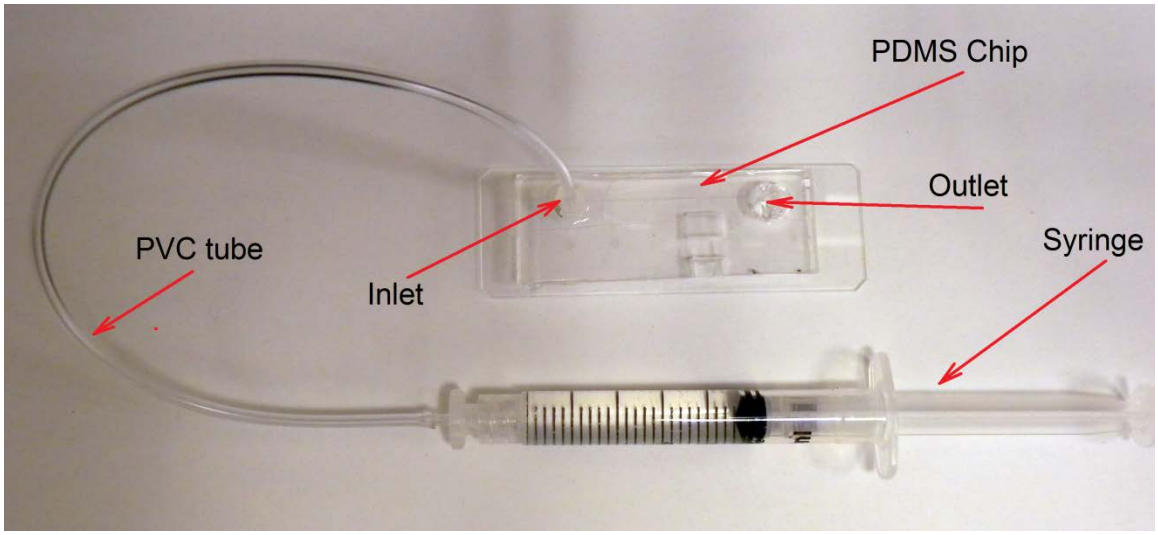

Figure 5. 2: The device setup for worm loading. The 3 mL syringe was connected to a 20 cm PVD tube and subsequently into the inlet of the PDMS chip.

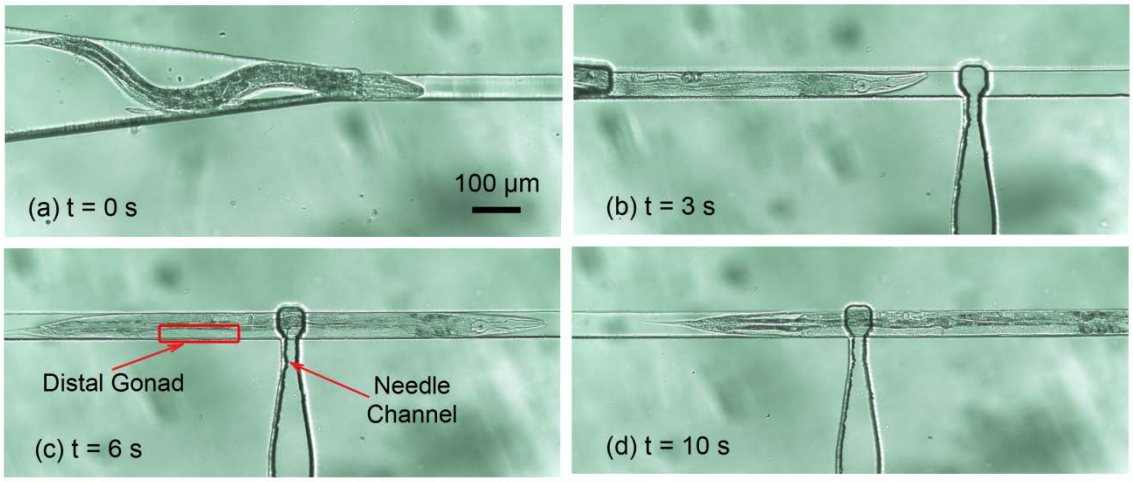

Figure 5. 3: image sequence of worm loading process. a) The worm was introduced into the immobilization channel, b) the worm was pushed into the immobilization channel, c) the worm was fully inserted into the immobilization channel and d) the distal gonad of the worm was aligned with needle channel for needle insertion

The functioning of the complaint mechanism and the microinjection were tested next by inserting the microneedle into the worm, once the worm was aligned in the right position in the immobilization channel (as in Figure 5. 3b). The microneedle was moved using the micropositioner described in section 5.2.. The displacement of the needle was observed and under microscope and its image sequence recorded as shown in Figure 5. 4. During this process, the needle was moved continually at steady rate (20 µm/s). Once its tip touched the worm, the needle deformed the body of the worm (Figure 5. 4b) and after certain deflection (~25 % of the width of the immobilization channel), the tip was inserted into the worm. The nematode body plan consists of an outer shell (including the cuticle, hypodermis, excretory system, neurons, and longitudinal muscles) separated from an inner compartment (including the pharynx, intestine, and gonad) by a fluid-filled pseudocoelom which is under a pressure of approximately 2-30 kPa. The tissue cut caused spillage of the fluid-filled in the pseudocoelom due to the internal pressure in it. This spillage can affect the viability of the worms. However, the size of the needle (the outer diameter) has a critical role on the amount of the liquid spilled and smaller diameter needles cause smaller spillage and have a lesser effect on viability. The total time to move the microneedle was approximately 5 s while displacement of the microneedle could be precisely controlled to increments of 5 µm under visual feedback. The experiments performed on compliant mechanism showed that the system worked successfully for *C. elegans* worm microinjection. However, a complete characterization of the mechanism was required, which is described in the following section.

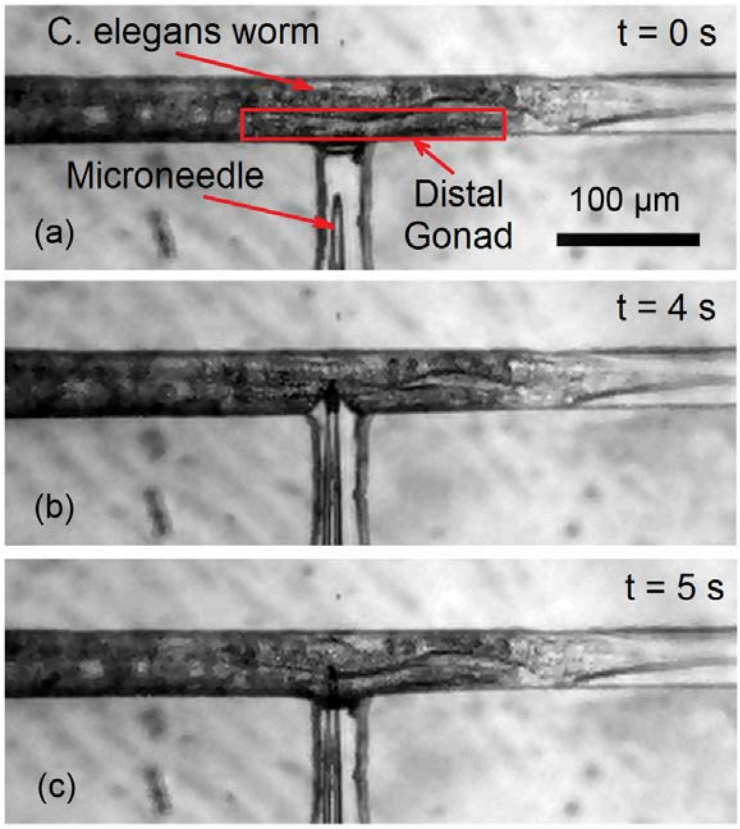

Figure 5. 4: image sequence of the needle insertion, a) the microneedle was aligned with distal gonad of the worm, b) the microneedle was moved and penetrated into the worm, c) the microneedle was inserted into the gonad and suitable for the reagent delivery

5.4.2. Characterization

5.4.2.1 Worm Loading

As described in the section 5.4.1, a constant manual pressure was applied to introduce the worms into the immobilization channel. For a certain defined immobilization channel (25 µm depth and 55 µm width here), the required time to introduce and align the worms (relative to the needle) into the immobilization channel was dependent on the applied

pressure. In order to characterize the required pressure with loading time, constant pressure in range of 50-200 (kPa) was applied inside the loading channel to load the worm in the immobilization channel. Subsequently, the immobilization process (Figure 5. 3) was observed and recorded from which the required loading time was calculated. The result of the experiment, loading time versus the loading pressure, has been plotted in Figure 5. 6. The results showed that at 50 (kPa) loading pressure or below, the worms could not be fully inserted into immobilization channel (see Figure 5. 5). When 50 (kPa) pressure was applied on the worms, only $1/3^{rd}$ of the length of the worm could be compressed into narrowed channel and the rest of worm was remained in the loading channel as shown in Figure 5. 5. (The experiment was performed on 5 worms and after 120s, the worms could not be inserted more than $1/3^{rd}$ of its length).

There are two forces, which were acting on the worm. One is the force due to pressure that pushes the worm through the narrow channel. The other was the frictional force on the body as it moves through the narrow channel, which was dependent to the length of the worm, inserted into the channel. At low pressures, the frictional force was greater and hence the worm stops to move at the certain length ($1/3^{rd}$ of the worm here). In contrast, at 200 (kPa) loading pressure or higher, the worm could not trapped by narrowed channel and all worms (n=5) passed the narrow channel (the loading time was reported as zero for these situation). The reason was that the friction force was overcome by loading pressure and the worm could freely move inside the immobilization channel. The pressure range from 75-100 (kPa) allowed a relatively fast loading process with a reasonable immobilization control inside the narrowed channel for all worms (n=5) in this geometry.

At this pressure range, the balance between pushing and friction forces was well controllable. Since this immobilization mechanism was of a passive design, the friction force caused by immobilization channel on certain *C. elegans* worm was dependent to the geometry of the channel. Therefore, the pressure range obtained in this experiment could be shifted to the lower pressure range by increasing the width and/or depth of the immobilization channel and via versa. The required time to load the worms was decreased from 37s to 3.5s while the pressure was increased from 75 (kPa) to 150 (kPa).

.

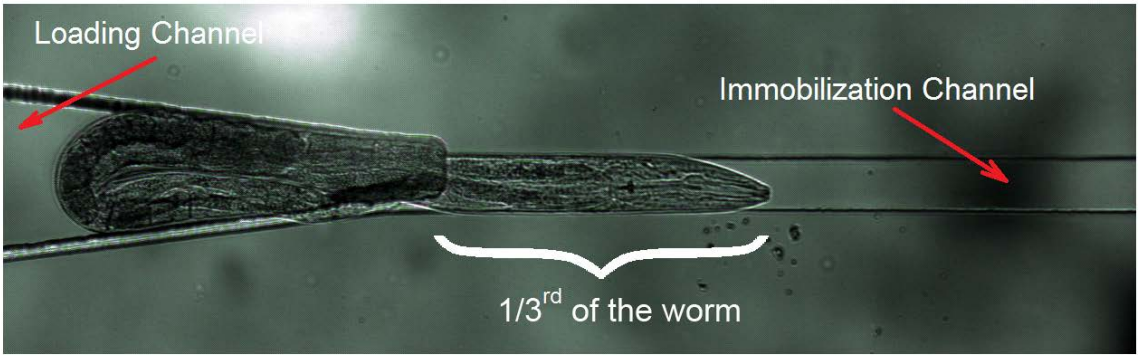

Figure 5. 5: At the loading pressure less than 50 (kPa), the worms could not be fully inserted into immobilization channel. When 50 (kPa) pressure was applied on the worms, only 1/3rd of the length of the worm could be compressed into narrowed channel and the rest of worm was remained in loading channel

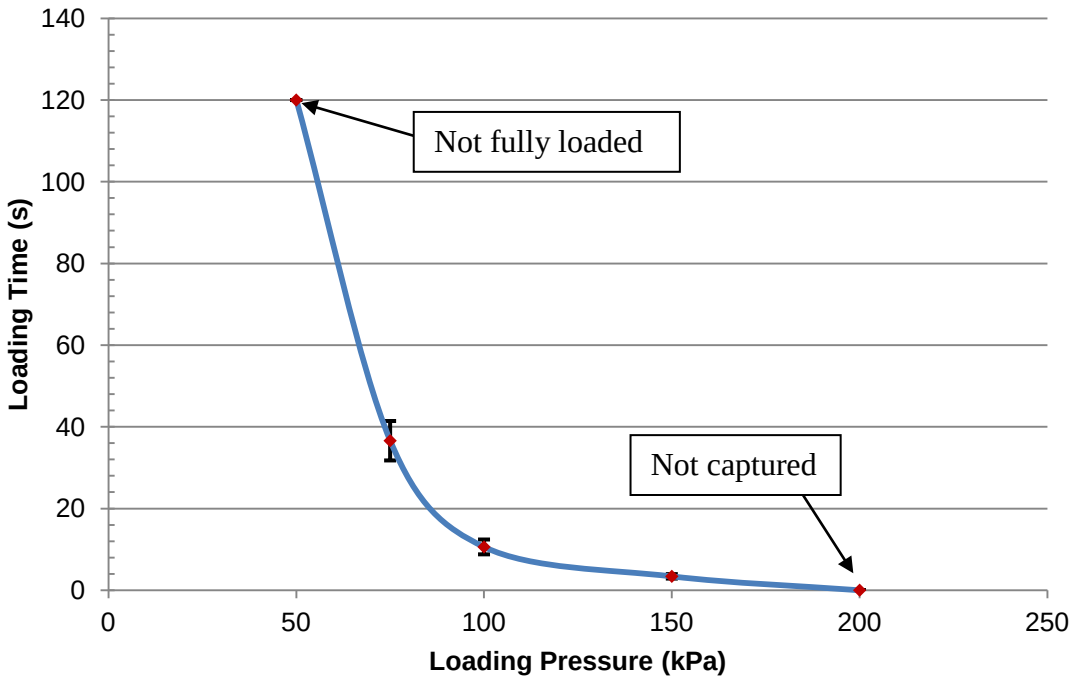

Figure 5. 6: The loading time versus the loading pressure. At *t = 120s*, the worm was not fully loaded and at *t = 0s*, the worm was not captured in the immobilization channel

5.4.2.2 Immobilization system

Once the worm was loaded, the immobilization channel was used to keep the worm inside for needle insertion. A young adult *C. elegans* worm (45 µm diameter and 1000 µm length) is a live and mobile worm. The primary characteristics for immobilization system were that it should be simple and fast to operate and, fixes the position of the body and various internal organs of the worm for injection. Additional criteria include that the immobilization system does not damage the worm and allows visualization of the internal organs of subsequent injection. These factors were dependent on the geometry of the immobilization channel including depth and width, which could be changed to obtain

the optimal design. The optimum geometry for immobilization and visualization for young adults has 55 µm width and 25 µm depth (see Figure 5. 7) as discussed in section 3.3.2.

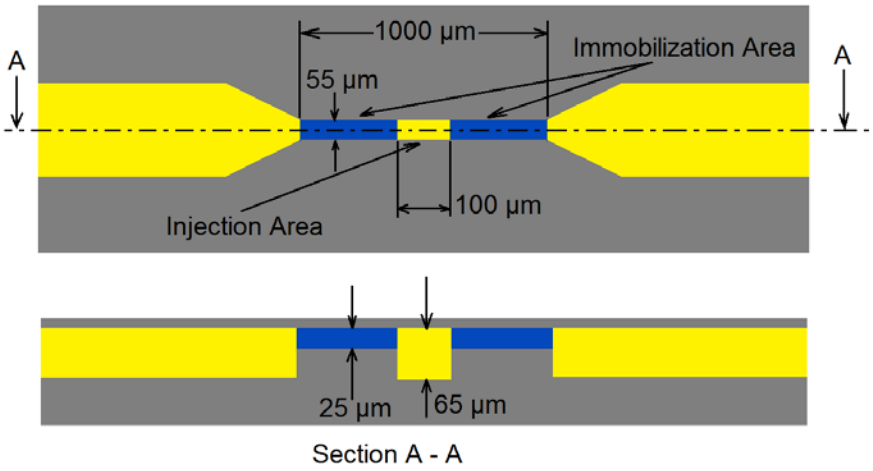

Figure 5. 7: The final design of the immobilization system. the narrowed channel had 25 µm depth with 55 µm width. The depth in the middle of the narrowed channel with length of 100 µm was increased to 65 µm where called as “injection area”.

Although, the compression of the worm was effective in immobilizing the animal, it could potentially have an impact on its viability [3]. In order to study the effect of mechanical stress caused by compression into narrowed channel (in this specific geometry) on the viability and reproduction rate of the worms, a set of experiments was conducted, as described below.

A total of 15 young adult Wild-type N2 *C. elegans* worms were loaded into narrowed channel consecutively by using method described in section 3.3.1 and immobilized. Then they were kept inside the channel for 5 minutes and subsequently unloaded and

distributed evenly (5 worms) on three agar plates (standard nematode growth (NG) agar plates containing OP50 Escherichia coli as a food source) to study the viability and reproduction of the worm after 72 (hr). A similar number of worms from the same batch was cultivated on the agar plates without putting them through the microdevice and used as control for comparison. The number of progenies on the plate after 72 (hr) was counted for each plate. To do this, first the worms on each plate were washed off with 2 mL of M9 solution into a 15 mL test tube. Next, the worm was distributed uniformly into the M9 solution by shaking the test tube and then, 50 μL of the suspension was dropped on a glass slide and then placed under the microscope (repeated 3 times for each plate). Subsequently, the image of the suspension spread on the slide was used to identify L4 and young adult worms from the L1, L2 and L3 worms and the younger worms were counted. Since we had started with only L4 worms, the L1, L2 and L3 worms present in the suspension must be the progenies of the older worms. Finally, the count of the worms in each plate was averaged, multiplied by the dilution factor (in order to obtain the total number of progenies in the entire sample) and divided by the number of L4 worms in each plate (n=5) in order to arrive at the average number of progenies for each condition as shown in Figure 5. 8.

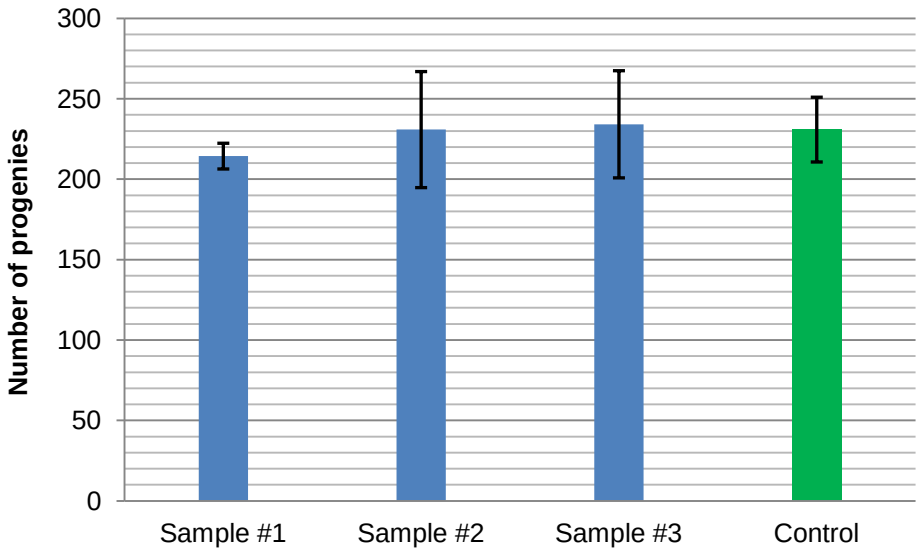

Figure 5. 8: Worms (n=5 for each plate) reproduction rate 72 hrs after 5 minutes immobilization compared to not immobilized control animals

The results demonstrate that the worms recovered well after being immobilized transferred to E. coli-bacteria (OP50) seeded agar plates (100% viable after 72 hrs). As compared to control sample, they moved normally and were indistinguishable from the control animals in their movement behavior (the frequency of their curling movement was visually compared with control sample and no significant difference was observed) . Moreover, their reproduction was not affected indicating that there was minimal stress or tissue damage due to immobilization in this format.

5.4.2.3 Compliant system

The compliant mechanism (described in more detail in section 3.3.3) is composed of three parts: (1) movable block, (2) PDMS membrane and (3) fixed block as previously show in Figure 3. 9a. The microinjection needle is attached to movable block. When the movable block is pushed using a micropositioner, it deflects the PDMS membrane and subsequently moves the microneedle inside needle channel (created on fixed block) as previously show in Figure 3. 9b.

The actuation mechanism employed for the needle movement should have the resolution of at least 5 µm ($1/4^{th}$ of the size of the gonad) for successful insertion. Moreover, the range of the needle motion should be at least as large as 400 µm along the length of the worm (2 times of the gonad length) and 100 µm across the width of the worm (2 times of the gonad diameter) to fully span the gonad region during the injection.

In this design, the movement of the worm in the direction along its length and its relative position with respect to the needle is controlled by the external syringe at the inlet and the pressure applied to it. The movement of the needle along the width of the worm is controlled by the compliant mechanism whose design has been described in section 3.3.3. The PDMS membrane, which forms the crucial element of the compliant mechanism, has the dimension of 7x5x1 mm (LxWxH).

The compliant mechanism provides a simple yet quick method for insertion of needle into the worm as seen in Figure 5. 10 where the needle tip is moved from its original position into the immobilization channel in fewer than 5s. The performance of the

compliant mechanism attached to the micropositioner was characterized by applying a known displacement to the micropositioner and measuring the actual movement of the microneedle tip. The needle motion was recorded under microscope and then, the videos were analyzed to obtain needle displacement by using a custom image processing procedure. Figure 5. 10 shows the displacement applied by the micropositioner (x-axis) and the resultant needle motion as measured through image analysis (y-axis). Since the initial position of the needle is not the same for all the devices, the needle position was normalized to the original position. It can be seen that the microneedle can be moved in a controllable and repeatable manner by using a micropositioner and a compliant mechanism. The relationship between the displacement of the needle tip and that of the micropositioner is not linear. This may be because the stiffness of the micropositioner was not constant and varied with the displacement.

In order to study the effect of the combination immobilization and injection on the viability and reproduction rate of the worms, a set of experiment (similar to the experiment was perform in section 5.4.2) was performed, as described below. Young adult Wild-type N2 *C. elegans* worms (n=15) were immobilized into narrowed channel and then the microneedle was inserted into the gonad for 2s and then removed. Subsequently, the worms were unloaded and plated to examine the effect of the microneedle insertion and the ensuing tissue damage on the viability and reproduction by using similar assay performed in section 5.5.2.

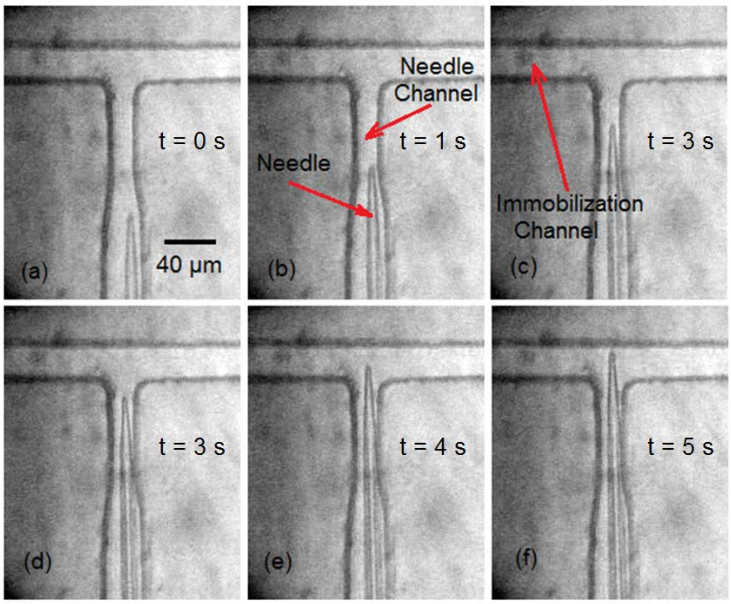

Figure 5. 9: The pictures of the time evolutions of the needle tip position. A known displacement (motion with the segment of 20 µm) was applied to the compliant mechanism (to the movable block) using a micropositioner and the actual movement of the microneedle tip was recorded and measured.

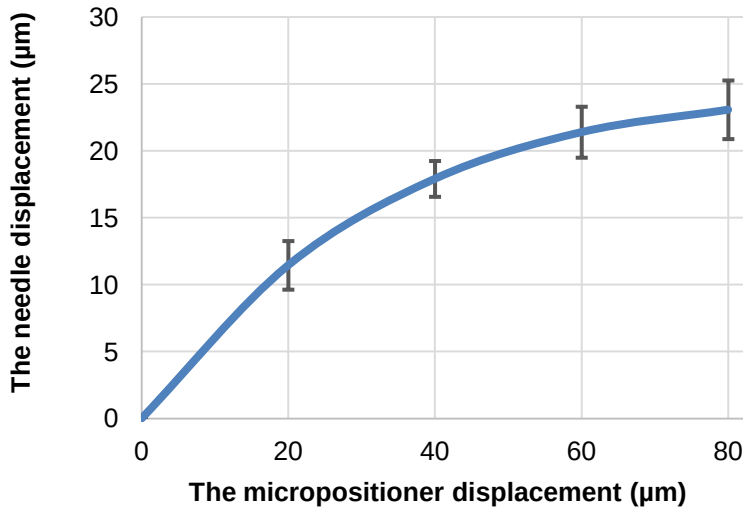

Figure 5. 10: The characterization of the compliant mechanism. A known displacement has been applied to the micropositioner and measuring the movement of the microneedle was calculated using images of the tip of the microneedle. The experiment has been repeated for 8 times on one device. The minimum resolution of the micropositioner was 20 um

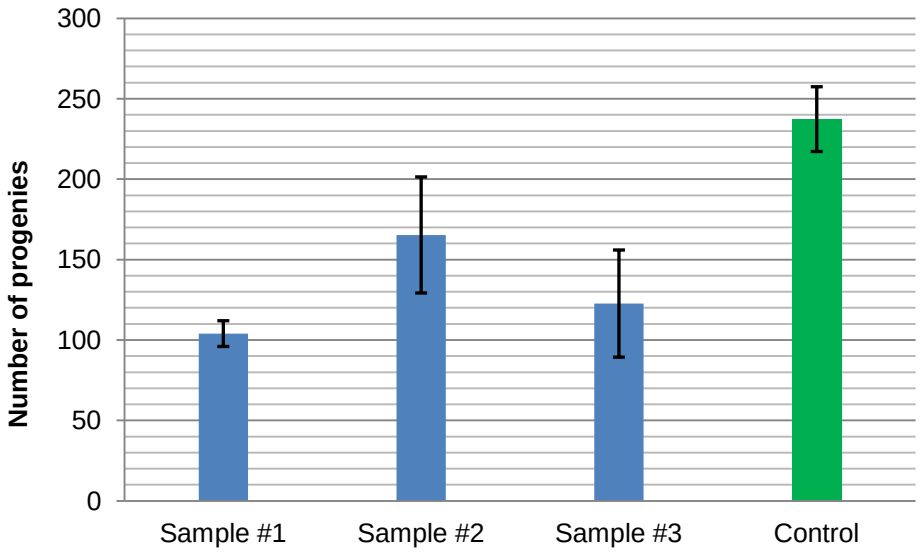

Figure 5. 11: Worms (n=5 for each plate) reproduction rate 72 hrs after needle insertion compared to not inserted control worms. Using the same assay used in section 5.5.2, a number of 15 worms distributed evenly (5 worms) on three agar plates and after 72 (hr), the number of the progenies per mother was counted for each plate.

The results (Figure 5. 12) demonstrated that number of the progenies for the injected worms were reduced (105-165 progenies) compared to the control worms (238 progenies) due to the effect of immobilization and injection (the error bar in Figure 5. 12 shows the standard deviation from three sample that were taken to count the number of the progenies). Since the immobilization alone does not cause any significant variation in the number of progenies, it can be concluded that the needle insertion and the ensuing tissue damage cause the reduction in the number of progenies produced by the worms. This decrease in the number of progenies is similar to the case of other microinjection procedures for *C.elegans*. Observation of the worms post injection on agar plate showed

that the worms were able to recover normal motion and were indistinguishable from the wild type within 24 hours after needle insertion.

5.4.2.4 Reagent delivery

The design for the reagent delivery system presented in section 3.3.4 consisted of a glass capillary (ID = 0.5 (mm), OD = 1 (mm) and length = 25 (mm)) that served as the reagent chamber attached to the end of the microneedle (5 µm inner diameter of needle tip, 250 µm taper length and 20 µm inner diameter of the shank of the needle). An automated pressure pulse was used to drive the reagent from the chamber through the microneedle into the worm. It was also determined that the reagent delivery system should have ability to transport 200 ± 20 pL of the reagent into the gonad. The volume of reagent delivered can be controlled by changing the pressure level as well as the duration of the pulse. In order to characterize the delivery characteristics of the system, and experiment setup as shown in Figure 5. 13 was used.

Here, the solenoid valve controlled by the computer was used to control the duration (set as 1s) of the pressure pulse and a pressure regulator connected to the gas cylinder was used to control the pressure level (200 kPa). The microneedle was inserted into a block of agar gel (1%) (Figure 5. 13) to mimic the consistency of the interior of the worm. Methylene blue dissolved in DI water (0.01 M) was used as a model injection reagent to visualize the movement of the liquid. Since the volume delivered in each pulse was small and cannot be easily visualized, a set of 1000 pulses (freq 0.5 Hz) were delivered and the

total volume injected calculated by the displacement of the solution interface in the reagent chamber. The volume delivered in each pulse was calculated by simply dividing the total volume delivered by the number of pulses applied and is plotted for five different attempts in Figure 5. 14. The results show that the delivery system was consistently able to deliver ~ 160 pL per pulse and the variation between different attempts was small which meets the design criteria for delivery.

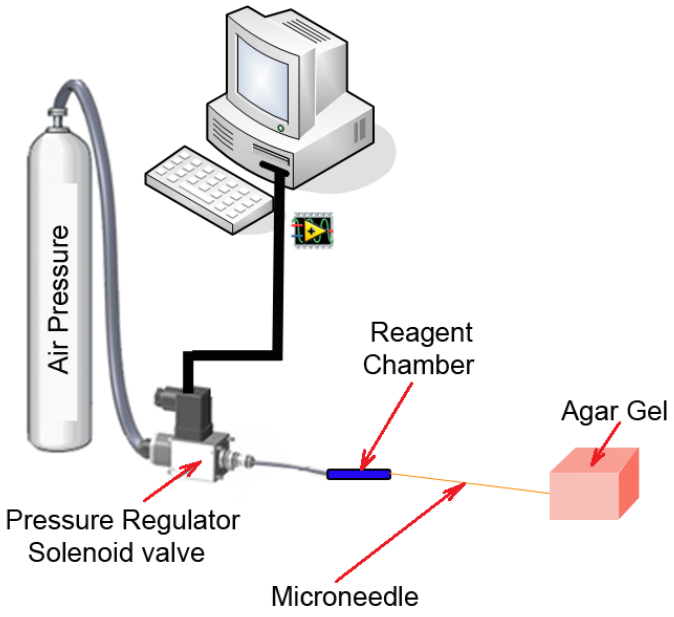

Figure 5. 12: The experiential setup used to characterize the reagent delivery system.

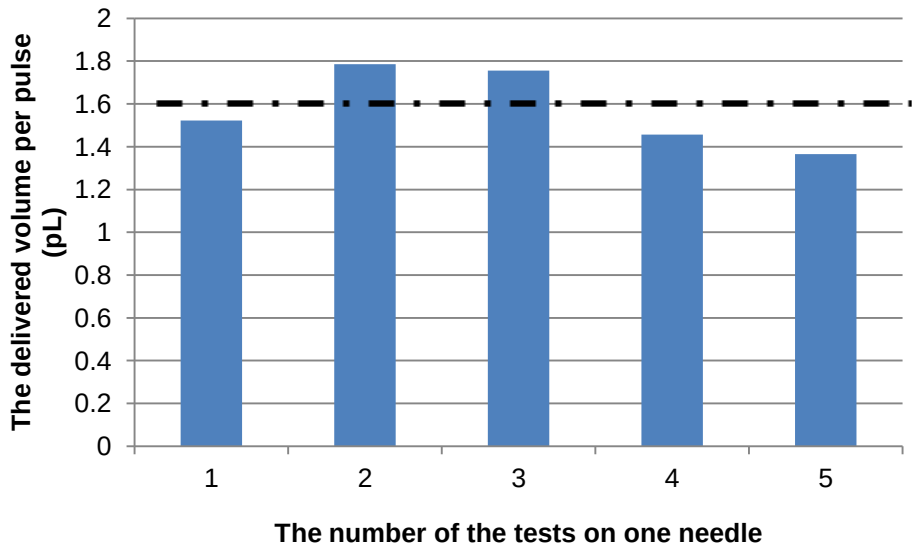

Figure 5. 13: The characterization of the reagent delivery system. For each pulse 200 kPa was applied for a duration of 1s . In average, 160 pL reagent can be delivered for each pulses. By controlling the duration of the pulses or the pressure level, the delivered volume can be controlled to achieve lower injected reagent per pulses.

5.4.3. Microinjection into the worm

5.4.3.1 Methylene blue injection

In order to visualize the delivery of reagents into the body of the worm, Methylene blue (0.05 M) was injected into the distal arm of the gonad using the microinjection device. The sequence of steps involved in the microinjection process is shown in Figure 5. 15. The L4 wild-type N2 C. elegans at 56 (hr) were loaded at the inlet. Subsequently, they were pushed into the immobilization channel and one of the two gonads was aligned with the tip of the needle (Figure 5. 15a), pneumatically under visual feedback. Following this, a micropositioner connected to the complaint mechanism was used to gradually move the

needle and penetrate the distal end of the gonad (Figure 5. 15b). Then, by applying 2 pressure pulses with the magnitude of 200 KPa and 1(s) duration, the reagent in the microneedle was delivered into the gonad (Figure 5. 15c). Afterwards, the worm was unloaded and transferred into outlet chamber (Figure 5. 15d).

The results showed that the reagent could be successfully injected into the worm and the dye was distributed in worm after injection. As illustrated in Figure 5. 15d, the injected dye did not come out of the injection spot during the unloading process, which indicated that compression pressure in the immobilization channel does not affect the ability of the dye to remain in the worm in a significant way. However, visualization with Methylene blue did not provide sufficient contrast to identify the movement of the dye inside the worm post injection. Therefore, a DNA solution bound to fluorescent dye was used in the next section to study the distribution of the dye into the gonad after injection.

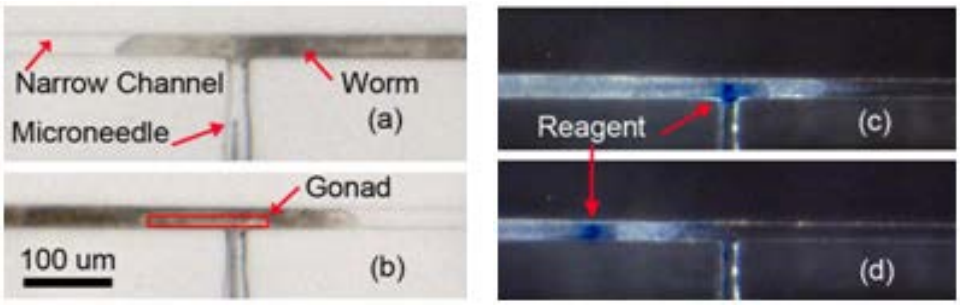

Figure 5. 14: The sequence of four steps for microinjection: a) loading and immobilization, b) needle penetration, c) reagent injection and d) unloading.

5.4.3.2 DNA injection

A DNA solution bounded to green fluorescent dye was injected into the gonad using the same process as described in previous section in order to visualize the distribution of the dye inside the body of the worm post injection. First, the fluorescent DNA reagent consisted of 1 µL UltraPure™ Salmon Sperm DNA Solution (concentration of 10 mg/mL, Life Technologies Co., Canada), 1 µL Acridine Orange (concentration of 10 mg/mL, SIGMA-ALDRICH, Canada) and 1 mL DI water was prepared (the components were mixed and the solution was kept 30 minutes at room temperature and then stored into -20^{o} fridge). Acridine Orange is a nucleic acid binding dye that emits green fluorescence when bound to dsDNA such as sperm (red fluorescence when bound to ssDNA or RNA). Next, the 2 µL reagent chamber was filled by the green fluorescent dye. Then, the Wild-type N2 *C. elegans* were loaded, injected and unloaded as described previously and the fluorescent image of the injected worms were recorded and shown in Figure 5. 16a and 5.16c. In order to compare, other worms were injected at multiple locations using conventional method described in section 2.5 and the fluorescent image of the injected worms were recorded and shown in Figure 5. 16b and 5. 16d.

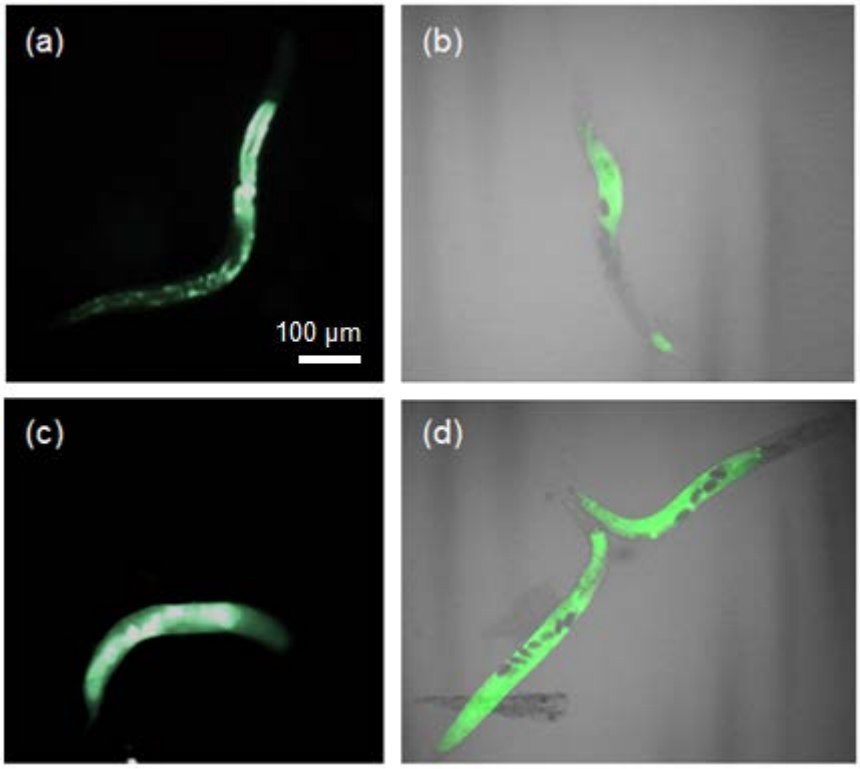

Figure 5. 15: GFP dye was delivered into gonad (a-b) and the intestine (c-d) in both conventional (right) and microfluidic method (left). The scale bar shown in (a) is the same on (b-d)

It can be seen from Figure 5. 16a, b that the DNA solution is located to a small region in the body, while in the case of Figure 5. 16c and d, the dye is distributed throughout the body of the worm. This can be explained by the location of delivery. Figure 5. 16a, b are typical when the injection occurred in the gonad which is located in the mid section of the worm. Figure 5. 16c, d are typical of delivery into the intestine which extends throughout the entire stretch of the worm. In order to identify the probability of injection into the gonad, a group of 30 young adult *C. elegans* worms were immobilized, gonad aligned to the microneedle and injected with DNA solution in the microdevice. Analysis of

fluorescent images post injection revealed that 63% (19 worms) of the injections were delivered into the gonad and 37% (11 worms) into the intestine. The reason that 37% of the injections into the intestine can be explained based on the cross sectional orientation of the worm body with the microneedle tip at the time of injection as shown in Figure 5. 17. The cross-section of young adult *C. elegans* worm shows that if the orientation of the gonad were aligned with needle (Figure 5. 17a), the injection would happen into the gonad. However, any misalignment between the needle and the gonad would lead the needle injection into the intestine of the worm (see Figure 5. 17b) which was happened into 37% of the injections in this experiment. These two situations cannot be distinguished from each other, as the visualization mechanism is top down and 2D.

The results showed that the DNA solution could be successfully (with success rate of 63%) injected into the distal gonad. However, the DNA solution used in this experiment was only a model reagent to track the distribution of the reagent after injection and it could not be used to create transgenic worms which is the main goal of this project. In order to show the capacity of the microinjector for creating transgenic *C. elegans* worm, the next set of the experiment was performed.

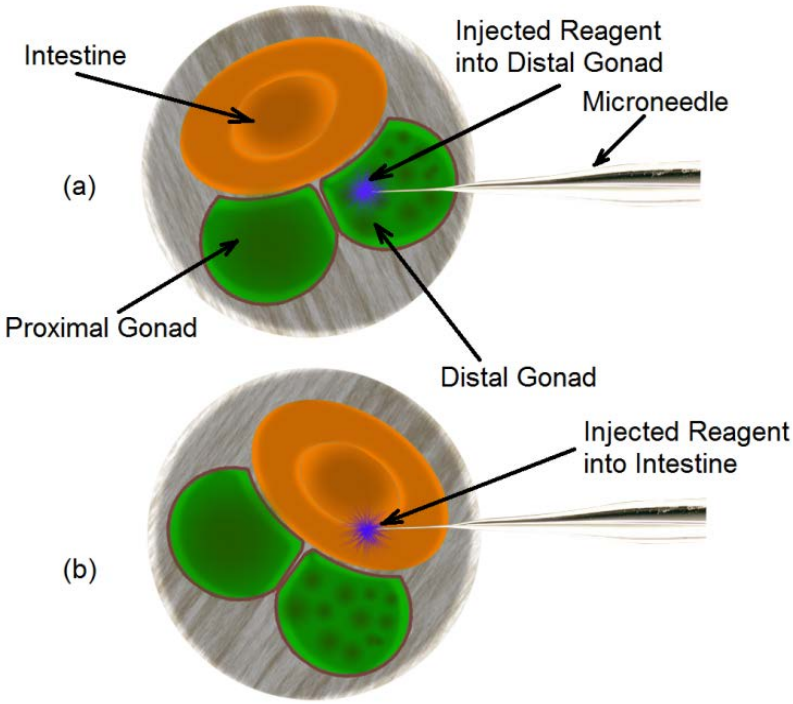

Figure 5. 16: The cross-section of the young adults *C. elegans* and its alignment relative to the microneedle inside the microinjector. a) The microneedle is properly aligned with the distal gonad b) the microneedle is aligned with the intestine instead of distal gonad and the reagent is delivered into the intestine

5.4.3.3 DNA Plasmid injection

In this set of experiments, a DNA plasmid that introduces gene modification in the MYO-2 gene as well as expresses GFP simultaneously was injected into young adult *C. elegans* worm. As described in section 2.4, transgenesis is a relatively new technology to introduce new inherent characteristics into organisms by deliberate modification of DNA sequences. By using RNAi, it is possible to change the expression levels (up regulate or down regulate) of a specific gene. The resulting modifications to the anatomy, physiology

or behaviour would then indicate the role of that gene in the functioning of the organism. MYO-2 encodes a pharyngeal muscle-specific myosin heavy chain isoform. Along with other myosins, MYO-2 is an ATP-dependent motor protein with an important role in muscle contraction, where it mediates actin-based motility. RNAi-mediated knockdown of MYO-2 produces animals that develop severe abnormalities in pharyngeal morphology and exhibit both embryonic and larval arrest phenotypes [95]. The myo-2::GFP plasmid encodes for both the MYO-2 gene as well as a GFP gene and produces robust fluorescence throughout the pharynx when successfully incorporated. Therefore, this gene transcript was used as a model to demonstrate the generation of transgenic species in *C.elegans*.

In order to show the capability of the microinjector chip for creating transgenic *C. elegans*, the volume of ~150 pL (corresponding to 1 pulse at pressure level of 2 bar) of myo-2::GFP was injected into distal gonad of 25 wild-type N2 *C. elegans* worm at 56 (hr) by using procedure described in section 5.6.3. The adult ovary is composed of a common compartment of cytoplasm containing multiple nuclei (syncytium) and once the plasmid DNA was injected into the distal gonad, the plasmid will randomly go into multiple nuclei existing in cytoplasm of the syncytium. Therefore, the Oocytes, which are formed when plasma membranes enclose individual germ-line, will contain the desired gene as an extra chromosome and the next generation of injected worm will express the gene. the next generation of injected worms were cultivated by equally distributing the injected worms on 5 agar plates for recovery and reproduction. The GFP image of the

first generation (F1) progeny shown in Figure 5. 18 clearly demonstrate the incorporation of gene into the genome of the worm.

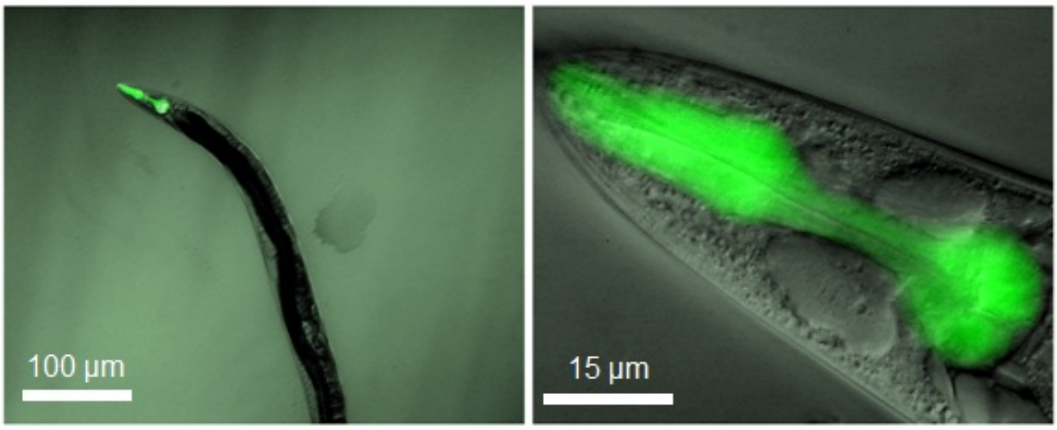

Figure 5. 17: Myo-2::GFP construct is commonly employed as a co-injection marker to label extrachromosomal arrays. The GFP image shows that the microinjector is applicable for creating transgenic *C. elegans*.

The results demonstrated that out of the 5 plates, one plate contained transgenic worms which means that the efficiency of the injection was between 4% to 20% depending on the number of the mothers which created transgenic line. Comparing it to conventional method, both methods have the same success rate (5%-15%), while microfluidic injection was faster and easier than conventional microinjection.

In this example, the procedure of loading and gonad aligning, needle actuation, reagent delivery and unloading took 10s, 5s, 5s and 5s respectively and 30s in total. The time required for the injection was strongly depended on the speed of gonad aligning, actuation speed of the needle and the delivery speed of required reagent. The loading

process and needle actuation, both were achieved using a manually-operated syringe and linear micropositioner, respectively. However, it was expected that the injection time can be reduced to 5–10s by using an automated loading (unloading) and actuation mechanisms. Since the gonad of the *C. elegans* worm is visually distinguishable (see Figure 5. 19), a real-time image processing software (e.g. MATLAB©) could be could be used to detect and control the loading process to achieve a high-speed loading process. The needle actuation could be accelerated by using high-speed step motor to perform a fast and an accurate open-loop control system for needle actuation.

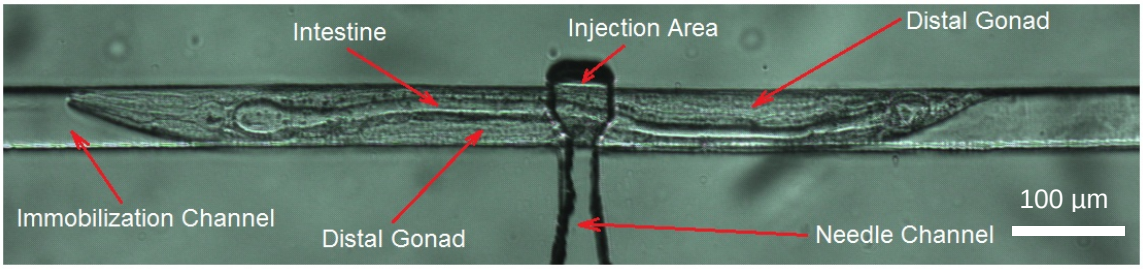

Figure 5. 18: An immobilized *C. elegans* worm inside the narrowed channel. The picture shows that the narrowed portions of the immobilization channel would allow easy visualization of the internal organs as well as allow consistent immobilization

5.5. Summary

This chapter presented the experimental setup, characterization and results obtained from the injection device. The setup used for the device, and the characterization of the loading system, immobilization channel, compliant mechanism and reagent delivery system of the device were described. From the results, the pressure range 0.75-1 (bar) was appropriate for a

fast and controllable loading process. The single DOF compliant mechanism, showed a robust and smooth motion for needle insertion. The chapter then highlighted the characterization of the reagent delivery system, The pressure pulses with pressure level of 200 (bar), duration of 1 (s) and frequency of 0.5 (Hz) was successfully deliver 160 pL reagent for each pulse. Subsequently, the results obtained in the injection of *C. elegans* worm with Methylene blue and GFP dye were presented in order to study the and track the location of the delivered reagent inside the gonad. Finally, the results showed the capability of the microinjector chip for creating transgenic *C. elegans* by injecting myo-2::GFP into wild-type N2 *C. elegans* at 56 (hr).

Chapter 6: Conclusion and Future Work

6.1. Conclusion

In conclusion, we have presented a microfluidic device for microinjection of *C. elegans* worm. The microinjector designed in this research was capable of simultaneously immobilizing a freely mobile animal such as *C.elegans* and performing microinjection by using a simple and fast mechanism for needle actuation. The entire process of the microinjection takes ~30 seconds which includes 10s for worm loading and aligning, 5s needle penetration, 5s reagent injection and 5s worm unloading. The capability of the microinjector chip for creating transgenic *C. elegans* was illustrated (with success rate between 4% to 20%) by injecting ~150 pL (corresponding to 1 pulse at pressure level of 2 bar) of myo-2::GFP DNA plasmid into distal gonad of 25 wild-type N2 *C. elegans* worm at 56 (hr).

Simple operation and low cost of making the devices are key to successful uptake of this device among end users. By using microcapillaries and embedding them in cast microchannels and using integrated compliant mechanism, the cost of manufacture was reduced compared to micropositioner used in conventional method. Moreover, the device is fabricated by low cost materials such as PDMS, glass slide and microcapillaries which further decreases the cost of the device.

A passive immobilization mechanism was also developed. The passive immobilization mechanism design in this research was suitable for rapid and high throughput immobilization which is simple to operate and easy to fabricate. The design allowed complete immobilization of *C.elegans* worm for large durations of time (more than 10 minutes) as well as in enabling clear visualization of the gonad with minimum viability effect on the worms.

Although, the microinjector designed in this research addressed many problems involved in current microinjection methods (e.g. slow, low throughput and complex protocols, requiring expensive equipment and skilled operator), the system still works manually and the transfection efficiency of the microinjector is still low. In order to automate the system for higher throughput and increase the transfection efficiency, some correction would be applied on this design, which can be pursued in the future.

6.2. Future work

The first aspect that can be investigated in future in order to automate the system for higher throughput (in the range of 1000 injection/hr) the system, is parallel microinjection. By placing several microneedles in parallel with several immobilization microchannel, the throughput of the device can be increased. Currently, the loading process and needle actuation, both were achieved using a manually-operated syringe and linear micropositioner, respectively. However, it was expected that the injection time can

be reduced to 5–10s by using an automated loading (unloading) and actuation mechanisms. Therefore, an effect of an automated system on the throughput of the microinjector can be investigated.

The other aspect, which can be investigated to increase the trasfection efficiency, is Electroosmotic delivery. In this research, capillary pressure microinjection (CPM), which uses pressure driven flow (PDF) was used to transport the reagent into the distal gonad which is a well established and the simplest technique to inject a wide range of substances, including naked DNA, RNA, antibodies and nanoparticles into cells with high transfection efficiency (up to 100%) and low cytotoxicity. However, pressure driven into the distal gonad might affect the transfection efficiency since the sudden flow into the goad mixed material inside the gonad. Electroosmotic flow (EOF), which is caused by the movement of charge within the fluid, for reagent transport would be an option to examine the effect of the sudden flow on the trasfection efficiency. For the reason that the electroosmosis flow is a gentle flow and it does not blend the liquid inside the gonad.

Finally, the effect of the insertion angle on the trasfection efficiency can be examined in future works. The insertion angle with respect to the tissue might be a factor to affect the transfection efficiency. The length of the needle, which travels through the gonad, defines the location of the reagent delivery. If the delivery location were closer to the insertion location, the chance that the reagent spill out after delivery would be higher. The insertion length can be controlled by changing the insertion angle. Therefore, the effect of

various insertion angles on the transfection efficiency and its variation as function of the inserted length into the gonad can be investigated.

In short, by overcoming the existing problems in designed microinjector, the efficiency and thoroughput of the microinjector injector can be significantly increased. Such an automated design, will allow high-throughput microinjection that could be used for drug discovery assays. Through this process, active molecules, antibodies or genes, which modulate a particular biomolecular pathway, can be identified quickly.

Appendix A: Device Fabrication

1. SU-8 Mold Fabrication

A) First layer

1. Wash silicon wafer in Acetone and Methanol solution each one for 1 minutes.

2. Rinse the wafer with DI water for 5 minutes and then blow nitrogen gas to dry it.

3. After putting the wafer on 150 ^{o}C hotplate for 2 minutes, place the wafer in plasma etcher at 50Watt for 50 seconds.

4. Spin SU8-3035 photoresist on the wafer at 500 rpm for 20 second and then Ramp up the speed to 3900 rpm at an acceleration of 100 rpm/s and spin at final speed for 30 second.

6. Prebake the wafer at 95 ºC for 10 minutes.

9. Align the wafer and mask on mask aligner by using the first layer mask.

10. Expose the wafer to UV light for total exposure energy of 150 mJ/cm^2.

11. Post bake at 65 ºC for 1 minute.

12. Increase post bake temperature to 95 ºC and maintain the temperature for 3 minutes.

13. Submerge wafer into developer solution and slowly stir until the features are clear.

14. Use Isopropyl alcohol (IPA) to check the complete removal of unexposed photoresist.

15. Re-submerge wafer back in developer solution if white residual appears.

16. Rinse with DI water and blow nitrogen air to dry the wafer.

17. Hard bake at 120 ºC for 10 minutes.

A) Second layer

1. Wash silicon wafer in Isoproponal alcohol (IPA) for 1 minutes.

2. Rinse the wafer with DI water for 5 minutes and then blow nitrogen gas to dry it.

4. Spin SU8-3035 photoresist on the wafer at 500 rpm for 20 second and then Ramp up the speed to 2000 rpm at an acceleration of 100 rpm/s and spin at final speed for 30 second.

6. Prebake the wafer at 95 ºC for 10 minutes.

9. Align the wafer (the first pattern) with second pattern by using aligner.

10. Expose the wafer to UV light for total exposure energy of 150 mJ/cm^2.

11. Post bake at 65 ºC for 3 minute.

12. Increase post bake temperature to 95 ºC and maintain the temperature for 5 minutes.

13. Submerge wafer into developer solution and slowly stir until the features are clear.

14. Use Isopropyl alcohol (IPA) to check the complete removal of unexposed photoresist.

15. Re-submerge wafer back in developer solution if white residual appears.

16. Rinse with DI water and blow nitrogen air to dry the wafer.

17. Hard bake at 120 ºC for 10 minutes.

18. Manually mix base to curing agent of PDMS at ratio 10:1 for 3 minutes.

19. Put a small droplet of PDMS mixture (< 2 µL) on the base of the (5x5x2 mm^2) 3D printed fixture

20. Place the 3D printed fixture on the needle channel with distance of ~5 mm from the immobilization channel

2. Channel replica

1. Manually mix base to curing agent of PDMS at ratio 10:1 for 3 minutes.

2. Degas PDMS the mixture in vacuum chamber for 5 minutes.

3. Cut 10 mm segment of silicone tubing (1.5/4.8 mm ID/OD) and place them on SU8 mold (on the reservoir of worm inlet and washing channel)

4. Pour PDMS mixture onto SU8 mold for the thickness of 3 mm.

5. Bake at 85 ºC on hotplate for 2 hours

6. Peel the PDMS channel off and use 2 mm hole puncher (Harris Inc.) to clean the PDMS pieces in the silicone tubing.

7. Disconnect the PDMS membrane and movable block from the rest of the PDMS substrate.

3. Device assembly

1. Place the PDMS substrate upside down under optical microscope (100-200x magnification); therefore, the needle channel was accessible for the needle assembly.

2. After filling the needle chamber with DI water, genteelly put the microneedle on the PDMS substrate and then move and align it into the needle channel, so that the tip of the microneedle had the distance of ~100 µm to 200 µm from the immobilization channel.

3. Insert the shank of the needle into needle channel on the movable block.

4. Spread a droplet (~1 uL) of the PDMS (4: 1 ratio of the base and crosslinker) on the movable block to fully attach the microneedle to the movable block.

5. After curing the PDMS glue using the flame of the match, drive some reagent through the microneedle to make sure that the needle is still open and then take off the PDMS

chip from the microscope for bonding. If the microneedle was clogged, genteelly touch the tip of the microneedle by using a sharp scalpel and then pressurized the chamber again. Repeat the process as more as required to open the needle.

6. Expose the PDMS substrate and a 75x25 mm^2 glass slide to 50W oxygen plasma for 70s.

7. Since the plasma machine worked in low level of the pressure, the DI water available inside the reagent chamber would be evaporated. Therefore, after taking off the PDMS chip from the plasma machine, fill the reagent chamber with reagent required for microinjection.

8. Spread a thin layer of grease on the movable block to reduce the friction of the motion during the needle actuation.

9. Place the PDMS chip under microscope and connect a 10 mL syringe to the reagent chamber. By pressurizing the reagent chamber, examine the clogging of the needle. If the needle was clogged, by touching the tip of the microneedle via a sharp and clean scalpel, the tip of the needle could be opened. It is important to be note that the force during the touching should not be high that breaks the needle.

10. Genteelly place the microneedle into needle channel in PDMS substrate by using a forceps.

11. Finally, bond the glass slide to the PDMS chip to complete the fabrication process.

GLOSSARY

Anus	Is an opening at the opposite end of an animal's digestive tract from the mouth. Its function is to control the expulsion of feces, unwanted semi-solid matter produced during digestion, which, depending on the type of animal, may include matter which the animal cannot digest.
AutoCAD	Is a software application for 2D and 3D computer-aided design (CAD) and drafting .
Cell toxicity	Cell toxicity or *Cytotoxicity* is the quality of being toxic to cells.
Deflexed	Bent or turned abruptly downward at a sharp angle.
Degree of Freedom	In statistics, the number of degrees of freedom or DOF is the number of values in the final calculation of a statistic that are free to vary.
DI water	Deionized Water (We call it "DI water" in the chemistry labs) is just what it sounds like Water that has the ions removed. Tap water is usually full of ions from the soil (Na+, Ca2+), from the pipes (Fe2+, Cu2+), and other sources. Water is usually deionized by using an ion exchange process.
DNA	Deoxyribonucleic acid (DNA) is a molecule that encodes the genetic instructions used in the development and functioning of all known living organisms and many viruses.
Drug discovery	Is the process by which new candidate medications are discovered.
Electrophoretic potential **Electrophoresis**	Is the motion of dispersed particles relative to a fluid under the influence of a spatially uniform electric field.
Endocytosis	A process which cell absorbs required molecules such as protein by engulfing the particle and use of that required energy.

Endosomal	Is a membrane-bounded compartment inside eukaryotic cells involved in endocytosis pathway.
Ex vivo	Ex vivo (Latin: "out of the living") means that which takes place outside an organism. In science, ex vivo refers to experimentation or measurements done in or on tissue from an organism in an external environment with the minimum alteration of natural conditions.
Exogenous	An action or object brought in from outside of the cell.
F1 Generation	The first generation of a model organism
Fluid-filled pseudocoelom	That arises from an embryonic cavity and contains the internal organs free within it.
Gene therapy	Is the use of DNA as a drug to treat disease by delivering therapeutic DNA into a patient's cells.
Genotype	Is the genetic makeup of a cell, an organism, or an individual usually with reference to a specific characteristic under consideration.
GFP marker	The green fluorescent protein (GFP) is a protein composed of 238 amino acid residues (26.9 kDa) Green fluorescent protein as a marker for gene expression
Gonad	A primary reproductive organ producing reproductive cells(gametes). In males the gonads are called testes; the gonads in females are called ovaries.
ID	Inner diameter
Immunogenicity	Is the ability of a particular substance, such as an antigen or epitope, to provoke an immune response in the body of a human or animal.
Insertional mutagenesis	Is mutagenesis of DNA by the insertion of one or more bases.
In vitro	Are those that are conducted using components of an organism that have been isolated from their usual biological surroundings in order to permit a more detailed or more convenient analysis than can be done with whole organisms.

In vivo	Is experimentation using a whole, living organism as opposed to a partial or dead organism, or an in-vitro.
iPS cell	Induced pluripotent stem cells are a type of pluripotebt stem cell that can be generated directly from adult cells.
Knock-down mutants	Is a genetic technique in which one of an organism's genes are made inoperative. These organisms are used in learning about a gene that has been sequenced, but which has an unknown or incompletely known function.
Lysosomal	The cell's waste disposal system which can digest some compounds.
Model organisms	A non-human species that is extensively studied to understand particular biological phenomena, with the expectation that discoveries made in the organism model will provide insight into the workings of other organisms.
OD	Outer Diameter
Phagocytosis	A process by which a cell engulfs particles to form an internal vesicle known as a phagosome.
Pharynx	Is an organ found in animals, including humans. It is part of the digestive system and also the respiratory system.
Phenotype	A phenotype is the composite of an organism's observable characteristics or traits, such as its morphology, development, biochemical or physiological properties, phenology, behavior, and products of behavior.
Plasmid DNA	A small DNA molecule that is physically separate from, and can replicate independently of, chromosomal DNA within a cell.
siRNA	Small interfering RNA (siRNA) or short interfering RNA or silencing RNA, is a double stranded RNA molecules. Important in RNA interference (RNAi) pathway and expression of specific genes.
The permeability of the cell	The cell membrane is selectively permeable to ions and organic molecules and controls the movement of substances in and out

	of cells.
Transduction	A process by which DNA is transferred to a virus form a bacteria.
Translocation	a chromosome translocation is a chromosome abnormality caused by rearrangement of parts between nonhomologous chromosomes.
Viability	Capable of living, developing, or germinating under favorable conditions.

LIST OF REFERENCES

[1] F. Recillas-Targa, “Multiple strategies for gene transfer, expression, knockdown, and chromatin influence in mammalian cell lines and transgenic animals”, *Mol Biotechnol*, Vol. 34, No. 3, PP. 337–354, 2006

[2] D.J. Glover, H.J. Lipps and D.A. Jans, “Towards safe, non-viral therapeutic gene expression in humans”. *Nat Rev Genet* , Vol. 6, No. 4, PP. 299– 310, 2005

[3] F.M.Wurm, “Production of recombinant protein therapeutics in cultivated mammalian cells”. *Nat Biotechnol*, Vol. 22, No. 11, PP. 1393–1398, 2004

[4] A. Pfeifer and I.M. Verma, “Gene therapy: promises and problems”. *Annu Rev Genomics Hum Genet*, Vol. 2, pp. 177–21, 2001

[5] K. Takahashi and S.Yamanaka, “Induction of pluripotent stem cells from mouse embryonic and adult fibroblast cultures by defined factors s”. *Cell*, Vol. 126, No. 4, PP. 663–676, 2006

[6] A.J. Hamilton and D.C. Baulcombe, “A species of small antisense RNA in posttranscriptional gene silencing in plants”. *Science*, Vol. 286, No. 5441, PP. 950–952, 1999.

[7] R. L. Brinster, “The effect of cells transferred into the mouse blastocyst on subsequent development”, *The Journal of experimental medicine*, Vol. 140, No. 4, pp. 1049-1056, 1974.

[8] Palmiter, D. Richard and Ralph L. Brinster, “Germ-line transformation of mice”, *Annual review of genetics*, Vol. 20, No.1, pp. 465-499, 1986.

[9] E.T. Schenborn and V.Goiffon, “DEAE-dextran transfection of mammalian cultured cells”. *Meth Mol Biol*, Vol. 130, PP. 147–153, 2000.

[10] S.L. Holmen, M.W. Vanbrocklin, R.R. Eversole, S.R. Stapleton and L.C. Ginsberg, “Efficient lipid-mediated transfection of DNA into primary rat hepatocytes”. *In Vitro Cell Dev Biol Anim*, Vol. 31, No. 5, PP. 347–351, 1995

[11] P. Washbourne and A.K. McAllister, “Techniques for gene transfer into neurons”. *Curr Opin Neurobiol*, Vol. 12, No. 5, PP. 566–573, 2002.

[12] T.K. Kim and J.H. Eberwine, “Mammalian cell transfection: the present and the future”. *Anal Bioanal Chem*, Vol. 397, No. 8, PP. 3173–3178, 2010.

[13] J.K. Rose, L. Buonocore, M.A. Whitt, “A new cationic liposome reagent mediating nearly quantitative transfection of animal cells”, *Biotechniques*, Vol. 10, No. 4, pp. 520-525, 1991.

[14] A. Mortellaro, R. J. Hernandez, M. M. Guerrini, F. Carlucci, A. Tabucchi, M. Ponzoni, ... & A. Aiuti, “Ex vivo gene therapy with lentiviral vectors rescues adenosine deaminase (ADA)–deficient mice and corrects their immune and metabolic defects”, *Blood*, Vol. 108, No. 9, pp. 2979-2988, 2006.

[15] A. C. Nathwani, E. G. Tuddenham, S. Rangarajan, C. Rosales, J. McIntosh, D. C. Linch, ... & A. M. Davidoff, “Adenovirus-associated virus vector–mediated gene transfer in hemophilia”, *B. New England Journal of Medicine*, Vol. 365, No. 25, pp. 2357-2365, 2011

[16] N.B. Woods, A. Muessing, M. Schmidt, J. Flygare, K. Olsson, P. Salmon, D. Trono, C. Von Kalle and S. Karlsson, “Lentiviral vector transduction of NOD/ SCID

repopulating cells results in multiple vector integrations per transduced cell: risk of insertional mutagenesis". *Blood* , Vol. 101, No. 4, PP. 1284–1289, 2003

[17] S. Mehier-Humbert, T. Bettinger, F. Yan and R.H. Guy, "Ultrasound-mediated gene delivery: Kinetics of plasmid internalization and gene expression" *Journal of Controlled Release* Vol. 104, No. 1, PP. 203-211, 2005

[18] D.C. Lo, A.K. McAllister and L.C. Katz, "Neuronal transfection in brain slices using particle-mediated gene transfe"r. *Neuron*, Vol. 13, No. 6, PP. 1263–1268, 1994

[19] J.A. O'Brien , S.C. Lummis, "Biolistic transfection of neuronal cultures using a hand-held gene gun", *Nat Protoc*. Vol. 1, No. 2, PP. 977–981, 2006

[20] A.L. Parker, C. Newman, S. Briggs, L. Seymour and P.J. Sheridan, "Nonviral gene delivery: techniques and implications for molecular medicine", *Expert Reviews in Molecular Medicine*, Vol. 5, No. 22, PP. 1-15, 2004

[21] F. M. Cheng and K. E. Joho, "Effect of biolistic particle size on the efficiency of transfection of oocytes in Xenopus ovary tissue", *Nucleic acids research*, Vol. 22, No. 15, pp. 3265-3266, 1994.

[22] C. W. Liu, C. C. Lin, J. C. Yiu, J. J. Chen, and M. J. Tseng, "Expression of a Bacillus thuringiensis toxin (cry1Ab) gene in cabbage (Brassica oleracea L. var. capitata L.) chloroplasts confers high insecticidal efficacy against Plutella xylostella", *Theoretical and Applied Genetics*, Vol. 117, No. 1, pp. 75-88, 2008.

[23] A. Adamo, O. Roushdy, R. Dokov, A. Sharei, and K. F. Jensen, "Microfluidic jet injection for delivering macromolecules into cells", *Journal of micromechanics and*

microengineering: structures, devices, and systems, Vol. 23. Pp. pp. 35026-35033, 2013.

[24] J. Gehl, "Electroporation: theory and methods, perspectives for drug delivery, gene therapy and research", *Acta Physiologica Scandinavica*, Vol. 177, No. 4, PP. 437-447, 2003

[25] T. Inoue, R. Krumlauf, "An impulse to the brain-using in vivo electroporation", *Nat Neurosci*, No.4, PP. 1156–1158, 2001

[26] H. Potter, "Electroporation in biology: Methods, applications, and instrumentation", *Analytical Biochemistry*, Vol. 174, No. 2, PP. 361-373. (1988).

[27] Mehier-Humbert, Sophie, and Richard H. Guy. "Physical methods for gene transfer: improving the kinetics of gene delivery into cells", *Advanced drug delivery reviews*, Vol. 57, No. 5, pp. 733-753, 2005.

[28] P. L. Felgner, T. R. Gadek, M. Holm, R. Roman, H. W. Chan, M. Wenz, and M. Danielsen, "Lipofection: a highly efficient, lipid-mediated DNA-transfection procedure", *Proceedings of the National Academy of Sciences*, Vol. 84, No. 21, pp. 7413-7417, 1987.

[29] Y.C. Lin, M. Li, C.S. Fan and L.W. Wu, "A microchip for electroporation of primary endothelial cells", *Sensors & Actuators: A. Physical*, Vol. 108, No. 1-3, PP. 12-19, 2003

[30] C. Ionescu-Zanetti, A. Blatz and M. Khine, "Electrophoresis-assisted single-cell electroporation for efficient intracellular delivery", *Biomedical Microdevices*, Vol. 10, No. 1, PP. 113-116, 2008

[31] M. Khine, C. Ionescu-Zanetti, A. Baltz, L.P. Wang and L.P. Lee, "Single-cell electroporation arrays with real-time monitoring and feedback control" *Lab on a Chip*, Vol. 7, No. 4, PP. 457-462, 2007.

[32] Y. Huang, and B. Rubinsky, "Flow-through micro-electroporation chip for high efficiency single-cell genetic manipulation", *Sensors & Actuators: A. Physical*, Vol. 104, No. 3, PP. 205-212, 2003.

[33] M.B. Fox, D. C. Esveld, A. Valero, R. Luttge, H.C. Mastwijk, P.V. Bartels, A. Van Den Berg and R.M. Boom, "Electroporation of cells in microfluidic devices: a review", *Analytical and Bioanalytical Chemistry*, Vol. 385, No. 3, PP. 474-485, 2006.

[34] H.Y. Wang and C. Lu, "Electroporation of Mammalian Cells in a Microfluidic Channel with Geometric Variation", *Analytical Chemistry*, Vol. 78, No. 14, PP. 5158-5164, 2006.

[35] O. Kurosawa, H. Oana, S. Matsuoka, A. Noma, H. Kotera and M. Washizu, "Electroporation through a micro-fabricated orifice and its application to the measurement of cell response to external stimuli", *Measurement Science and Technology*, Vol. 17, No. 12, PP. 3127-3133, 2006.

[36] Y. Liu, H. Yang and A. Sakanishi, "Ultrasound: Mechanical gene transfer into plant cells by sonoporation", *Biotechnology Advances*, Vol. 24, No. 1, PP. 1-16, 2006

[37] H.J. Kim, J.F. Greenleaf, R.R. Kinnick, J.T. Bronk, and M.E. Bolander, "Ultrasound-mediated transfection of mammalian cells", *Hum Gene Ther*, Vol.7, No. 11, PP. 1339–1346, 1996

[38] D.L. Miller, S.V. Pislaru, and J.F. Greenleaf. “Sonoporation: mechanical DNA delivery by ultrasonic cavitation”, *Somatic cell and molecular genetics*, Vol. 27, No. 1-6 pp. 115-134, 2002.

[39] Siu, Tung, R. Rohling, and M. Chiao. “Microdevice-based delivery of gene products using sonoporation”, *Biomedical microdevices*, Vol. 9, No. 3, pp. 295-300, 2007.

[40] L.S. Gac, E. Zwaan, A. Van Den Berg and C.D. Ohl, “Sonoporation of suspension cells with a single cavitation bubble in a microfluidic confinement”, *Lab on a Chip*, Vol.7, No. 12, PP. 1666-1672, 2007

[41] I. Martinou, P.A. Fernandez, M. Missotten, E. White, B, Allet, R. Sadoul and J.C. Martinou, “Viral proteins E1B19K and p35 protect sympathetic neurons from cell death induced by NGF deprivation”, *The journal of Cell Biology*, Vol. 128, No. 1–2, PP. 201–208, 1995

[42] S.R. Ikeda, D.M. Lovinger, B.A. McCool and D.L. Lewis, “Heterologous expression of metabotropic glutamate receptors in adult rat sympathetic neurons: subtypespecific coupling to ion channels”, *Neuron*, Vol. 14, No. 5, PP. 1029–1038, 1995

[43] Chun, Kyoseok, G. Hashiguchi, H. Toshiyosh, and H. Fujita. “Fabrication of array of hollow microcapillaries used for injection of genetic materials into animal/plant cells”, *Japanese journal of applied physics*, Vol. 38, No.3A, pp. L279, 1999..

[44] S. Lee, W. Jeong, and D.J. Beebe, "Microfluidic valve with cored glass microneedle for microinjection", *Lab on a Chip*, Vol. 3, No. 3, PP. 164-167, 2003

[45] O. Guillaume-Gentil, E. Potthoff, D. Ossola, P. Dörig, T. Zambelli, and J. A. Vorholt, "Force-Controlled Fluidic Injection into Single Cell Nuclei. Small, Vol. 9, No. 11, pp. 1904-1907, 2013.

[46] A. Adamo and K. F. Jensen, "Microfluidic based single cell microinjection", *Lab on a Chip*, Vol. 8. No. 8, PP. 1258-1261, 2008

[47] D. Delubac, C. B. Highley, M. Witzberger-Krajcovic, J. C. Ayoob, E. C. Furbee, J. S. Minden, and S. Zappe, "Microfluidic system with integrated microinjector for automated Drosophila embryo injection". *Lab on a Chip*, Vol. 12, No. 22, pp. 4911-4919, 2012.

[48] A. Noori, P. R. Selvaganapathy, and J. Wilson. "Microinjection in a microfluidic format using flexible and compliant channels and electroosmotic dosage control", *Lab on a Chip*, Vol. 9, No.22, pp. 3202-3211, 2009.

[49] I. Martinou, P.A. Fernandez, M. Missotten, E. White, B. Allet, R. Sadoul and J.C. Martinou, "Viral proteins E1B19K and p35 protect sympathetic neurons from cell death induced by NGF deprivation", *Journal of Cell Biology*, Vol. 128, No. 1, PP. 201–208, 1995.

[50] S. R. Ikeda, R., D. M. Lovinger, B. A. McCool, and D. L.Lewis, "Heterologous expression of metabotropic glutamate receptors in adult rat sympathetic neurons: subtype-specific coupling to ion channels", *Neuron*, Vol. 14, No. 5, pp. 1029-1038. Chicago, 1995.

[51] M. Rieckher, N. Kourtis, A. Pasparaki, and N. Tavernarakis, “Methods In Molecular Biology – Chapter 2”, School of Life Sciences University of Hertfordshire Hatfield, Hertfordshire, AL10 9AB, UK.

[52] Z. Xi and S.L. Dobson, “Characterization of Wolbachia transfection efficiency by using microinjection of embryonic cytoplasm and embryo homogenate”, *Applied and environmental microbiology*, Vol. 71, No. 6, PP. 3199-3204, 2005.

[53] Y.M, Shen, R.R. Hirschhorn, W.E. Mercer, E. Surmacz, Y. Tsutsui, K.J. Soprano and R. Baserga, “Gene transfer: DNA microinjection compared with DNA transfection with a very high efficiency.” *Molecular and cellular biology*, Vol. 2, No. 9, PP. 1145-1154, 1982.

[54] W. Ansorg, and R. Pepperkok, “Performance of an automated system for capillary microinjection into living cells”, *Journal of biochemical and biophysical methods*, Vol. 16, No. 4 , PP. 283-292, 1988.

[55] T. Muramatsu, Y. Mizutani, Y. Ohmori, and J. I. Okumura, “Comparison of Three Nonviral Transfection Methods for Foreign Gene Expression in Early Chicken Embryos in Ovo”, *Biochemical and biophysical research communications*, Vol. 230, No. 2, pp. 376-380. 1997.

[56] J. Drews, “Drug discovery today–and tomorrow”, *Drug Discovery Today*, Vol. 5, No. 1, PP. 2-4, 2000

[57] A. C. Hart, ed. “Behavior”, *WormBook, ed*. July 3, 2006.

[58] T. C. Evans, ed. “Transformation and microinjection”, *WormBook, ed*, April 6, 2006.

[59] X. Zhao1, F. Xu1, L. Tang, W. Du, X. Feng, B. F. Liu. "Microfluidic chip-based *C. elegans* microinjection system for investigating cell–cell communication in vivo", *Biosensors and Bioelectronics*, Vol. 50, pp. 28-34, 2013.

[60] S.X. Guo, F. Bourgeois, T. Chokshi, N.J. Durr, M.A. Hilliard, N. Chronis and A. Ben-Yakar, "Femtosecond laser nanoaxotomy lab-on-a-chip for in vivo nerve regeneration studies" *Nat. Methods*, Vol. 5, No. 6, PP. 531–33, 2008

[61] C.B. Rohde, F. Zeng, R. Gonzalez-Rubio, M. Angel and M.F. Yanik, "Microfluidic system for on-chip high-throughput whole-animal sorting and screening at subcellular resolution", *Proceedings of the National Academy of Sciences*, Vol. 104, No. 35, PP. 13891–95, 2007

[62] F. Zeng, C.B. Rohde and M.F. Yanik, "Sub-cellular precision on-chip small-animal immobilization, multiphoton imaging and femtosecond-laser manipulation", *Lab Chip*, Vol. 8, No. 5, PP. 653–56, 2008

[63] K. MacMillan, D. Mahdaviani and D. Matuszewski, "Effect of Temperature on Caenorhabditis elegans Locomotion", *The Expedition 1*, 2012.

[64] K. Chung, M.M. Crane and H. Lu, "Automated on-chip rapid microscopy, phenotyping and sorting of C. elegans", *Nat. Methods*, Vol. 5, No. 7, PP. 637–43, 2008

[65] M.S. Bodri, "Nematodes" In *Invertebrate Medicine*, ed. GA Lewbart, pp. 221–34. Ames, Iowa: Blackwell. 1st ed. 327 pp. 2006.

[66] T.V. Chokshi, A. Ben-Yakar and N. Chronis, "C_{O2} and compressive immobilization of *C. elegans*", *Lab on a chip*, Vol. 9, No. 1, PP. 151–57, 2009

[67] S.E. Hulme, S.S. Shevkoplyas, J. Apfeld, W. Fontana and G.M. Whitesides, "A microfabricated array of clamps for immobilizing and imaging *C. elegans*", *Lab On a Chip,* Vol. 7, No. 11, PP. 1515–23, 2007.

[68] D. J. van Gerwen, J. Dankelman, and J. J. van den Dobbelsteen, "Needle–tissue interaction forces–A survey of experimental data", *Medical engineering & physics*, Vol. 34,.No. 6, pp. 665-680, 2012.

[69] N. Abolhassani, R. Patel and M. Moallem, "Needle insertion into soft tissue: a survey", *Medical Engineering and Physics*, Vol. 29, No. 4, PP. 413–431, 2007

[70] S. Misra, K.T. Ramesh and A.M. Okamura, "Modeling of tool-tissue interactions for computer-based surgical simulation – a literature review", *Presence: Teleoperators and Virtual Environment,* Vol.17, No. 5, PP. 463–91, 2008

[71] N.J. Cowan , K. Goldberg, G.S. Chirikjian, G. Fichtinger, R. Alterovitz, K.B. Reed, V. Kallem, W. Park, S. Misra and A.M. Okamura, "Robotic needle steering: design, modeling, planning, and image guidance", In: Surgical Robotics, Vol. 3, PP. 557–582, 2011

[72] Y. Kobayashi, A. Onishi, T. Hoshi and K. Kawamura, "Modeling of conditions where a puncture occurs during needle insertion considering probability distribution", *Intelligent Robots and Systems, IROS 2008. IEEE/RSJ International Conference on*, PP. 1433–1440, 2008.

[73] F. Mueller, "Biomechanical test report on hsw fine-ject needles", *Tech. Rep*, 2011.

[74] J.T, Hing, A.D. Brooks and J.P. Desai, "Reality-based needle insertion simulation for haptic feedback in prostate brachytherapy", *Robotics and Automation. ICRA. Proceedings IEEE International Conference on*, PP. 619–624, 2006

[75] M. Heverly and P. Dupont, "Trajectory optimization for dynamic needle insertion", *Robotics and Automation, 2005. ICRA 2005. Proceedings of the IEEE International Conference on*, PP. 1658–166, 2005

[76] M. Mahvash and P.E. Dupont, "Mechanics of dynamic needle insertion into a biological material", *Biomedical Engineering, IEEE Transactions on,*Vol. 57, No. 4, PP. 934-943, 2010.

[77] Rousche, Patrick J., and Richard A. Normann. "A method for pneumatically inserting an array of penetrating electrodes into cortical tissue." *Annals of biomedical engineering* 20.4 (1992): 413-422.

[78] N. Abolhassani, R. Patel and M. Moallem, "Experimental study of robotic needle insertion in soft tissue", *International Congress Series*, Vol. 1268, PP. 797–802, 2004

[79] M. Meltsner, N. Ferrier and B. Thomadsen, "Observations on rotating needle insertions using a brachytherapy robot", *Physics in Medicine and Biology*, Vol. 52, No. 19, PP. 6027–6037, 2007

[80] H.M. Langevin, D.L. Churchill, J.R. Fox, G.J. Badger, B.S. Garra and M.H. Krag , "Biomechanical response to acupuncture needling in humans", *Journals of Applied Physiology*, Vol. 91, No. 6, PP. 2471–2478, 2001

[81] T. Suzuki, A. Tanaka, H. Fukuyama, J. Nishiyama, M. Kanazawa, M. Oda and M. Takahashi, "Differences in penetration force of intravenous catheters – effect of

grinding methods on inner needles of intravenous catheters", *Tokai J Exp Clin Med*, Vol. 29, No. 4, PP. 175–181, 2004.

[82] T. Podder D. Clark, J. Sherman, D. Fuller, E. Messing, D. Rubens, and et al., "*In vivo motion and force measurement of surgical needle intervention during prostate brachytherapy*", *Med Phys*, Vol. 33, No. 8, pp. 2915–22, 2006.

[83] D. Okuno, T. Togawa, H, Saito and K.Tsuchiya, "Development of an automatic blood sampling system: control of the puncturing needle by measuring forces", *Engineering in Medicine and Biology Society,Proceedings of the 20th Annual International Conference of the IEEE,* Vol. 4, PP. 1811–1812, 1988.

[84] A.M. Okamura, C. Simone and M.D. O'Leary, "Force modeling for needle insertion into soft tissue", *Biomedical Engineering, IEEE Transactions on*, Vol. 51, No. 10, PP. 1707–1716, 2004.

[85] M. D. O'Leary, C. Simone, T. Washio, K. Yoshinaka, A. M. Okamura, "Robotic needle insertion: effects of friction and needle geometry", IEEE international conference on robotics and automation, ICRA, pp. 1774, 2003.

[86] S. P. Davis, B. J. Landis, Z. H. Adams, M. G. Allen, and M. R. Prausnitz,, "Insertion of microneedles into skin: measurement and prediction of insertion force and needle fracture force", *Journal of biomechanics*, Vol. 37, No. 8, pp. 1155-1163, 2004.

[87] J.L. Westbrook, D.R. Uncles, B.T. Sitzman and L.E. Carrie, "Comparison of the force required for dural puncture with different spinal needles and subsequent leakage of cerebrospinal fluid", *Anesthesia & Analgesia*, Vol. 79, No. 4, PP. 769–72, 1994.

[88] Y. Zhang, L.C. Yu, "Single-cell microinjection technology in cell biology", BioEssays, Vol. 30, No. 6, PP. 606-610, 2008

[89] G. Minaschek, J. Bereiter-Hahn and G. Bertholdt, "Quantitation of the volume of liquid injected into cells by means of pressure", *Experimental Cell Research*, Vol. 183, No. 2, PP. 434-42, 1989

[90] J.R. Walton, J.D. Murray, J.T. Marshall and C.D. Nancarrow, "Zygote viability in gene transfer experiments", *Biology of Reproduction,* Vol. 37, No. 4, PP. 957-967, 1987

[91] D. C. Spanner, "Electroosmotic flow", *Transport in Plants I. Springer Berlin Heidelberg,* pp. 301-327, 1975.

[92] R.D. Purves, "The physics of iontophoretic pipettes", *Journal of Neuroscience Methods*, Vol. 1, No. 2, PP. 165-78, 1979

[93] Brenner, Sydney, "The genetics of Caenorhabditis elegans", *Genetics*, Vol. 77, No. 1, pp. 71-94, 1974.

[94] T. Stiernagle, "Maintenance of C. elegans", *WormBook, ed,* February 11, 2006

[95] A. Fire, S. Xu, M. K. Montgomery, S. A. Kostas, S. E. Driver, C. C. Mello "Potent and specific genetic interference by double-stranded RNA in Caenorhabditis elegans", *Nature*, Vol. 391 No. 6669, pp. 806-811, 1998.